UNIVERSIDADE FEDERAL DO ESPIRITO SANTO

DEPARTAMENTO DE ENGENHARIA AMBIENTAL

DAVI DE FERREYRO MONTICELLI

USING GAUSSIAN DISPERSION MODELS AS A TOOL TO IMPROVE SOURCE APPORTIONMENT OF SETTLEABLE PARTICLES

VITÓRIA

2018

DAVI DE FERREYRO MONTICELLI

USO DE MODELOS DE DISPERSÃO ATMOSFÉRICA GAUSSIANOS COMO FERRAMENTA DE MELHORIA NA IDENTIFICAÇÃO E QUANTIFICAÇÃO DA CONTRIBUIÇÃO DE FONTES PARA PARTICULAS SEDIMENTADAS

Trabalho de Conclusão de Curso apresentado ao Departamento de Engenharia Ambiental do Centro Tecnológico da Universidade Federal do Espírito Santo, como requisito parcial para a obtenção do título de Bacharel em Engenharia Ambiental.
Orientador: Dra. Jane Meri Santos
Coorientador: Dr. Harerton Oliveira Dourado

VITÓRIA

2018

Dedico este trabalho aos meus pais Renato Monticelli e Fernanda Ferreyro Monticelli que proporcionaram todo possível para que eu recebesse minha educação. Serão sempre os primeiros mestres que tive.

“Che meraviglia! Noi viviamo sommersi nel fondo d’um pelago d’aria.” - Torricelli

AGRADECIMENTOS

Inicialmente gostaria de agradecer aos meus pais Renato Monticelli e Fernanda Ferreyro Monticelli, por todo incentivo que me deram desde o início até a conclusão deste projeto. Também por todo o esforço que colocaram para proporcionar a vida que tive. A vocês, serei eternamente grato.

Em segunda linha agradeço toda a minha família que direta ou indiretamente contribuiu neste trabalho. Incluo aqui meu irmão Eduardo de Ferreyro Monticelli que vez em quando buscava saber o que eu fazia tanto em frente ao computador diariamente. Ah! E claro, por ter cedido o próprio computador para as modelagens! Sua atitude foi crucial para cumprimento dos prazos deste projeto.

Não poderia me esquecer do meu grande pilar, agora mestranda, e incentivadora, da qual tenho imensa admiração: meu amor Thais Ayres Rebello, que por várias vezes me ajudou neste projeto, e sempre esteve por mim quando precisei.

Gostaria de agradecer, também, a Prof(a). Dra. Jane Meri Santos que me encarregou desta tarefa e acreditou em mim para realizá-la. Esteve sempre acompanhando meu desempenho e disposta a discutir o progresso. Neste sentido, gostaria de aproveitar a lacuna e estender ao Dr. Harerton Oliveira Dourado, que aceitou ser meu coorientador, e demonstrou interesse em me auxiliar principalmente na correção do texto e discussão dos resultados.

Agradeço ao Dr. Neyval Costa Reis Junior, que desde minha Iniciação Cientifica mostrou veemência em meu desenvolvimento e sugeriu parte do tema desta pesquisa. Não poderia me esquecer dos colegas do NQualiAr, em especial Elson Galvão que me incentivou servindo de exemplo de pesquisador. Vitor Lavor, Igor e Alexandre que me ajudaram com o computador que utilizei no laboratório para as modelagens (e com o HD que queimou e fomos capazes de restaurar!). Agradeço também os colegas da AIRES Serviços Ambientais em especial ao Vinicius Sarnaglia que tirou dúvidas minhas durante o processo de modelagem.

Aos professores que tive ao longo da vida e participaram direta ou indiretamente desta conquista e que colaboraram na formação profissional que tive.

ABSTRACT

MONTICELLI, D. F. **Using gaussian dispersion models as a tool to improve source apportionment of settleable particles.** Graduation Project – Environmental Engineering Department, Universidade Federal Do Espírito Santo, Vitória, 107p. 2018.

Particulate matter emitted to the atmosphere can settle inside households, on top of roofs, art pieces, roads and other surfaces causing nuisance. Over the years, the Air Quality Monitoring Network of Great Vitoria Region has monitored Settleable Particulate Matter (SPM) and from the monitored data, studies have been conducted to estimate the deposition flux of particles, their disturbance from the point of view of the population affected, their chemical and morphological characteristics and finally, its formation and contribution sources. One way to study SPM is through dispersion modelling that characterize the dispersal behavior of pollutants and their deposition onto surfaces. Another way is through receptor modelling that identify sources contribution correlating emission and samples' chemistry. However, despite the advances in receptor modelling, there is still a major problem caused by collinearity of sources, that is, when two or more emissions from different sources have chemical similarities. When these sources profiles are added linearly in receptor modeling equations, standard errors on source contributions are often very high. In this context, this study aims to investigate the use of two of the preferred (recommended) dispersion models by USEPA (AERMOD and CALPUFF) to estimate deposition fluxes of particles in urban area and to improve source apportionment of settleable particles. The elected best-fit model is used to ungroup the sources contributions of SPM obtained using the USEPA CMB 8.2 Model. The results showed that CALPUFF presented better adjustment towards monitored data with few overestimations. It also successfully ungrouped the "Coal" and "Steel industry" groups, which consists of similar sources and therefore are not well distinguished by the source apportionment model.

LIST OF TABLES

LIST OF FIGURES

LIST OF ABBREVIATIONS

ABNT	Brazilian Association of Technical Normatives (*portuguese*)
AERMAP	AERMOD Terrain Preprocessor
AERMET	AERMOD Meteorological Preprocessor
AERMOD	AMS/EPA Regulatory Model
AP 42	Compilation of Air Emission Factors from USEPA
ASTM	American Standard Test Method
CALMET	CALPUFF Meteorological Preprocessor
CALPOST	CALPUFF Postprocessor
CALPUFF	Californian Puff Model
CMB	Chemical Mass Balance
COC	Correlation Coefficient
CONAMA	National Council of the Environment (*portuguese*)
EI	Emission Inventory
FAC2	Factor of Two
FB	Fractional Bias
FSD	Fractional Standard Deviation
GMMD	Geometric Mass Mean Diameter
GSD	Geometric Standard Mass Mean Diameter Deviation
GVR	Great Vitória Region
IEMA	ES-State Institute of the Environment and Water Resources (*portuguese*)
METAR	Meteorological Aerodrome Report
NCDC	National Climatic Data Center
NMSE	Normalized Mean Square Error
NOAA	National Oceanic Atmosphere Administration
PBL	Planetary Boundary Layer
PM	Particulate Matter
PM10	Particulate matter with aerodynamic diameter less than 10μm
PM2.5	Particulate matter with aerodynamic diameter less than 2.5μm
RAMQAR	Air Quality Monitoring Network (*potuguese*)
RHC	Robust Highest Concentration
SPM	Settleable Particulate Matter

TPM	Total Particulate Matter
USEPA	United States Environmental Protection Agency
WEBMET	Meteorological Resource Center
WHO	World Health Organization
WNNR	Weighted Normalized Mean Square Error of the Normalized Errors
WRPLOT	Wind Rose Plot Software

TABLE OF CONTENTS

1. INTRODUCTION

According to Brazilian legislation's Resolution CONAMA Nº.3 of 28/06/1990, an air pollutant consists of:

> "(…) matter or energy with intensity and in quantity, concentration, time or characteristics in disagreement with the established levels, and that make air: (i) Improper, harmful or offensive to health, (ii) inconvenience to public welfare, (iii) harmful to materials, fauna and flora and/or (iv) harmful to the security, enjoyment of property and normal activities of the community."

Therefore, particulate matter (PM) is considered an atmospheric pollutant as it can cause damage to the flora, affects the climate on a regional and global scales, and act as a potential cause of disturbance due to its deposition on surfaces and buildings. It is also detrimental to human health as it can penetrate the respiratory system leading to acute and chronicle diseases (WHO, 2006).

Settleable Particulate Matter (SPM) is defined as particles that deposit onto surfaces, in most cases varying from 5μm to 100μm knowing that the presence of particles smaller than 5μm can occur (ASTM D1739-98). Notably, larger particles deposit closer to the emission source than smaller particles (PM_{10} and $PM_{2.5}$) due to the gravitational force. SPM can decrease the visibility of a region close to their emission and can cause nuisance that generates complaints among the inhabitants of urban areas.

Different countries have established thresholds for particles deposition rate, which is calculated from a mass amount deposited per unit area in a time interval (Machado et *al.,* 2018). In Brazil, the states of Minas Gerais, Rio de Janeiro and Amapá have adopted standards for particle deposition. Recently, the Government of the State of Espírito Santo has established state air quality standards, through Decree No. 3463-R/2013, including thresholds for SPM as well.

A dispersion model can be used for environmental risk assessment and for planning the abatement/mitigation of pollutants concentration in the environment. The USEPA recommends two Gaussian dispersion models AERMOD and CALPUFF to estimate dry deposition of particles.

Another approach for the assessment of sources contribution to SPM levels is receptor modelling. One of the most used receptor model is the Chemical Mass Balance (CMB), which works correlating the source chemical profile and the chemical composition of a sample. It is used to identify and quantify the contribution of each source present in the region. However, receptor models present some difficulties in identifying sources and their contribution if facing the problem of collinearity. Collinearity occurs if two or more sources present similar chemical profile. If added linearly, it can lead to improbable solutions (such as negative contribution). In this context, dispersion models can assist receptor-modeling results by identifying the specific mass contribution of sources that rely amid the collinear ones. Thus, this integrated source apportionment segregates grouped sources making it more feasible to isolate possible contributors.

In the Great Vitória Region (GVR), a recent source apportionment study conducted by Santos et *al.* (2017) showed that the deposition rate of particles during April of 2009 to March of 2010 ranged between 2 and 20g/m².30days (being 14g/m².30days the state standard). Among the main constituents of SPM were Elemental Carbon (EC), Organic Carbon (OC), and non-carbon compounds such as Fe, Al and Si. Through USEPA CMB 8.2 model, the authors concluded that the main contributors to SPM loadings in the region were steel and iron ore pelletizing industries. However, iron ore and pellet stockpiles contributions could not be differentiated due to the collinearity of sources.

Therefore, the aim of this work consists in quantifying the dry deposition flux of particles using CALPUFF and AERMOD dispersion models and through the models output assist the CMB receptor model in identifying the contribution of number sources of settleable particles in GVR.

2. OBJECTIVES

2.1 General objective

Investigate the use of the CALPUFF and AERMOD dispersion models to estimate particles' dry deposition rate and to assist the CMB receptor model to identify contributions of similar sources.

2.2 Specific objectives

i. Analyze the formulations contained in the CALPUFF and AERMOD models to determine particle deposition rate;

ii. Estimate the dry deposition rate of the particles, through the CALPUFF and AERMOD dispersion models, in the GVR for April/2009 to March/2010;

iii. Compare the results obtained by the models with the monitored data and elect a best-fit model for GVR;

iv. Use the elected dispersion model outputs to assist the CMB receptor model on identifying and ungroup sources contribution of SPM loadings.

3. LITERATURE OVERVIEW

3.1 Settleable particulate matter (SPM)

Particulate matter is a form of air pollution. It causes loss of visibility as light is scattered and atmosphere becomes hazy. This haziness alters the amount of solar radiation reaching earth's surface and, by consequence, alters the structure and stability of the atmosphere. Particles generate other forms of impacts, for example, if deposited on surfaces they can cause vegetation decay, health effects on animals and humans and damage to infrastructure and art pieces (Finlayson-Pitts and Pitts Jr, 2000). One can see that the understanding of particles and their sources, physical and chemical properties, formation (due to chemical reactions in air) and fates, are crucial for determining the effects aforementioned.

The *American Standard Test Method for Collection and Measurement of Dustfall (Settleable Particulate Matter)* – ASTM D1739-98 defines this type of particulate matter as any material made of particles small enough to pass screening of 1mm and large enough to fall, due to their weight, on a container exposed to ambient air. The *Brazilian Association of Technical Normative* – (ABNT – MB 3402, 1991) defines SPM, as dustfall in the atmosphere that is susceptible to sampling by free sedimentation and it is composed of solid or liquid particles large enough to deposit on a collector glass, however small enough to pass through screening of 0.8mm.

SPM present themselves with a variety of chemical properties (Santos et *al.,* 2017; Zheng et *al.,* 2005; Sakata and Asakura, 2011; Engelbrecht et *al.,* 2017) and in diverse morphologies and sizes (Conti, 2013; Coe and Lindberg, 1987; Tomašević et *al.,* 2005; Panas et *al.,* 2014) which are correlated with the main sources in the region.

Particles can settle due to dry/wet deposition and sedimentation. Dry deposition, as it will be further explored in the next section, comprehends the transference of a particle (or gas) from the atmosphere onto the surface without precipitation, and without dissolution in atmospheric water droplets (wet deposition). Whereas sedimentation corresponds to when a particle sinks at their fall speed, and is usually accountable for larger particles and has limited to no importance for small particles.

These mechanisms, specifically dry deposition, play a significant role in the global biochemical cycles (Bobbink et *al.,* 2010; Duce et *al.,* 1991; Chu *et al.*, 2008) since it is responsible for half of the total deposition of a variety of chemical compounds present in the atmosphere.

3.2 Dry deposition

By definition, dry deposition is the transport of a contaminant (particles our gases) from the atmosphere onto the surface without precipitation, and without being firstly dissolved in atmospheric water droplets (Seinfeld and Wiley, 2006; Finlayson-Pitts and Pitts Jr., 2000).

According to Seinfeld and Pandis (2006), three factors govern dry deposition of particles: (a) the level of atmospheric turbulence, (b) the physical-chemical properties of the species (size and morphology) and (c) the nature of the surface itself. In the following articles, each author explores one or more factors.

Petroff *et al.* (2008) presented a review on dry deposition and discussed the aerosol dynamics and the mechanical processes controlling aerosol deposition. They focused in the problematic of dry deposition onto vegetation, addressed through analytical and differential model comparisons. Overall, their founding were that friction velocity and surface adhesion affects coarse particles (>20μm) more than vegetation surface roughness or morphology. However, for accumulation and Aitken modes the canopy geometry is an important factor. In Petroff *et al.* (2008b), the authors proposed a new approach for modelling aerosol's dry deposition onto vegetation, based on their findings from the previous study. The new model produced good agreements with existing measurements of deposition for different aerosols and atmospheric flow regimes. However, this model still requires further improvement, since it ignores the physical and chemical interactions between particles-and-particles and particles-and-gases.

Following the Petroff *et al.* (2008) and Petroff *et al.* (2008b) studies, Petroff and Zhang (2010) developed a size-resolved particle dry deposition scheme. The new model accounts not only the leaf size, shape and area index but also the height of the vegetation canopy. Therefore, land cover influences the model more than previously ones do. The authors tested their parameterizations onto six different scenarios,

including: (i) two vegetation covers, (ii) bare soil, (iii) short grass, (iv) coniferous forests, (v) liquid water surfaces and (vi) snow and ice surfaces. Their results compared with actual measurement and surfaces (i) to (v) appeared to be well fit. They suggest that a further analysis can improve the model even more, accounting surface roughness, temperature gradients, and rebounding, resuspension and particle-particle or particle-gas interactions.

Moving to an urban scenario, Jonsson, Karlsson and Jönsson (2008) investigated the aspects of particle dry deposition in urban environment adapting micro-scale deposition models to outdoor situations, using Computational Fluid Dynamics. They found that the deposition velocity depends not only on the friction velocity but also in the variation of micro-scale roughness and temperature on the surfaces.

Liu *et al.* (2016) studied the dry deposition velocity, fluxes and vegetation collection in Beijing Olympic Park, over daytime in an artificial forest, wetland and water surface. According to these authors, the deposition velocity is influenced by weather seasons, i.e., larger fine particle deposition over winter and larger coarse particle deposition in the spring. Moreover, it is higher onto forest canopy than the other types of surfaces.

Chen *et al.* (2012) analyzed meteorological and land cover influence in deposition velocity of particles. In order to do this, the authors set an experiment at four different sites: (i) urban commercial landscape, (ii) urban forest landscape, (iii) urban residential landscape and (iv) country landscape. In their conclusions, landscapes with the highest dry deposition velocities were (i) > (ii) > (iii) > (iv) suggesting that wind speed appears to have the strongest positive correlation with dry deposition velocity. In contrast, temperature and relative humidity had a negative correlation, indicating that the series behavior do not properly follows the fluctuations in these meteorological variables.

3.3 Gaussian diffusion models

3.3.1 The AERMOD modelling system and its formulation for dry deposition

AERMOD is a Gaussian dispersion model widely used for estimation of species concentration and deposition fluxes. It is a regulatory model indicated by the United States Environmental Protecting Agency (USEPA) that includes treatment of surface

and elevated sources, simple and complex terrain features. This section describes some key information over this model and how it is able to perform such analysis. For further details, the author recommends the following readings, and one video channel (see Table 1):

Table 1. References for AERMOD model.

Reference	Link
User's Guide for the AERMOD Meteorological Preprocessor (AERMET) - 2016;	https://www3.epa.gov/ttn/scram/7thconf/aermod/aermet_userguide.pdf
User's Guide For The AERMOD Terrain Preprocessor (AERMAP) - 2006;	http://www.energy.ca.gov/sitingcases/orangegrovepeaker/documents/applicant/afc/Volume_2/Section%206.2%20-%20Air%20Quality/Appendix%206.2-E_Modeling%20Files/01_aermap/AERMAP_06341/AERMAP_USERGUIDE_ADDENDUM_06341.pdf
AERMOD Model Formulation and Evaluation - 2016;	https://www3.epa.gov/ttn/scram/models/aermod/aermod_mfed.pdf
AERMOD Implementation Guide - 2016;	https://www3.epa.gov/ttn/scram/7thconf/aermod/aermod_implmtn_guide_3August2015.pdf
User's Guide for the AMS/EPA Regulatory Model (AERMOD) - 2016;	https://www3.epa.gov/ttn/scram/models/aermod/aermod_userguide.pdf
AERMOD Training	https://www.youtube.com/channel/UCAJ-s7Us1jeGYpdgC9bObMg

Source: Monticelli (2018).

The AERMIC Model – AMS/EPA Regulatory Model (AERMOD) has some advantages to its predecessor ISC3 Model, which includes the treatment of pollutants' dispersion in the Planetary Boundary Layer (PBL) for convective and stable conditions. AERMOD also includes the effect of quasi-reflection of the plume at the top of the mixing layer and the plume penetration in the stable layer above the Convective Boundary Layer (CBL) as well as its re-entry, those represented by virtual plumes (DOURADO, 2013).

To calculate the contribution of direct, penetrated and indirect sources, the system utilizes variations of the Eulerian approach, shown in Table 2:

Table 2. AERMOD formulation for direct, penetrated and indirect sources' contribution.

Direct source	$C_d(x,y,z) = \frac{Qf_p}{\sqrt{2\pi}u} F_y \sum_{f=1}^{2} \sum_{m=0}^{\infty} \frac{\lambda_f}{\sigma_{zj}} [\exp\left(-\frac{\left(z-\psi_{dj}-2mz_i\right)^2}{2\sigma_{zj}^2}\right) + \exp\left(-\frac{\left(z+\psi_{dj}+2mz_i\right)^2}{2\sigma_{zj}^2}\right)]$
Penetrated source	$C_d(x,y,z) = \frac{Q(1-f_p)}{\sqrt{2\pi}u} F_y \sum_{f=1}^{2} \sum_{m=0}^{\infty} \frac{\lambda_f}{\sigma_{zj}} [\exp\left(-\frac{\left(z-\psi_{dj}-2mz_i\right)^2}{2\sigma_{zj}^2}\right) + \exp\left(-\frac{\left(z+\psi_{dj}+2mz_i\right)^2}{2\sigma_{zj}^2}\right)]$
Indirect source	$C_p(x,y,z) = \frac{Qf_p}{\sqrt{2\pi}u\sigma_{zp}} F_y \sum_{m=-\infty}^{\infty} [\exp\left(-\frac{\left(z-h_{ep}-2mz_{ieff}\right)^2}{2\sigma_{zp}^2}\right) + \exp\left(-\frac{\left(z+h_{ep}+2mz_{ieff}\right)^2}{2\sigma_{zp}^2}\right)]$
Variables: $C_d(x,y,z)$ is the concentration due to a direct source at distance (x,y,z); Q = stack emission strength; u = wind velocity; λ_f = distribution coefficient; ψ_{dj} = difference height between source base and plume centreline; f_p = fraction of emitted contaminant (by the source) that stays in the CBL ($0<f_p<1$); z_i = height above the reflected surface in a stable layer; σ_{zp} = total vertical dispersion of penetrated force; h_{ep} = plume height that penetrate beyond the CBL.	

Source: Adapted from USEPA (2016).

The AERMOD system presents three modules:

- AERMET (pre-processor)
- AERMAP (pre-processor)
- AERMOD

Essentially, AERMET reads inputs of meteorological data, obtained from field measurements and adjusted by the user. It generates vertical profiles of wind direction and velocity, also temperature profiles, potential temperature gradient and turbulence in the PBL. AERMAP processes the location of sources and receptors (chosen accordingly to the users' study purpose) and terrain data. AERMOD is the final module which acquire the outputs from AERMAP and AERMET and generates concentration estimations for a pollutant desired within the domain specified (DOURADO, 2013). Figure 1 summarizes AERMOD Modeling System including other features.

Figure 1. AERMOD complete system.

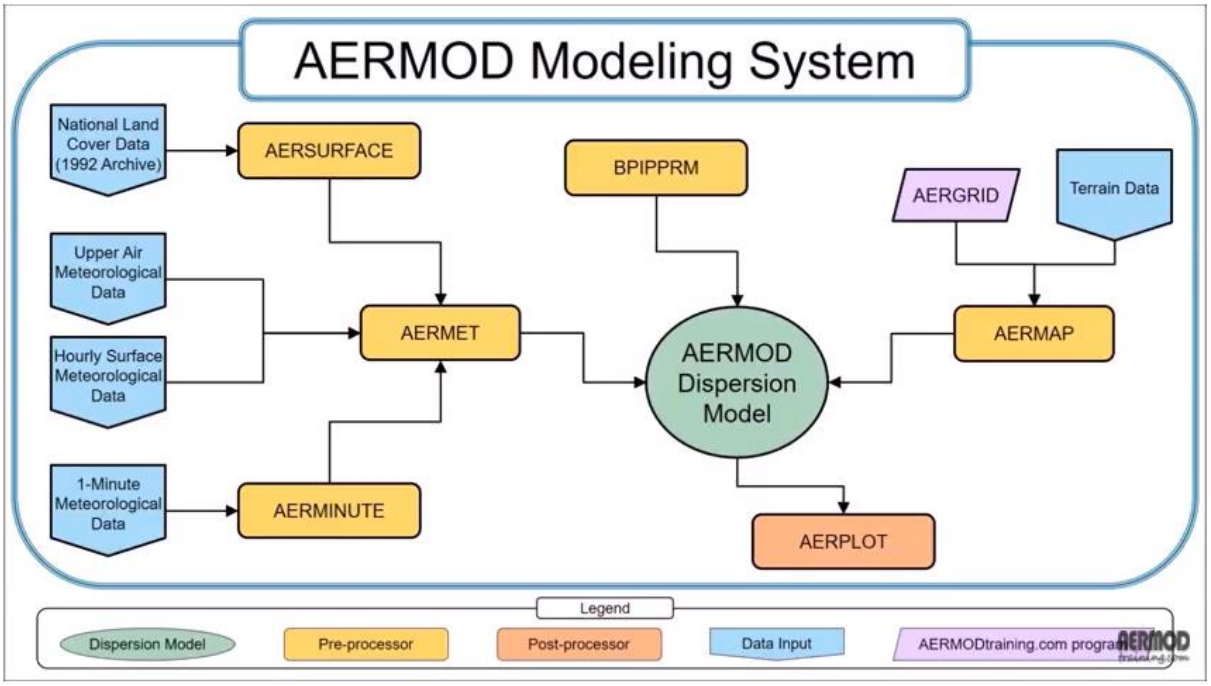

Source: from AERMODtraining.com (2018)

One disadvantage of this model is that is restricted to non-realistic situations, such as idealized uniform flows within the 1-hour step (the dispersion of a plume each hour rely in the direction of the flow straight-line trajectory in that period) and homogeneous turbulence. In addition, it has difficulties representing concentrations under low wind stagnant conditions, especially during nighttime hours (USEPA, 2016).

According to the *User's Guide for the AMS/EPA Regulatory Model (AERMOD) -2016*:

> "*The AERMOD model includes two methods for handling dry and/or wet deposition of particulate emissions. Method 1 is used when a significant fraction (greater than about 10 percent) of the total particulate mass has a diameter of 10 μm or larger, or when the particle size distribution is known. The particle size distribution must be known reasonably well in order to use Method 1. Method 2 may be used when the particle size distribution is not well known and when a small fraction (less than 10 percent of the mass) is in particles with a diameter of 10 μm or larger. The deposition velocity for Method 2 is calculated as the weighted average of the deposition velocity for particles in the fine mode (i.e., less than 2.5 μm in diameter) and the deposition velocity for the coarse mode" (pp. 3-96).*

a) Method 1:

Method 1 requires (i) the mass-mean aerodynamic particle diameter for each particle size categories in microns, (ii) their mass fractions ranging from 0 to 1 and (iii) the corresponding particle density (g/cm³) as inputs of the sources particulate emissions. With those parameters specified, the model applies Equation 1 for each particle size category and sums the results.

$$v_{dp} = \frac{1}{(r_a + r_p + r_a r_p v_g)} + v_g \quad (Eq. 1)$$

Where v_{dp} is the deposition velocity for particles (m/s) r_a represents the atmospheric resistance (s/m), r_p the quasilaminar sublayer resistance (s/m) and v_g the gravitational settling velocity of the particle.

Three keywords on the SO pathway, PARTDIAM, MASSFRAX, and PARTDENS, compose the controlling input of source variables for particle deposition using Method 1. The particle variables may be input for a single source, or to a range of sources (see Figure 2).

Figure 2. Method 1 Sytax, Type and Order.

Syntax:	SO PARTDIAM Srcid (or Srcrng) Pdiam(i), i=1,Npd SO MASSFRAX Srcid (or Srcrng) Phi(i), i=1,Npd SO PARTDENS Srcid (or Srcrng) Pdens(i), i=1,Npd
Type:	Optional, Repeatable
Order:	Must follow the LOCATION card for each source input

Source: (USEPA, 2015).

where the Srcid (Srcrng) identify the source(s) for which the inputs apply, and the Pdiam array consists of the mass-mean aerodynamic particle diameter (microns) for each of the particle size categories. The Phi array is the corresponding mass fractions (between 0 and 1) for each of the categories, and the Pdens array is the corresponding particle density (g/cm³) for each of the categories.

b) Method 2:

In Method 2, the user must specify for each source the fraction of fine mode particles emitted and the representative mass-mean aerodynamic diameter. The deposition velocity becomes a function of the weighted average of v_{dp} for particles in the fine mode (<2.5μm) and the coarse mode (2.5μm<d<10μm):

$$v_{dp} = f_p V_{dpf} + (1 - f_p) V_{dpc} \quad (Eq. 3)$$

Where v_{dp} is the overall deposition velocity for particles (m/s) f_p represents the fraction of particulates in the fine mode, V_{dpf} the deposition velocity (m/s) of fine particulate matter (v_g = 0) and V_{dpc} the deposition velocity (m/s) of coarse particulate matter (v_g = 0.002 m/s). Generally, Method 2 returns lower estimations of deposition fluxes than Method 1.

For Method 2, METHOD_2 keyword on the SO pathway inputs particles' emission information through the code (see Figure 3).

Figure 3. Method 2 Syntax, Type and Order.

Syntax:	SO METHOD_2 Srcid (or Srcrng) FineMassFraction Dmm
Type:	Optional, Repeatable
Order:	Must follow the LOCATION card for each source input

Source: (USEPA, 2015).

where the Srcid or Srcrng identify the source or sources for which the inputs apply. FineMassFraction is the fraction (between 0 and 1) of particle mass emitted in the fine mode and Dmm is the representative mass-mean aerodynamic particle diameter in micrometers.

For the model formulation AERMOD uses to calculate dry/wet deposition of particles and gases in the atmosphere, the reader may refer to *"AERMOD Deposition Algorithms – Science Document (Revised Draft)"* provided in EPA's website.

The AERMOD model allows concentration and deposition units to be quantified separately through the CONCUNIT and DEPOUNIT keywords.

The SOCONT option provides the average concentration (or total deposition) value (i.e., the contribution) from each source for the period corresponding to the event for the source group. The DETAIL option provides the basic source contribution information. In addition, the DETAIL option delivers the hourly average concentration (or total deposition) values for each source for every hour in the averaging period, and a summary of the hourly meteorological data for the event period.

AERMOD has seven functions for modelling removal of particles (and gases) from the atmosphere, shown in Table 3.

Table 3. AERMOD functions for particle and gas removal.

Functions	
DEPOS	Specifies that total deposition flux values (both dry and wet) will be calculated;
DDEP	Specifies that dry deposition flux values will be calculated;
WDEP	Specifies that wet deposition flux values will be calculated;
DRYDPLT	Option to incorporate dry depletion (removal) processes associated with dry deposition algorithms; this requires specification of dry deposition source parameters and additional meteorological variables; dry depletion will be used by default if dry deposition algorithms are invoked;
NODRYDPLT	Option to disable dry depletion (removal) processes associated with dry deposition algorithms;
WETDPLT	Option to incorporate wet depletion (removal) processes associated with wet deposition algorithms; this requires specification of wet deposition source parameters and additional meteorological variables; wet depletion will be used by default if wet deposition algorithms are invoked;
NOWETDEPLT	Option to disable wet depletion (removal) processes associated with wet deposition algorithms;

Source: Monticelli (2018).

The AERMOD outputs comes in the order of: (1) CONC, (2) DEPOS, (3) DDEP, and (4) WDEP. The model requires appropriate deposition parameters in order to output deposition fluxes using the keywords above mentioned. The use of the NODRYDPLT and/or NOWETDPLT options would result in a more conservative estimate of concentrations. Therefore, deposition fluxes for applications involving deposition processes would also be more conservative (U.S. EPA, 2015).

3.3.2 The CALPUFF modelling system and its formulation for dry deposition

CALPUFF is another Gaussian dispersion model widely used for estimation of species concentration and deposition fluxes and a regulatory model indicated by the United States Environmental Protecting Agency (USEPA). It is a non-steady-state puff dispersion model that incorporates the effects meteorological conditions on species dispersion (transport, transference and removal). This section describes some key information over this model and how it is able to perform such analysis. For further details, the author recommends the following readings (see Table 4):

Table 4. References for CALPUFF model.

Reference	Link
A User's Guide for the CALMET Meteorological Model (Version 5) - 2000;	http://www.src.com/calpuff/download/CALMET_UsersGuide.pdf
A User's Guide for the CALPUFF Dispersion Model (Version 5) - 2000;	http://www.src.com/calpuff/download/CALPUFF_UsersGuide.pdf
CALPUFF Modeling System Version 6 User Instructions - 2011;	http://www.src.com/calpuff/download/CALPUFF_Version6_UserInstructions.pdf

Source: Monticelli (2018).

While USEPA recommends AERMOD for near field (<50km) applications as preferred regulatory dispersion model, CALPUFF is for long distances (50 to 300km) or/and that include complex meteorological and terrain configurations. Three main processors compose the system: (1) CALMET, (2) CALPUFF and (3) CALPOST. CALMET is a 3D-meteorological model, a pre-processor that reads data from field measurements. This pre-processor also accepts inputs from prognostic meteorological models, for instance MM4, MM5 or WRF, the latter if properly configured (LEE *et al.*, 2014). CALPUFF estimates the concentrations under diverse meteorological and terrain settings. Finally, CALPOST is the postprocessor module, used to assemble the time-averaged concentration in the receptors specified by the user (DOURADO, 2013).

CALPUFF is often preferred and perceived as advantageous in the literature because include some effects that its competitors (eg. AERMOD) do not, like chemical transformation and overwater transport. Other effects included are: (a) plume rise, (b)

partial plume penetration in the stable layer, (c) pollutant removal, (d) vertical wind shear and (e) building downwash.

This dispersion model represents the continuous plume as a series of discrete packages of pollutant material, named *puffs*. These *puffs* travel in space and time through modelling steps, changing their position and size in each step (Figure 4(a)). Inside every *puff*, the dispersion of the pollutant follows a Gaussian distribution. As mentioned before, in puff-type dispersion modelling, the total concentration at a receptor point is the totality of the contributions of all *puffs* that are located nearby it, being averaged for all sampling steps within the averaging period (see Figure 4(b)) (DOURADO, 2013).

Figure 4. Representation of a plume by the puff-type approximation.

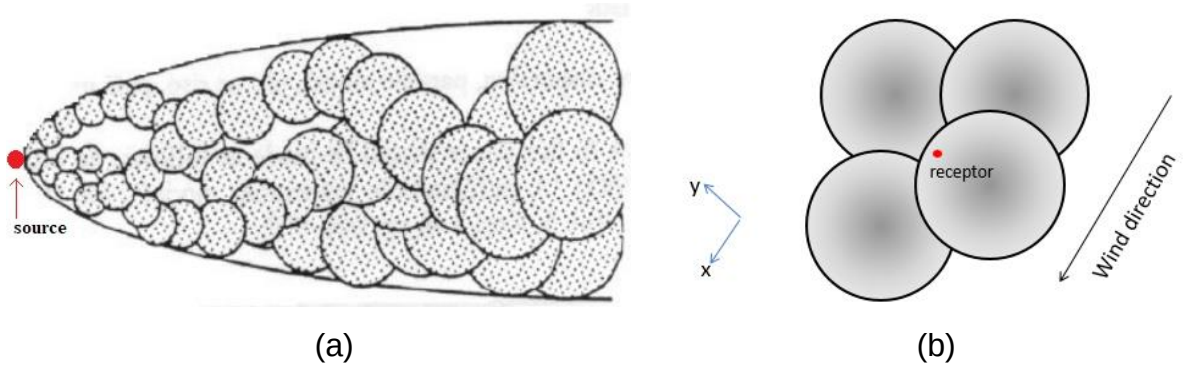

(a) (b)

Source: (a) adapted from (MORAES, 2004) and (b) total concentration at a receptor point, Monticelli (2018).

Equation 1 gives one isolated puff contribution to one receptor:

$$C = \frac{Q}{2\pi\sigma_x\sigma_y} g exp\left[-{d_a}^2/2{\sigma_x}^2\right] exp\left[-{d_c}^2/2{\sigma_y}^2\right]; \quad (Eq.1)$$

$$g = \frac{2}{(2\pi)^{1/2}\sigma_z} \sum_{n=-\infty}^{+\infty} exp\left[\frac{-(H_e + 2nh)^2}{2{\sigma_z}^2}\right] \quad (Eq.2)$$

In which C is the ground-level concentration (g/m³); Q is the pollutant mass (g) in the puff; σ_x is the standard deviation (m) of the Gaussian distribution in the along-wind direction; σ_y is the standard deviation (m) of the Gaussian distribution in the cross-wind direction; σ_z is the standard deviation (m) of the Gaussian distribution in the

vertical direction; d_a is the distance (m) from the puff center to the receptor in the along-wind direction; d_c is the distance (m) from the puff center to the receptor in the cross-wind direction, g (Eq.2) is the vertical term (m) of the Gaussian equation; H_e is the effective height (m) above the ground of the puff center, and h is the mixed-layer height (m). (SCIRE, STRIMAITIS and YAMARTINO, 2000). Equation 3 gives the total concentration at a receptor point:

$$C_{(x,y,z)} = \sum_{puff=1}^{\forall puff} C_{puff(x,y,z)} \quad (Eq.3)$$

CALPUFF has an advantage of tracing back the trajectories of the *puffs* that remain within the domain. This is particular important at low/calm wind conditions because it allows *puff*s path to tilt. In addition, it marks the deposition or particle settling at each hour-step.

Despite CALPUFF advantages, the model has some limitations since it requires a large quantity of emitted *puffs* to represent sufficiently a continuous emission. Not only that, but also the maximum distance between two consecutive *puffs* must be equal to the horizontal dispersion parameter (σ_y), which depends of atmospheric stability and wind speed (DOURADO, 2013).

The system modules work by first diagnosing the wind field and micrometeorology through CALMET, which is consisted of 5 main pre-processors, divided into geophysical and meteorological data processing. Afterwards, CALPUFF acquire the data processed by CALMET and calculates the concentration for each receptor and CALPOST estimate the averages and report concentration or wet/dry deposition flux results. Figure 5 present in form of flowchart the system usage.

For a broader flowchart representing each modules, the author recommend those found in *A User's Guide for the CALMET Meteorological Model (Version 5)* – Scire *et* al. (2000) and *A User's Guide for the CALPUFF Dispersion Model (Version 5) – Scire et* al. (2000).

Figure 5. CALPUFF modelling system

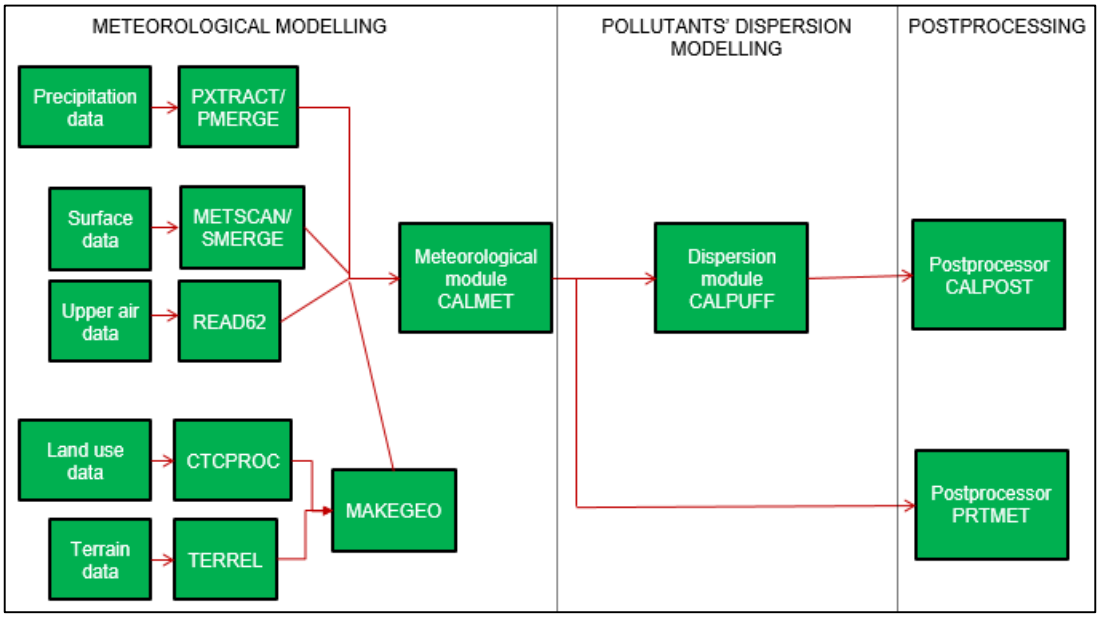

Source: Adapted from (SCIRE, STRIMAITIS and YAMARTINO, 2000).

In order to simulate dry deposition, the user must specify in form of a table in the CALPUFF.INP file the geometric mass mean diameter (in microns) of the particles and the geometric standard deviation (microns). The resistance deposition model for calculating the deposition velocities of particles will then use these inputs to estimate the dry deposition flux according to the Equation 4.

$$F = D_{bl}\frac{(x_m - x_S)}{(h - z_S)} = v_d.x_S \qquad (Eq.4)$$

Where x_m is the pollution concentration (g/m³) within the mixed-layer x_s is the pollutant concentration (g/m³) at the top of the surface layer, h is the mixed-layer height (m), z_S is the surface layer height (m), and D_{bl} is an overall boundary layer eddy diffusivity (m²/s).

Either the main output files from CALPUFF contain hourly concentrations (CONC.DAT) or hourly deposition fluxes (DFLX.DAT/WFLX.DAT) evaluated at designated receptor locations. CALPUFF provides a complete resistance model for the calculation of dry deposition rates of particulate matter (and gases) as a function of geophysical parameters, meteorological conditions, and pollutants species. Alternatives include user-specified, diurnally varying deposition velocities linked for one or more pollutants (e.g., for sensitivity testing) (Scire et *al*., 2000).

Since many variables influence dry deposition, it becomes impractical trying to include all in the deposition model. However, it is possible to parameterize the important effects based on the atmospheric, surface and pollutant properties. CALPUFF deposition module provides three options, detailed in the treatment of dry deposition (Scire et *al*., 2000).

In summary, CALPUFF can simulate gases and particulates dry deposition with full treatment of space and time variations of deposition with a resistance model. However, the user can specify it to address diurnal cycles for each pollutant or simply bypass it completely (Scire et *al*., 2000).

When is chosen by the user to account dry deposition, CALPUFF configures the *puff* centerline height for each receptor to enhance the accumulative effects of gravitational settling. In other words, the *puff* centerline height decreases accordingly with the Equation 5:

$$\Delta h_g = -v_g . t_{tot} \quad (Eq. 5)$$

Where, Δh_g is the change in *puff* height due to settling effects (m), v_g is the gravitational settling velocity and t_{tot} is the total travel time from the source to the receptor (s) (Scire et *al*., 2000).

3.3.3 PLUME versus PUFF Model

From the previous sections, it becomes clear that puff-type models have less assumptions associated with their formulation theory, and can simulate better the meteorology and terrain usage of a given domain. Therefore, may estimate better the concentrations and/or deposition fluxes of contaminants for a pre-established period. CALPUFF has improvements if compared to AERMOD since it can remember previous hourly information of *puffs* and has a chemical transformation model inputted. Nevertheless, the author searched for peer reviewed articles to elucidate which model has a better performance in general. Two articles came up in the subject.

Tartakovsky, Stern and Broday (2016) compared particles dry deposition estimated by AERMOD and CALPUFF using hypothetical point and area sources in flat terrain field to investigate what causes the differences in models estimations. They also simulated scenarios with diverse stability classes and compared the results with a complex

terrain simulation, performed by Tartakovsky, Stern and Broday (2016b). The authors concluded that for smaller topographical barriers between sources and receptors, were also smaller the differences in CALPUFF and AERMOD estimations of the plume centerline, hence, the dry deposition fluxes are closer. Moreover, for ground emissions (such as of an area source), AERMOD and CALPUFF predictions under F stability class (moderate stable) do not vary significantly, however they become larger under C class conditions (weakly unstable). Overall, AERMOD predicted concentrations were in better agreement with observations and thus the deposition fractions. CALPUFF representation of area sources was inferior to AERMOD (more suitable for nearby receptors). According with their findings, in complex terrain, dry deposition estimated by AERMOD is much higher than in CALPUFF.

Due to the scarcity of peer-reviewed articles on the problem, it is hard to elect one-good-for-all model between AERMOD and CALPUFF. Although Tartakovsky, Stern and Broday (2016) and Tartakovsky, Stern and Broday (2016b) showed the opposite, in many studies AERMOD appears to underestimate species concentrations while CALPUFF overestimate the concentrations predicted for some cases. Since the literature regarding the use of CALPUFF and AERMOD to calculate dry deposition fluxes is rather scarce, further studies/validations can indicate which is best.

3.4 Receptor models

3.4.1 Chemical Mass Balance (CMB version 8.2)

In order to determine the origin of the sampled PM, one can make use of the mathematical model called *Chemical Mass Balance* available in the version 8.2 by the US Environmental Protection Agency (USEPA). The CMB receptor model use two sets of data: (1) the chemical composition of the particulate matter collected at the site and (2) the chemical composition of the pollutant emitted from the main sources known in the region.

There are seven steps one may take to properly use this Receptor Model, which are shown in Figure 6:

Figure 6. CMB modelling steps.

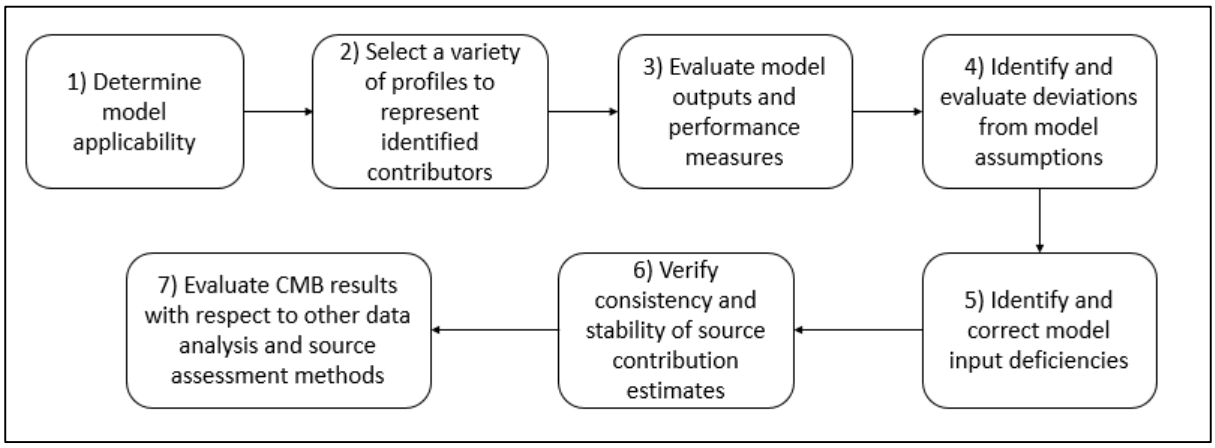

Source: adapted from (USEPA, 2004).

According to Santos et *al.* (2017), the most important limitations reported in the scientific literature for the use of this receptor model rely on the temporal variations in:

i. The composition of the samples of particulate material collected in the receivers distributed throughout the investigated region;

ii. The amount of particulate material emitted by each existing source, since the source profile used in the model is static; and;

iii. The composition of the emissions in each source due to changes in the industrial inputs that causes the chemical change of the material emitted.

Hopke (1991) describes the equation that the CMB 8.2 model tries to solve as it follows:

$$X_{ij} = \sum_{k=1}^{N} g_{ik} f_{kj} + e_{ij} \quad (i = 1\ to\ m); (j = 1\ to\ n); (k = 1\ to\ N) \quad (Eq. 6)$$

where, X_{ij} = concentration in the environment of species "j" in sample "i"; f_{kj} = mass fraction of species "j" at source "k"; g_{ik} = contribution of source "k" in sample "i"; e_{ij} = error.

Srivastava et *al.* (2008) emphasize the statistical parameters and their respective values associated to a good receptor modelling. They are: (1) Variation of calculated

concentrations (R^2)> 0.8; (2) Sum of squared weights of the differences between the calculated and measured concentrations of the species used (Chi-Square) < 4; (3) Degrees of freedom > 5; (4) Percentage of mass explained between 80-120%; (5) Ratio between calculated and measured concentration (C / M ratio) 0.5 -2 and Absolute value of residual uncertainty ratio (R / U) < 4.

For further understanding, one may refer to *"CMB Protocol for Applying and Validating the CMB Model for $PM_{2.5}$ and VOC"* (Watson *et* al., 2004).

CMB receptor model is also used for source apportionment of settleable particulate matter (Balakrishna and Pervez, 2009; Pervez, Balakrishna and Tiwari, 2009; Santos et *al.,* 2017). However, the sources profiles used often represent a category of source rather than individual emitters. The similarity between the chemical profiles of the sources limits the number and meaning of such categories, and due to the limitation of the representation of sources further investigation is frequently suggested in the conclusion of these studies.

There is a recent line of study that suggests a cooperative work of dispersion and receptor models as a way to overcome their limitations. In that sense, some applications involve (i) the correlation of sources contribution with wind directions and dispersion model results Contini et *al.* (2016), (ii) comparison of source apportionment using dispersion and receptor modes Li et *al.* (2015), (iii) using CMB to improve emission inventories and, therefore, the results of dispersion models PriyaDarshini, Sharma and Singh (2016) and (iv) identification of monitoring stations affected by specific group of sources using dispersion model, and results improvement trough CMB receptor model Roy, Singh and Yadav (2016).

4. CHARACTERIZATION OF THE STUDY REGION

The Great Vitoria Region (GVR) covers an area about 2.311km², which represents 5.0% of the State of Espírito Santo (46.078km²). The municipalities of Cariacica, Serra, Vila Velha, Vitoria, Viana, Fundão and Guarapari forms GVR possessing a population of 1.960.213 habitants (IBGE, 2010). Figure 7 to 9 shows the study region location.

Complex terrain features ranging from sea level at East to hills over West characterize GVR. The highest point is at Mestre Álvaro, with 833 meters, in Serra. There are also pikes of 200 to 800 meters in Cariacica and 293 meters in Vitória. Due to its proximity to the ocean and topography, the meteorological conditions and atmospheric circulation present many of the mesoscale phenomenon such as sea and land breeze, orthogonal precipitation, heat islands and temperature inversion (SANTIAGO, 2009).

GVR has twelve types of land use, being: (1) rocky outcrop, (2) flooded terrain, (3) agriculture, (4) planted forest, (5) mangrove, (6) forest, (7) mining areas, (8) pasture, (9) beach, (10) restinga, (11) urban and (12) water. In addition to this, important roads and highways cross the GVR from North to South as well as within its boundaries making it a region of considerable light (cars) and heavy (trucks) vehicle circulation (IJSN, 2012).

Figure 7. (a) Transport infrastructure for GVR.

Source: (IJSN, 2012).

Figure 8. (b) Land use for GVR.

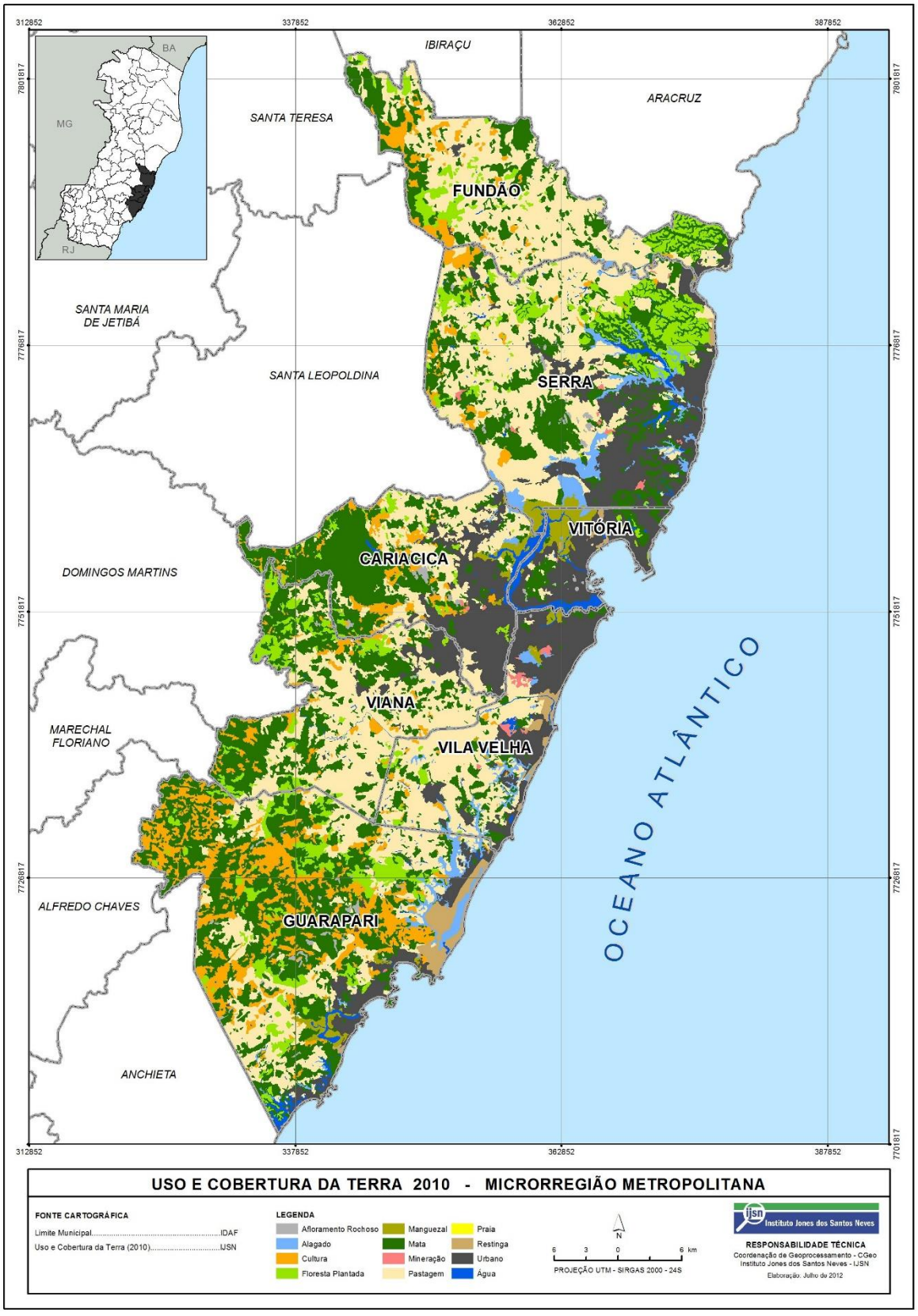

Source: (IJSN, 2012).

Figure 9. (c) Digital elevation model for GVR.

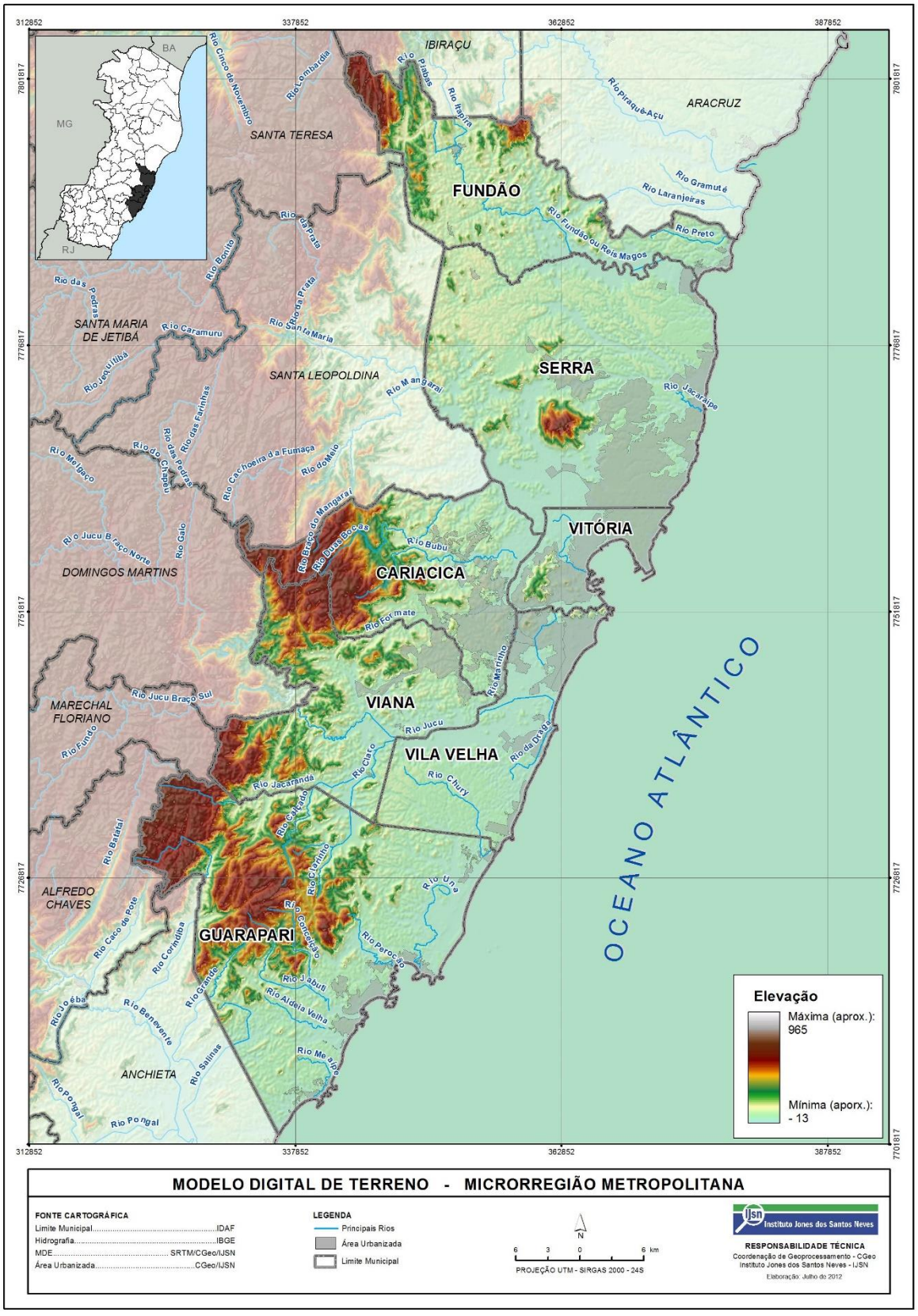

Source: (IJSN, 2012).

4.1 Meteorological conditions

The GVR has a hot and humid tropical climate (IEMA, 2013). In the winter period, it is common to have temperatures around 18°C, with sporadic fronts due to the polar anticyclone. The period with greater temperatures is extensive (approximately occurring between October and April) with higher solar radiation between December and January. The main atmospheric circulation systems are the subtropical anticyclone of the South Atlantic, which is responsible for winds with meteorological directions West and Southwest, provoking high intensity of solar radiation and temperatures. The polar mobile anticyclone is responsible for the south winds, low temperatures and cloudiness. Winds are predominant in the north and northeast quadrants, with intensities between 2.1 and 3.6m/s (SANTIGO, 2009).

Table 5. Interval for the main averaged meteorological values measured at Vitória-ES airport during 2009 to 2017.

Meteorological aspect	Minimum	Maximum
Rainfall	0 mm	300 mm
Wind speed	2.23 m/s	5.81 m/s
Pressure	1010 mb	1025 mb
Cloud cover	0%	100%
Humididty	75%	95%
Temperature	22 °C	30 °C

Source: WEBMET.com (2017)

In Appendix A, it is possible to visualize the temporal evolution of the main meteorological variables during 2009-2010 (study period).

4.2 Emission inventory

The GVR is a highly industrialized and expanding urban region, therefore its air quality is strongly affected by motor vehicles and industrial developments (IEMA, 2013). This section refers to the annual Air Quality Report for 2013 (IEMA, 2013) and the *"Atmospheric Emissions Inventory of the Great Vitória Region "* (ECOSOFT, 2010) report that describe the main pollutant emission sources in the region, specifying their location, amount of pollutants emitted and rank of the source groups based on the magnitude of their contributions (IEMA, 2010). Table 6 shows the ranked contribution results.

Table 6 Emission rate for GVR's main emission sources.

Activity	Emission Rate (kg/h)						
	PTS	**MP10**	**MP2.5**	**SO2**	**NOX**	**CO**	**VOC**
Food industry	4.8	3.7	3.1	3.1	19.0	9.0	0.7
Mineral Products Industry	78.5	43.5	15.5	9.4	22.8	40.7	2.7
Chemical Industry	9.9	9.3	3.7	20.2	6.8	66.1	269.6
Iron ore mining industry	954.4	538.2	271.5	2536	2369.8	15841.3	256.1
Total Industry emissions	**1047.5**	**594.7**	**293.8**	**2568.7**	**2418.4**	**15957**	**529**
Vehicles – Evaporative	107	107	107	46.2	1663	15965.8	1960.7
Vehicles – Breaks/Tire Wear	41.9	41.9	41/9	-	-	-	-
Vehicles - Ressuspension	2742.7	1904.2	944.2	-	-	-	-
Total Vehicles' Emission	**2891.6**	**2053.1**	**1093.1**	**46.2**	**1663**	**15965.8**	**1960.7**
Airport/Ports	98.6	97.3	96.8	74.3	853.9	146.5	75.8
Fuel Gas Stations	-	-	-	-	-	-	293.2
Residential and Comercial	2	1.1	1.1	2	32	20.9	7522.5
Landfill	0.5	0.5	0.5	-	0.7	46.1	43.2
Other emissions	3	2.6	2.1	1.2	9	11.2	0.8
Total emissions for the GVR	**4043.1**	**2749.3**	**1487.5**	**3358.4**	**4976.9**	**32147.6**	**3655.2**

Source: Adapted from IEMA (2013)

One can see through Table 6 that, among these sources, vehicles' emission stands out as the larger contributor to atmospheric particulate matter, being re-suspension predominant in this type of emission. Industry emissions appears after it, contributing with almost one quarter of total particulate emissions, being iron ore and mining industries the major emission source and food industry the minor in this particular group.

4.3 Manual and automatic air quality monitoring stations

Two paired sets of monitoring stations measures the air quality and meteorological conditions in the GVR: (i) the automatic air quality-monitoring network (RAMQAr) and (ii) the manual sediment-monitoring network, administrated by IEMA. The RAMQAr stations and the sediment particle monitoring manual network are located in four of the seven municipalities of the GVR, in locations considered strategic for directing management and control policies. However, according to IEMA, the number and distribution of the air quality monitoring stations operating in the GVR are not sufficient for the detailed characterization of air pollution throughout its territory (IEMA, 2013). Each monitoring station possesses the equipment required for quantification of dust deposition rate. The dust collection bases in the ASTM D173998 (2004), which consists in leaving the accumulating vessel exposed for 30 days and characterizing its contents gravimetrically after drying the sample in an oven. With the mass of deposited particles and an area of the container, determination of the flow of deposition in $g/m^2/30$ days comes naturally. The following map (Figure 10) show the

spatial distribution of the monitoring stations for dust deposition rate, and the usual collector applied is shown in Figure 11.

Figure 10. Spatial distribution of the RAMQAr and the emission sources in GRV..

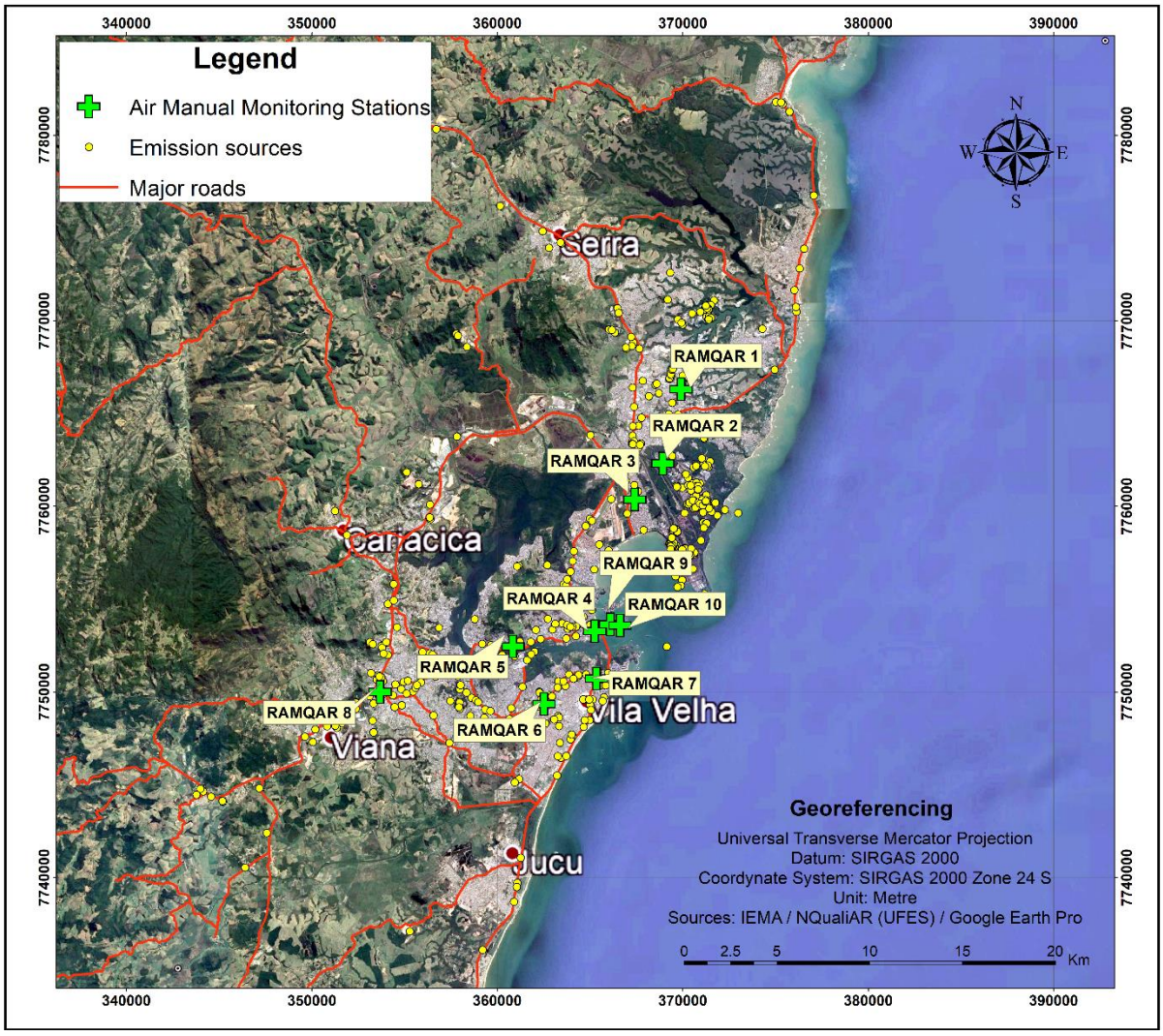

Source: Monticelli (2018).

One can observe that some of the monitoring stations are evidently close to not only major roads but also industrial sites. This can contribute to a source apportionment analysis; however has a major impact in modelling depending on AERMOD and CALPUFF formulation and treatment of those sources. For instance, USEPA (2012) showed that when modelling roads emissions, the user must know the relative position of the discrete receptors to the closest lane, if it is inside the exclusion zone, that source must be treated as an area source, however if it is outside of the exclusion zone, should be treated as packs of volume sources equally spaced.

Figure 11. The deposited dust collector utilized in the manual stations in GVR, units in meters (m).

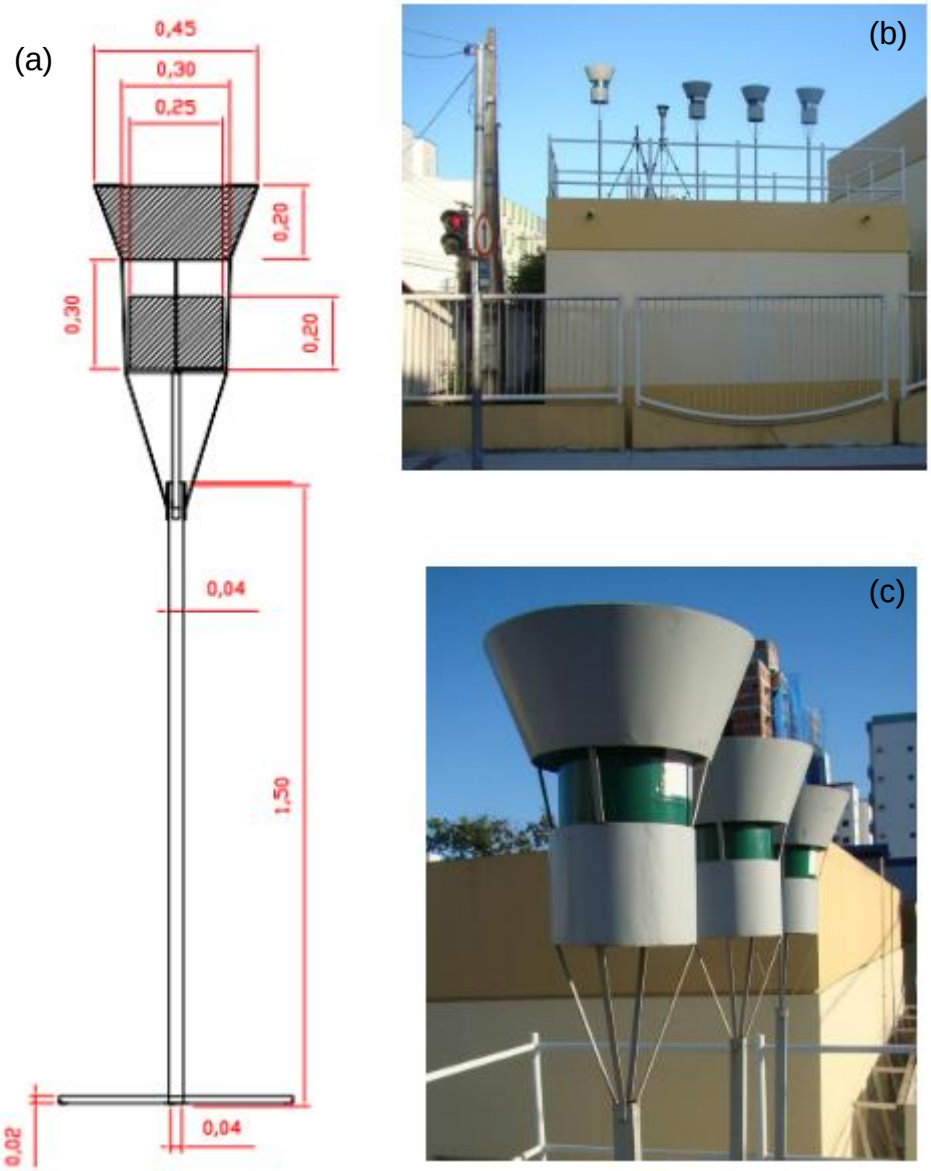

Source: (IEMA, 2013).

In Figure 12, one can observe the histogram of SPM in these monitoring stations alongside with the average source apportionment for the study period. During April/2009 to March/2010, RAMQAr 1, 4, 5, 6, 7 and 9 had values of SPM higher than the state decree (red line – 14 g/m².30days), being most of these exceeds on the month of November/2009. As for the source apportionment, one can notice the presence of the major emission contributor of GVR, steel industry and vehicles, being resuspension significant in RAMQAr 3, 4, 5 and 7 while Siderurgy is in RAMQAr 4 and expressively (77%) in RAMQAr 9.

Figure 12. Histogram and source apportionment of SPM for the monitoring stations of GVR (continue).

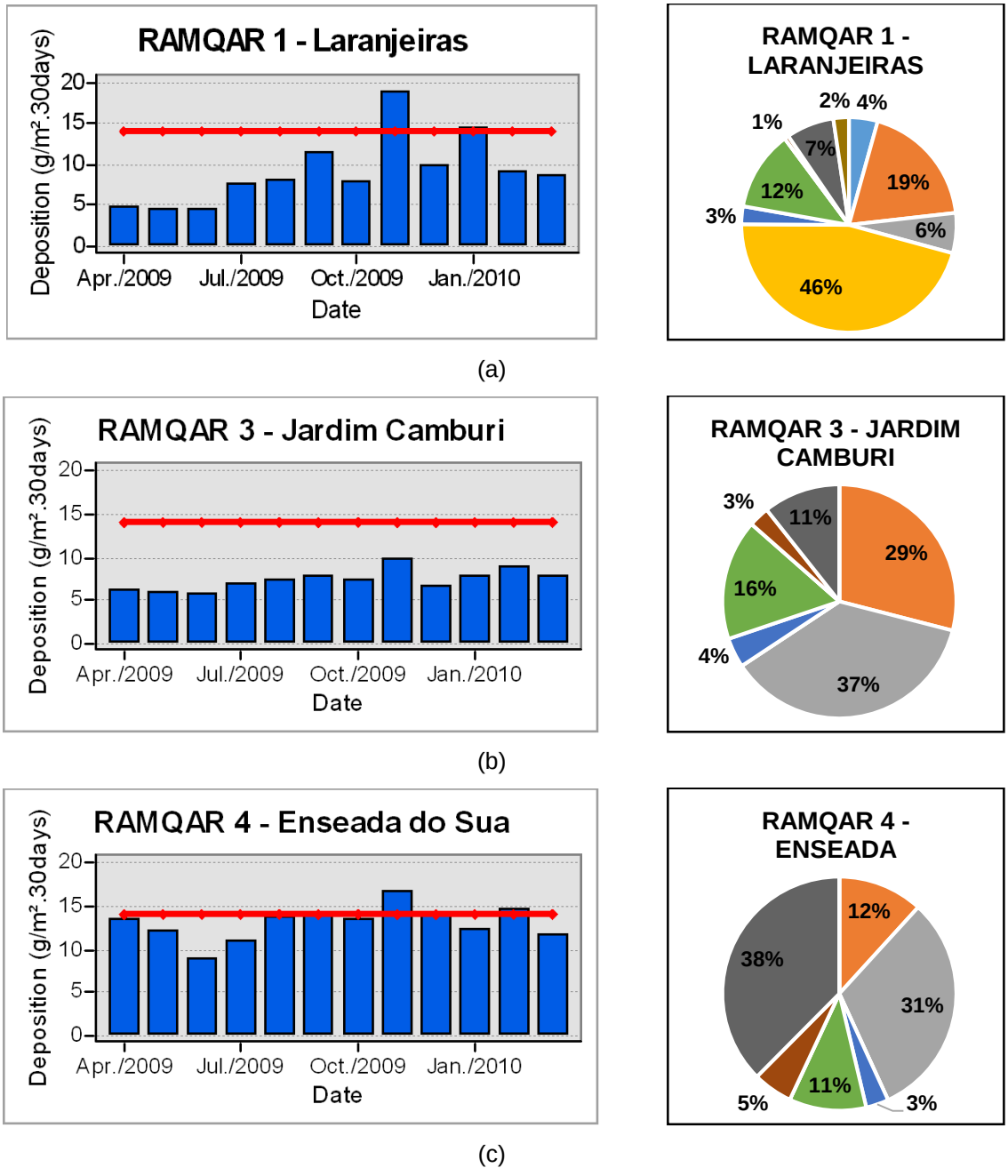

Source: Monticelli (2018), adapted from Santos et *al.* (2017).

Figure 12. Histogram and source apportionment of SPM for the monitoring stations of GVR (continue).

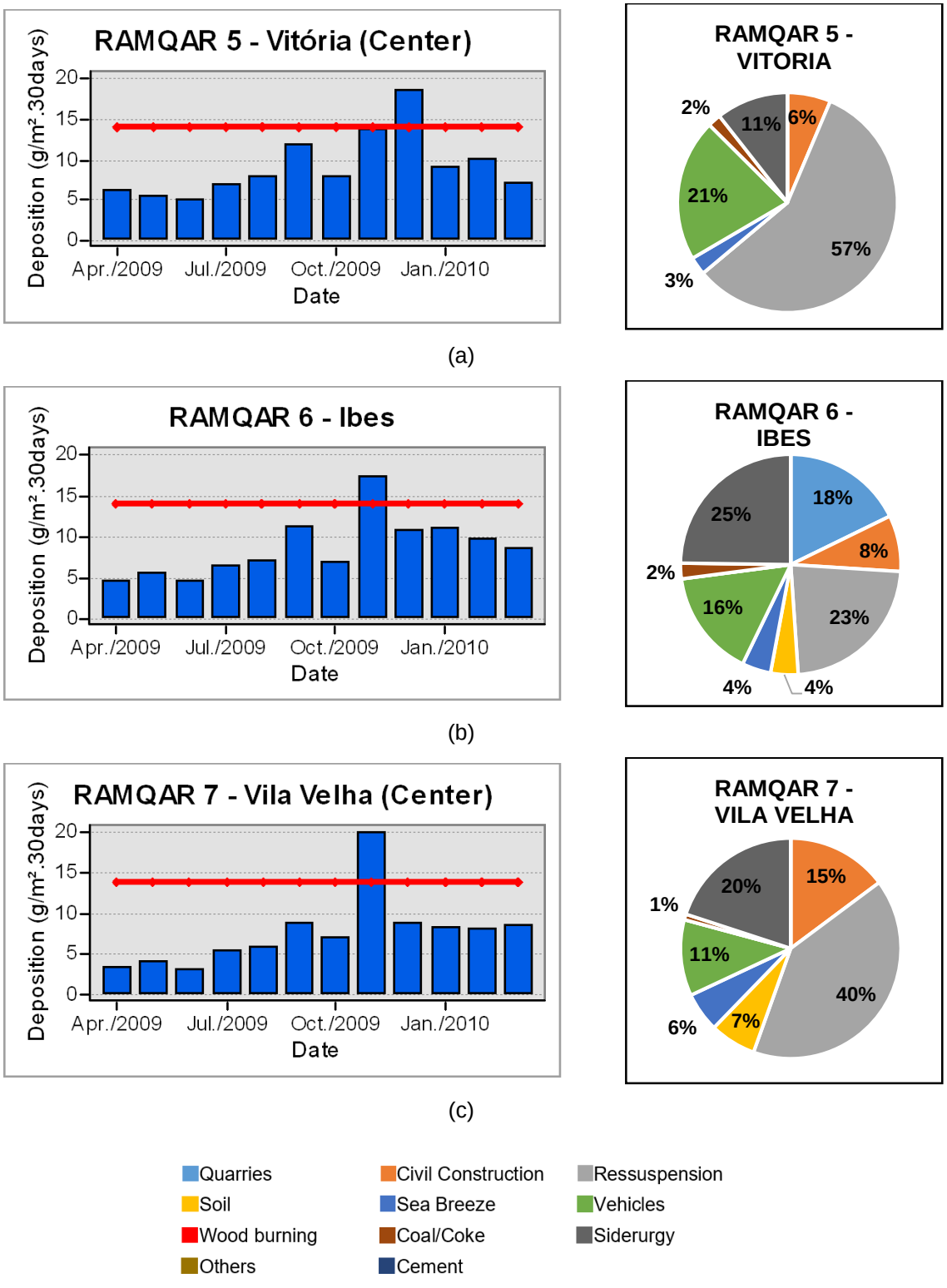

Source: Monticelli (2018), adapted from Santos et *al.* (2017).

Figure 12. Histogram and source apportionment of SPM for the monitoring stations of GVR (final part).

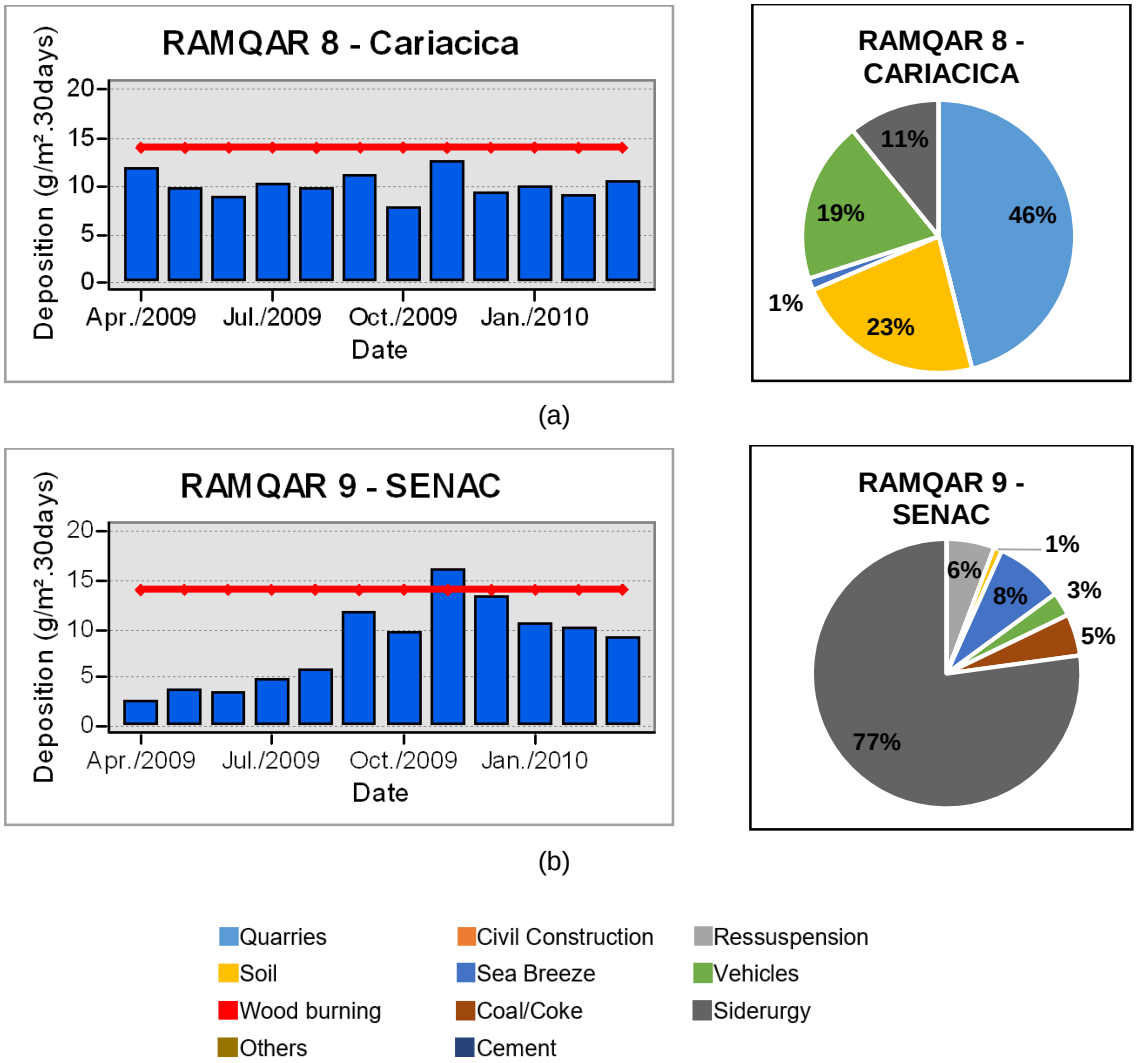

Source: Monticelli (2018), adapted from Santos et *al.* (2017).

5. METHODOLOGY

This section presents the methodology employed in the present research, first describing the study period of this work and the reasons why choosing it (5.1); moving to the emission sources that were part of this project, their manipulation and model accordance (5.2). Next, it goes to the AERMOD and CALPUFF input data, types of file used and those that required modification. Section 5.4 describes the employed models configuration whereas Section 5.5 describes the results analysis and the treatment of receptors location. At last, Section 5.6 describes the source apportionment results used in the Gaussian and Chemical Mass Balance integration and Section 5.7 gives the modelling flowchart.

5.1 Study period

The study period selected to run AERMOD and CALPUFF was from April/2009 to March/2010. The main reasons for choosing this period were: (i) The emission inventory publication date, (ii) The Settleable Particles Matter study, which conducted a source apportionment analysis for 2009-2010 samples and (iii) Available information on meteorological and air quality data.

i. Since the last emission inventory for the study region was relative to the year of 2009, and due to the progressive adjustments on the processes in the industry altering the emissions' composition and load in atmosphere, it is not reasonable to judge them constant and apply it to every year. In many modelling studies, the poor correlation of the results with the actual (measured) data is due to the lack of updates in the emission inventory.

ii. Santos et *al.* (2017) source apportionment study aimed to quantify the contribution of a selected group of sources. Since one of the objectives of this project is to evaluate the results of their CMB analysis, it is reasonable to use the same period in which it was conducted, especially because the wind direction and velocity are crucial to determine which sources may be contributing and needed to be considered in the receptor model for each run.

iii. A full year (12 months) period is relevant because it covers all the seasons and therefore possible meteorological scenarios as well as it is more evocative in

terms of the results' validation. Additionally, the author investigated the meteorological parameters for the study in order to judge the results from the meteorological pre-processors in both dispersion models. Appendix A exemplifies the meteorological variables observed.

5.2 Emission sources

In order to better represent the emission inventory in AERMOD and CALPUFF, the following sources were considered in this study:

i. Industrial emissions were categorized as point, area or volume sources, in accordance with the description provided for each category in the manuals for each model;

ii. Traffic lanes were categorized as a sum of volume sources, and the justification for it is based in the USEPA Research Group Report, the *Haul Road Workgroup Final Report Submission to EPA-OAQPS* (USEPA, 2012). For AERMOD, the inputs requirements were the same as a VOLUME source type; however, each road segregates in many small packs sources. For CALPUFF, the author used the same approach (it is recommended for researches to use the *"Haul Road Calculator"* incorporated in the newest versions of AERMOD View and CALPUFF View);

iii. Only sources emitting particulate matter were included in this study;

iv. Particles size fractions (TPM, PM_{10}, $PM_{2.5}$) of each source were inputted in the model, as a requirement for Method 1 in AERMOD Dry Deposition calculation and CALPUFF species data input.

In Figure 13 it is possible to visualize the domain, modelled sources and their location as point, area or volume emitters. In addition, one can observe the relative position of the receptors to the contributors of deposited particulate matter.

Figure 13. Spatial distribution of sources and receptors under the Domain of study.

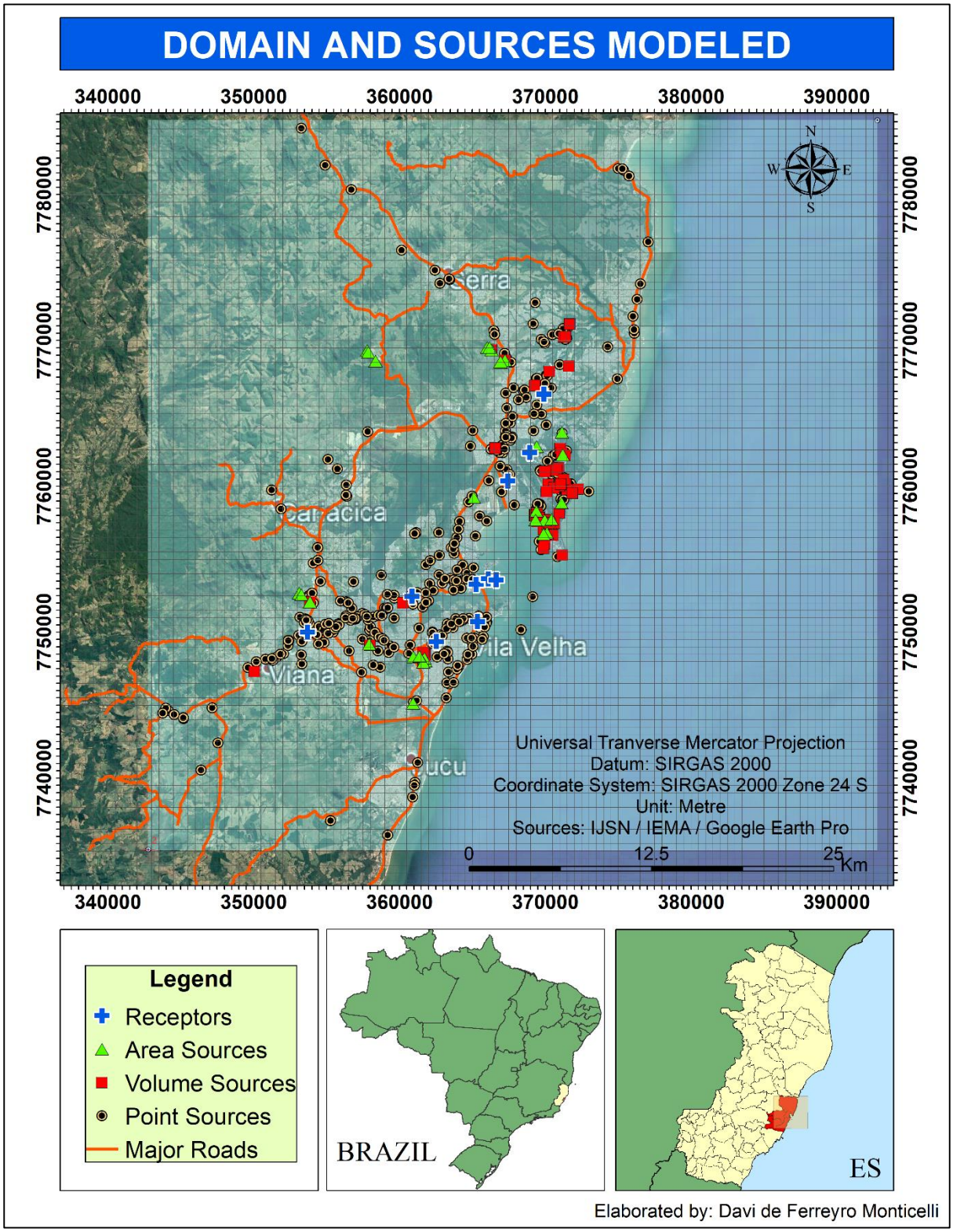

5.3 AEMOD and CALPUFF input data

The Meteorological and Topographical Data used in the models were in accord with their configuration. For AERMOD the following inputs were used (Table 7):

Table 7. Inputs files used in AERMOD.

AERMOD					
Processor	***Modeled File***	***Format***	***Situation***	***Observations***	***Link (Reference)***
AERMAP	Digital Elevation Model	.DEM	Ready to model	Checked in ArcGIS	S21W41.DEM (http://www.webgis.com/)
AERMET	Surface dataset	ISHD	Ready to model	No obs.	National Climatic Data Center (ftp://ftp.ncdc.noaa.gov//pub/data/noaa/)
	Upper air dataset	.FSL	Ready to model	Result altered for next stage	NOAA/ESRL Radiosondate Database (https://ruc.noaa.gov/raobs/)
	ONISTE data	(ONSITE)	Created by the author	No obs.	-
AERMOD	Point sources	Manual	Created by the author	Coordinates Converted in ArcGIS	IEMA (2010)
	Area sources	Manual	Created by the author	Coordinates Converted in ArcGIS	IEMA (2010)
	Volume sources	Manual	Created by the author	Coordinates Converted in ArcGIS	IEMA (2010)
	Major roads emission	Manual	Created by the author	Coordinates Converted in ArcGIS	IEMA (2010)
	All of above	Manual	Created by the author	Coordinates Converted in ArcGIS	IEMA (2010)

Source: Monticelli (2018).

For CALPUFF the methodology for the emission sources discretization and model configuration was extracted from SILVA and SARNAGLIA (2010) and the files presented in Table 8 were used.

Table 8. CALMET and CALPUFF used input files.

CALPUFF						
Processor	***Modeled File***		***Format***	***Situation***	***Observations***	***Link (Reference)***
CALMET	TERREL	Terrain file	.hgt	Ready to model	Compose the preprocessor MAKEGEO	S21W41.hgt (https://dds.cr.usgs.gov/srtm/version2_1/SRTM3/South_America/)
	CTGCOMP /CTGPROC	Use of soil file	.img	Ready to model		sausgs2_0l.img (https://edcftp.cr.usgs.gov/?dir=project/glcc/sa/lambert)
	COASTLINE	Coast line file	.b	Ready to model	Requires update.	gshhs_f.b (http://www.webgis.com/dlg_gshhs.html)
	READ62	Upper air file	.FSL	Required modification	Altered by the modeler	NOAA/ESRL (https://ruc.noaa.gov/raobs/)
	METSCAN /SMERGE	Surface file	.SAM	Created by the author	File generated then edited using WRPLOT	-
CALPUFF	Point sources		Manual	Created by the author	Coordinates Converted in ArcGIS	IEMA (2010)
	Area sources		Manual	Created by the author	Coordinates Converted in ArcGIS	IEMA (2010)
	Volume sources		Manual	Created by the author	Coordinates Converted in ArcGIS	IEMA (2010)
	Major roads emission		Manual	Created by the author	Coordinates Converted in ArcGIS	IEMA (2010)
	All of above		Manual	Created by the author	Coordinates Converted in ArcGIS	IEMA (2010)

Source: Monticelli (2018).

5.4 AERMOD/CALPUFF model configuration

The grid receptors' location is within 500m spaced range in AERMOD and 1km in CALPUFF for the modelling Domain. The author adopted this configuration due to the processing time for each model. Ten discrete receptors correspond to the manual monitoring stations of dustfall. Meteorological data gathered from the Vitoria's airport monitoring station served for comparison with the files provided by IEMA from different RAMQAr stations and as input data for surface and upper air observations in AERMET and CALMET. Furthermore, AERMOD and CALPUFF ran using the same terrain digital file resolution, however with major differences in land use due to AERMOD sectoring approach limitations. Table 9 presents the main parameters used for the dispersion model run in AERMOD and CALPUFF.

Table 9. AERMOD and CALPUFF in common configuration**.**

Parameters	**AERMOD**	**CALPUFF**
Surface/Altitude stations	SBVT/83649 (METAR)	SBVT/83649 (METAR)
Dry/Wet depletion	No	No
Dry deposition	Yes	Yes
Chemical transformations	No	No
Building Downwash	No	No
Terrain digital file resolution	90 m	90 m
Grid resolution	500 m	1 km
Domain	50 km	50 km
Vertical Levels	-	10

Source: Monticelli (2018).

5.5 Models performance

The results analysis from the AERMOD and CALPUFF simulations will rely on the *Protocol for Determining the Best Performing Air Quality Model,* from USEPA. The mass of settleable particulate matter deposited in the geographical location of the monitoring stations in contrast with the modelling values obtained for the same sites will justify the best-fit model. Table 10 summarizes the statistical indexes applied.

Table 10. Statistical parameters used in model evaluation.

Index	Abbreviation	Equation
Correlation Coefficient	COC	$\frac{\sum_1^n[(C_p - \overline{C_p})(C_o - \overline{C_o})]}{\sqrt{[\sum_1^n(C_p - \overline{C_p})^2]\,[\sum_1^n(C_o - \overline{C_o})^2]}}$
Fractional Standard Deviation	FSD	$2[\frac{(\sigma_p - \sigma_o)}{(\sigma_p + \sigma_o)}]$
Fractional Bias	FB	$2[\frac{(\overline{C_O} - \overline{C_p})}{(\overline{C_O} + \overline{C_p})}]$
Factor of 2	FAC2	$0.5 \leq \frac{C_o}{C_p} \leq 2$
Normalized Mean Square Error	NMSE	$\frac{\overline{(Cp - \overline{C_O})^2}}{C_p C_O}$
*C*p = dry deposition predicted; Co = dry depostion observed*		

Source: Monticelli (2018)

Other authors also suggest different statistical approaches such as the *Composite Performance Measure* (CPM). The CPM calculation involves using the *Absolute Fractional Bias* (AFB), and the *highest measured RHC* at any monitor and the *highest model-predicted RHC* at any monitor. Furthermore, it is recommended to evaluate from a temporal perspective and using Quantil-Quantil graphics (ROOD, 2014; DRESSER and HUIZER, 2011).

In this work, a Modelled vs Observed plot will provide the information required. They represent a common graphical technique for determining whether two sets of data have a mutual distribution. In this type of charts a good model will have a slope similar to that of a 1:1 line (indicating the same distribution) and, specifically for regulatory applications, will have the highest estimate values close to the measured ones.

5.6 CMB results to be reviewed

Once selected the best-fit model to determine the SPM deposited in the GVR, it will be applied to revise the grouped sources in the source apportionment study of Santos *et al.* (2017). In their study, not all of the RAMQAR stations were part of, for instance, Italo Club's location is very near to SENAC monitoring station and had fewer observational data. Another RAMQAR station taken out was Carapina, which have a bias location towards deposition and concentration values.

5.7 Modelling flowchart

Figure 14 explains the steps taken to integrate the US EPA recommended dispersion model and CMB model to improve source apportionment in this study.

Figure 14. Flowchart for explaining the methodology used in this study to integrate dispersion models to a receptor model and improve source apportionment of similar sources.

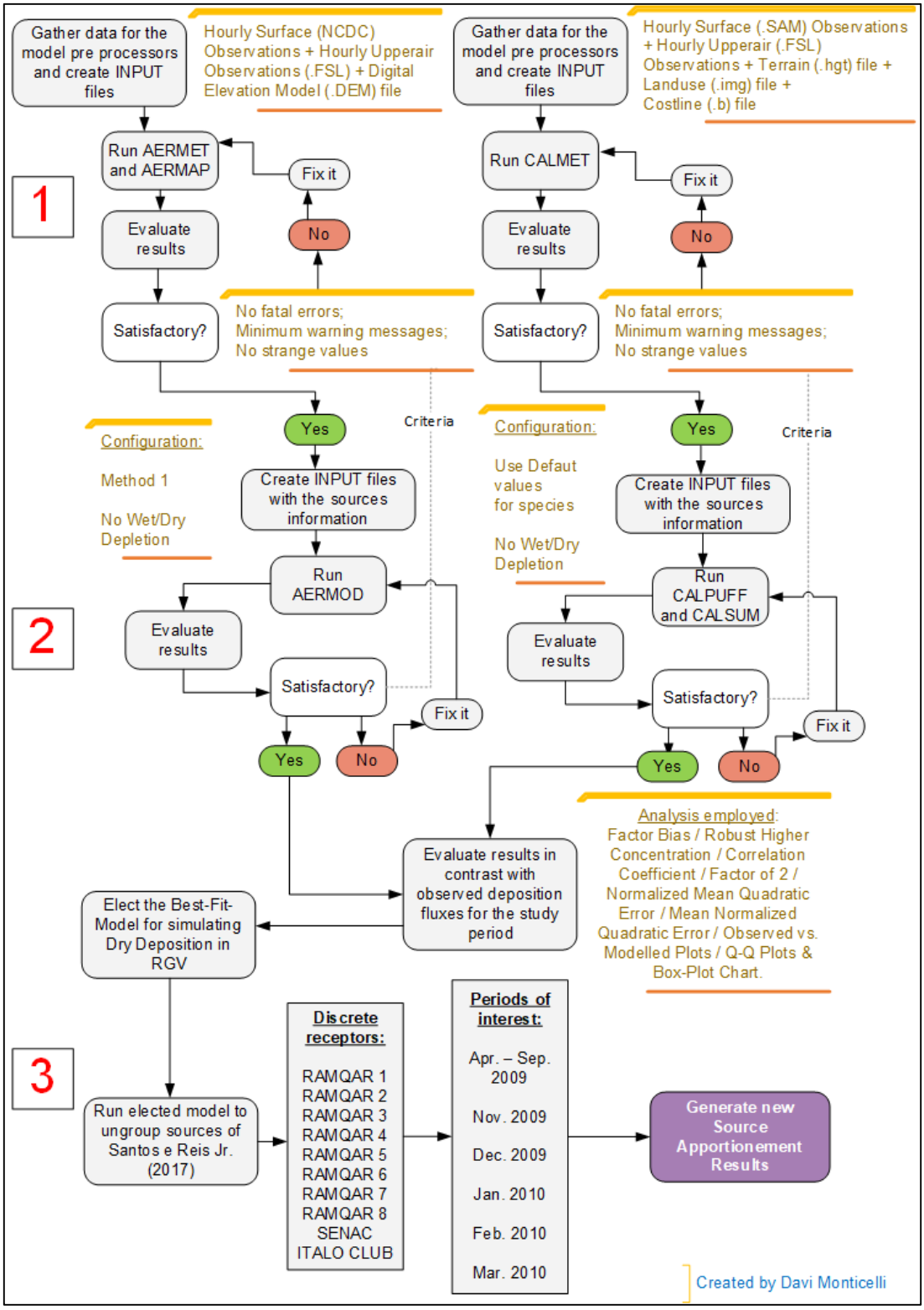

5.8 Modeling considerations

5.8.1 AERMOD

During AERMET pre-processing, the author could not manage to use the ONSITE option with the input data from the Meteorological Aerodrome Report (METAR) further than the second stage due to a fatal error of data reading. Therefore, to reduce the dependence in the reanalysis data from the National Oceanic and Atmosphere Administration (NOAA) and the National Climatic Data Center (NCDC), the AERMET outputs of stages 1 to 3 were analyzed using the plots in Appendix A as reference. The meteorological values listed as outputs of AERMET stage three (i.e. Monin-Obukhov length, sensible heat flux, surface friction velocity) had their values checked and due to lack of records from previous stages, some hours were missing. When applicable, an interpolation was carried out to fill the gaps. The reanalysis file with higher number of missing hours was the ASCII.txt (upper air data). For the land use sectoring in AERMET stage 3, the parameters adopted (see Table 11) were based on the pre-processor user's guide, chosen due to the high humidity and averages temperatures of the study region alongside with the information available on Figure 8.

Table 11. AERMET stage 3 land use input data.

Sector variables	Bowen Ratio (Bo)	Albedo (Ab)	Surface roughness (Zo)
Sector 1 (30° to 195°)	0.10	0.10	0.0001
Sector 2 (195° to 270°)	2.00	0.16	1.0000
Sector 3 (270° to 360°)	0.30	0.12	1.3000
Sector 4 (360° to 30°)	2.00	0.16	1.0000

Source: Monticelli (2018).

Since AERMOD possess two methods to quantify the dry deposition flux, a trial was carried out using Method 2, which is simpler in terms of modelling requirements. The output values of this trial run were much lower than observational data. A further investigation in the emission inventory (EI) resulted on the use of Method 1 with some considerations (see Table 12). The fractions of TPM, PM_{10} and $PM_{2.5}$ for each source emission was extracted directly from the EI, however the mass-mean aerodynamic particle diameter for each particle size categories (μm) and the corresponding particle

density (g/cm³) as inputs of the sources particulate emissions had their values gathered from the AP 42 documents and the literature available. For instance, in Tartakovsky, Stern and Broday (2016b), the authors state that the deposition velocity using 14µm particles with the density of 1.6 g/cm³ (for TPM) is approximately the same as the gravitational settling velocity in AERMOD and CALPUFF systems. Moreover, Hu et *al.* (2012) estimated several fractions of particle density having the coarse mode a result of 2 g/cm³. Table 12 illustrates the values employed for incomplete data in sources emissions using Method 1.

Table 12. Assumed values for implementation of AERMOD Method 1 to estimate particles' dry deposition.

Values used for:	TPM	PM10	PM2.5
mass-mean aerodynamic particle diameter (µm)	14	10	2.5
corresponding particle density (g/cm³)	2.0	1.85	1.60

Source: Monticelli (2018).

5.8.2 CALPUFF

CALMET is not a straightforward pre-processor as AERMET/AERMAP, having each file input (i.e. terrain, land use, surface observations) its own processing systems with their specific requirements. For instance, the surface observations file obtained via reanalysis in the NCDC website had missing values for pressure, temperature or humidity for some hours during April/2009 to March/2010 and that prevented the model to run properly. The author opted to use only one meteorological station in this study, since not all required meteorological variables were registered by the SPM monitoring stations. A SAMSON surface meteorological data was created using the WRPLOT software and information on the hourly wind speed and directions, then, this file was complemented with information obtained in METAR observations, having the meteorological values (i.e. cloud clover, cloud cover baseline height, sea level pressure) addressed to their specific columns. The structure of the SAMSON file is found in the WEBMET site. For the .FSL (upper air observations), it should be noted that the first option for download in the NOAA website had major flaws (with days lacking observations), therefore the author used the original FSL Format download option which presented fewer missing values. An interpolation was also carried for the upper air observations when applicable. Furthermore, no adjustments were carried on

the terrain/land use pre-processors; however, it should be noted that the modelling systems recognized that the input data should be updated.

Differently from AERMOD, CALPUFF dry deposition algorithms require the specification of parameters of the modelled pollutant, rather than information on the emission components. Since such information is not available in the emission inventory the author appealed to the literature and contrasted the information gathered with an self-made estimation for the geometric mass mean diameter (GMMD - microns) of the particles and the geometric standard deviation (GSD - microns), using a lognormal distribution and information from the EI. However, despite the effort, because the values found in the literature (GMMD = 20µm and GSD = 1.24µm from the Guidance Document of the Department of Environment & Conservation of Newfoundland Labrador) and those generated (GMMD = 0.885µm and GSD = 0.61µm) differ greatly, the author opted for using the Default parameters for PM_{10} in the CALPUFF system. This might has resulted in the best choice, once that accordingly with Conti (2013) at least 95% of settleable particles in two of the monitoring stations had diameters less than 10µm. Table 13 resumes the input values used in the CALPUFF dry deposition algorithms.

Table 13. Dry deposition parameters used in CALPUFF modelling system as input file.

Parameters	Value
Geometric mass-mean diameter (µm)	0.48
Geometric standard deviation (µm)	2.00
Reference cuticle resistance (s/cm)	30
Reference ground resistance (s/cm)	10
Reference pollutant reactivity	8
Number of particle-size intervals used to evaluate effective particle deposition velocity	9
Vegetation state in unirrigated areas	1 (active and unstressed vegetation)

Source: Monticelli (2018).

The CALPUFF.INP file specifies that for single species, the GMMD and the GSD are used to compute a deposition velocity for the number of particle-size intervals specified. Further, these values are averaged to obtain a mean deposition velocity.

6. RESULTS AND DISCUSSION

6.1 Modelled versus observed values of dry deposition flux

Figure 15 shows observed (RAMQAr) and predicted dry deposition fluxes by AERMOD and CALPUFF.

Figure 15. Temporal evaluation of modelled versus observed deposition fluxes for RAMQAR in GVR (continue).

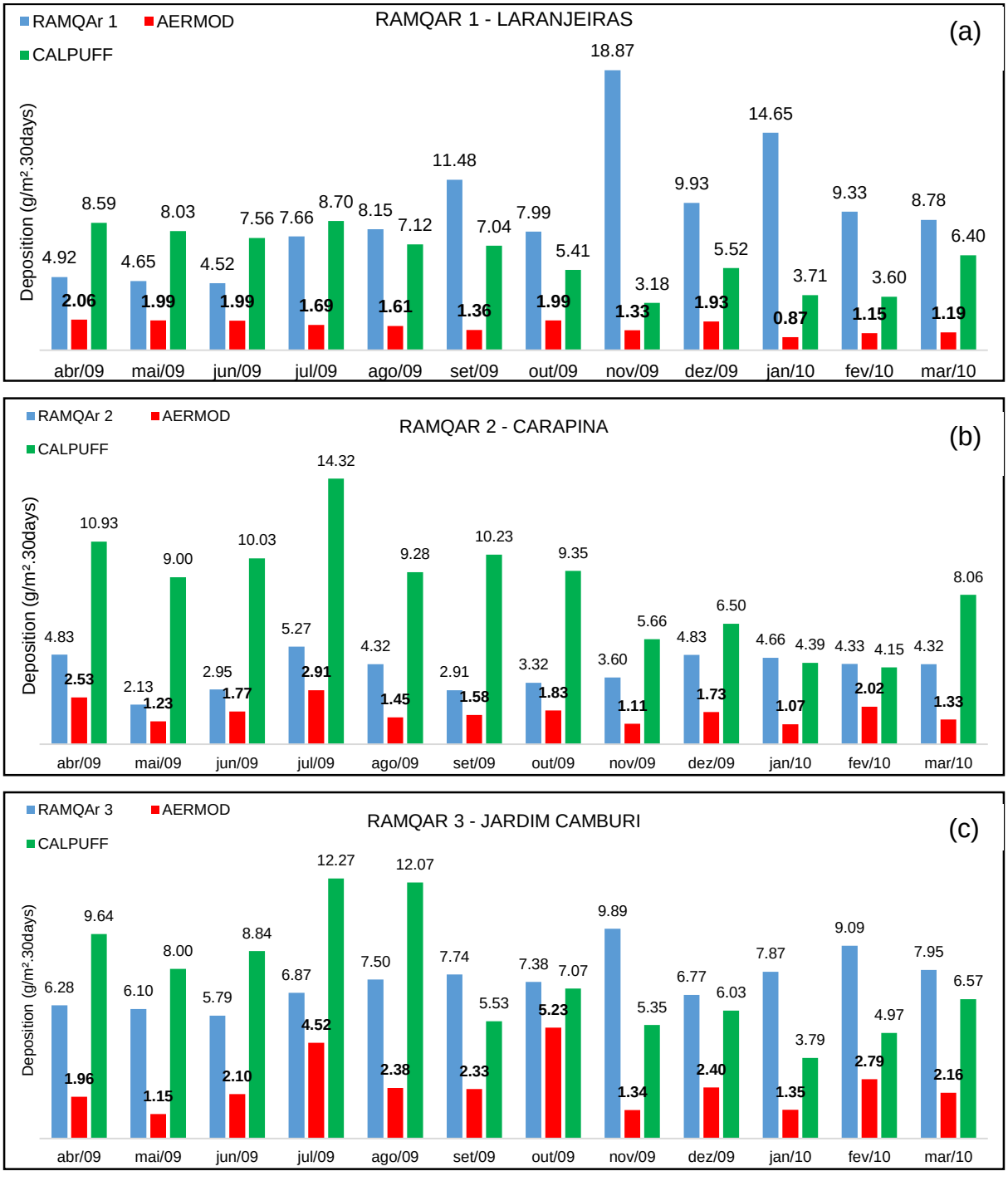

Source: Monticelli (2018).

Figure 15 Temporal evaluation of modelled versus observed deposition fluxes for RAMQAR in GVR (continue).

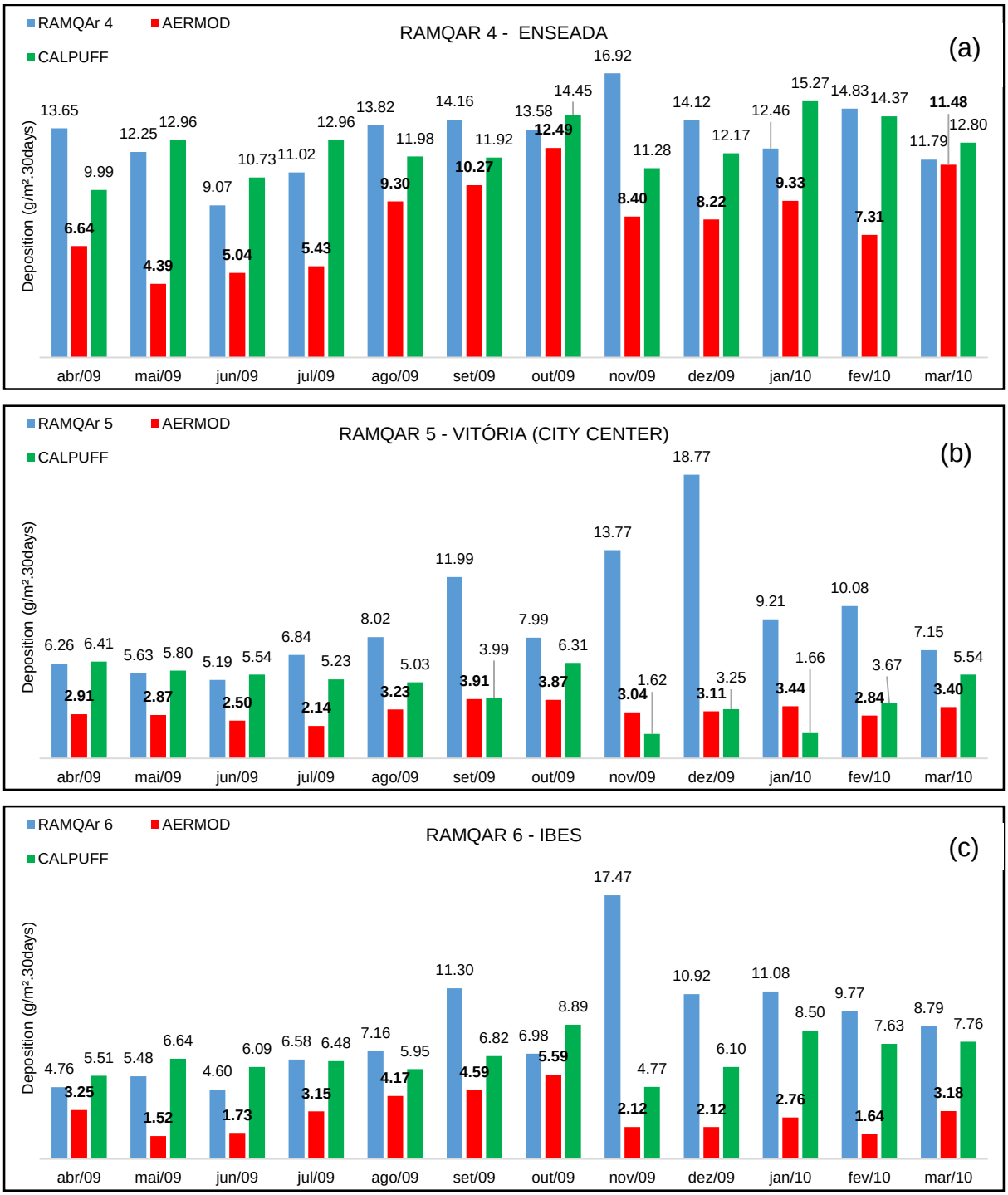

Source: Monticelli (2018).

Figure 15. Temporal evaluation of modelled versus observed deposition fluxes for RAMQAR in GVR (continue).

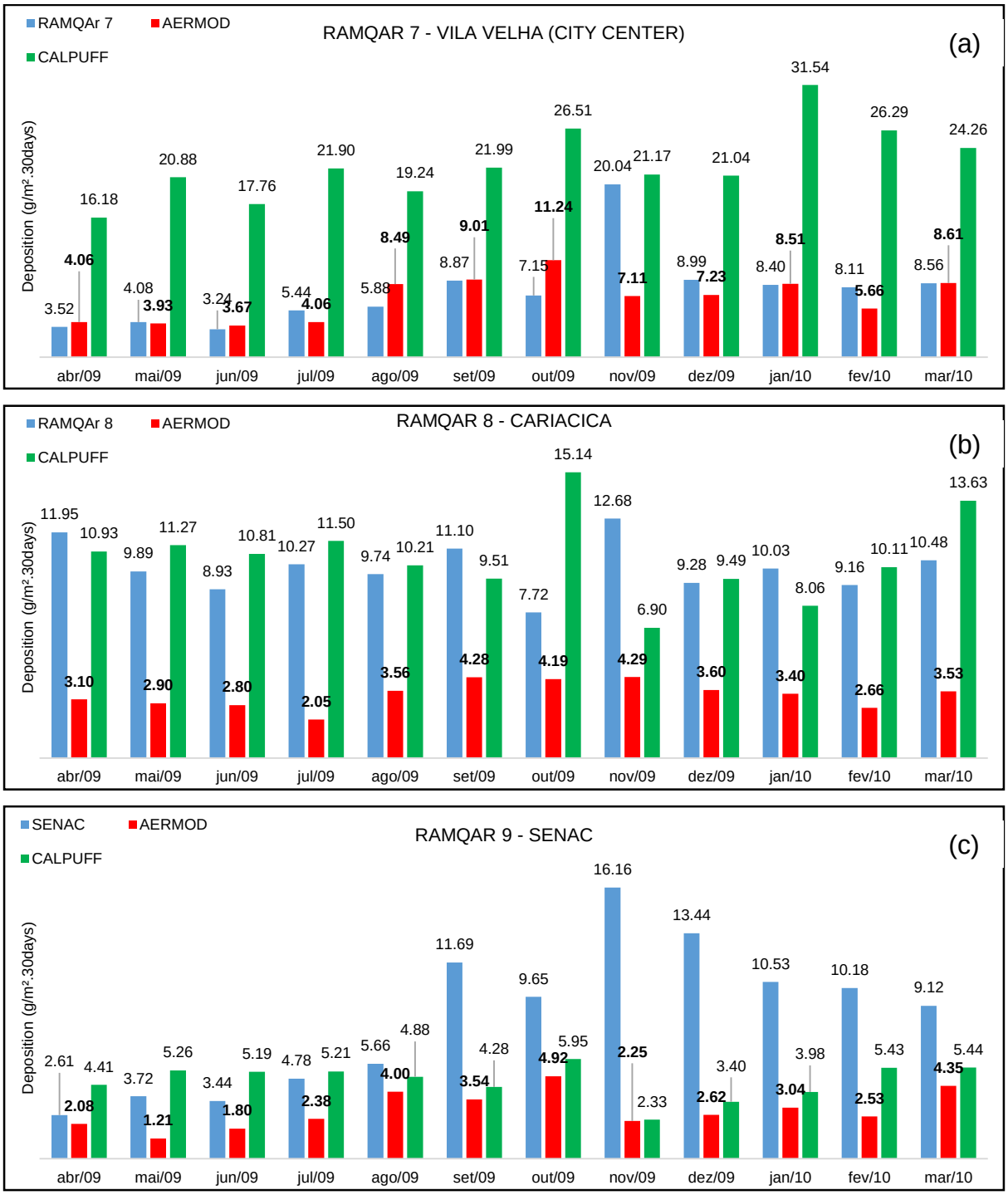

Source: Monticelli (2018).

Figure 15. Temporal evaluation of modelled versus observed deposition fluxes for RAMQAR in GVR (continue).

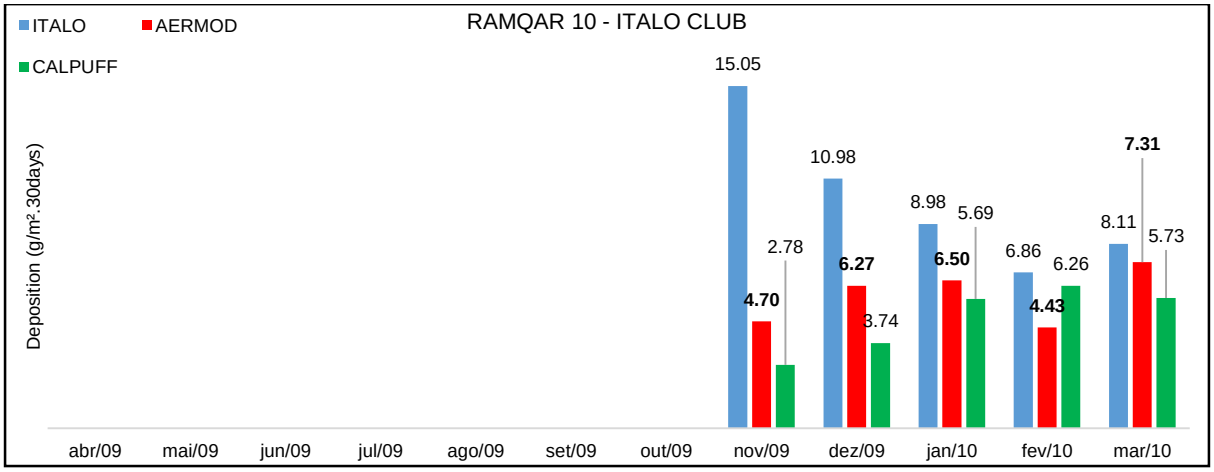

Source: Monticelli (2018).

Spatially, one get the perception that AERMOD mainly underestimates the deposition flux for numerous discrete receptors having the best results for RAMQAR 4 and 7 – Enseada and Vila Velha, respectively. From a temporal perspective, it appears that the months of September of 2009 to March of 2010 presented the highest predicted values (for most monitoring stations). Given that north and northeast winds predominates in this period (spring/summer) it is possible that the transport of particles from the emission carried them towards the RAMQAR.

For CALPUFF, more than one reference station had the deposition flux of particles overestimated; being RAMQAR 7 and 2 those with the highest absolute differences between modelled and observed data. In addition, the closer the stations are, more similar becomes the evolution of estimations over time. Temporally, it is hard to elect a period that appeared as the one with the highest predictions. For stations RAMQAr 1, 5, and 10, CALPUFF mainly underestimate dustfall deposition. Furthermore, for some stations (eg. RAMQAR 4 and 8) it is quite notable the better performance of the Lagrangian model.

In Figure 16, one can observe the dispersion pattern of the monthly averages of dry deposition fluxes for the study domain. It is notable that CALPUFF tend to provide spatially higher predictions than AERMOD. In these figures, all red zones comprehend locations where there was an exceedance of the state decree legislation regarding SPM.

Figure 16. Monthly averages of dry deposition fluxes modelled by AERMOD (left) and CALPUFF (right) for the study period (continue).

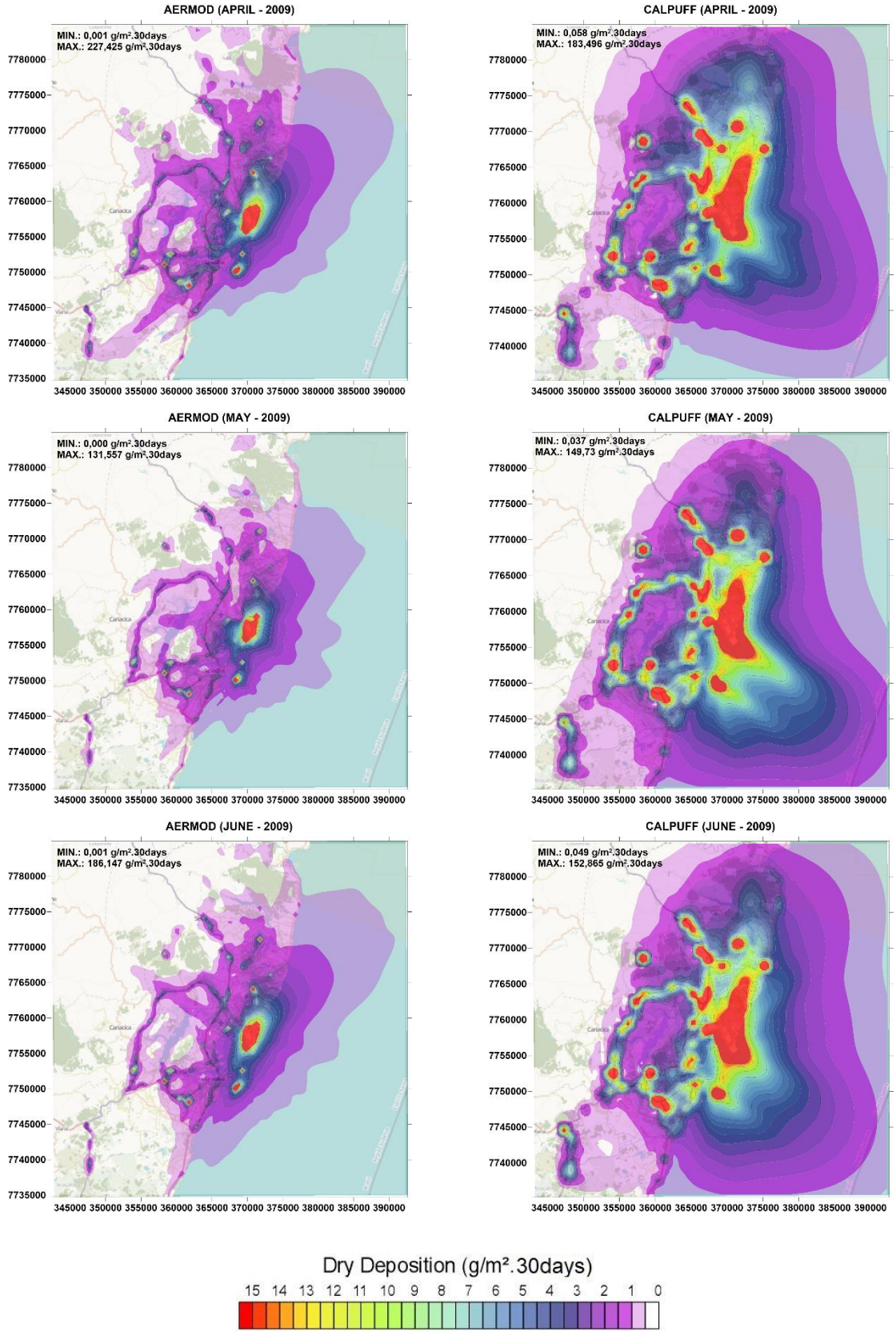

Source: Monticelli (2018).

Figure 16. Monthly averages of dry deposition fluxes modelled by AERMOD (left) and CALPUFF (right) for the study period (continue).

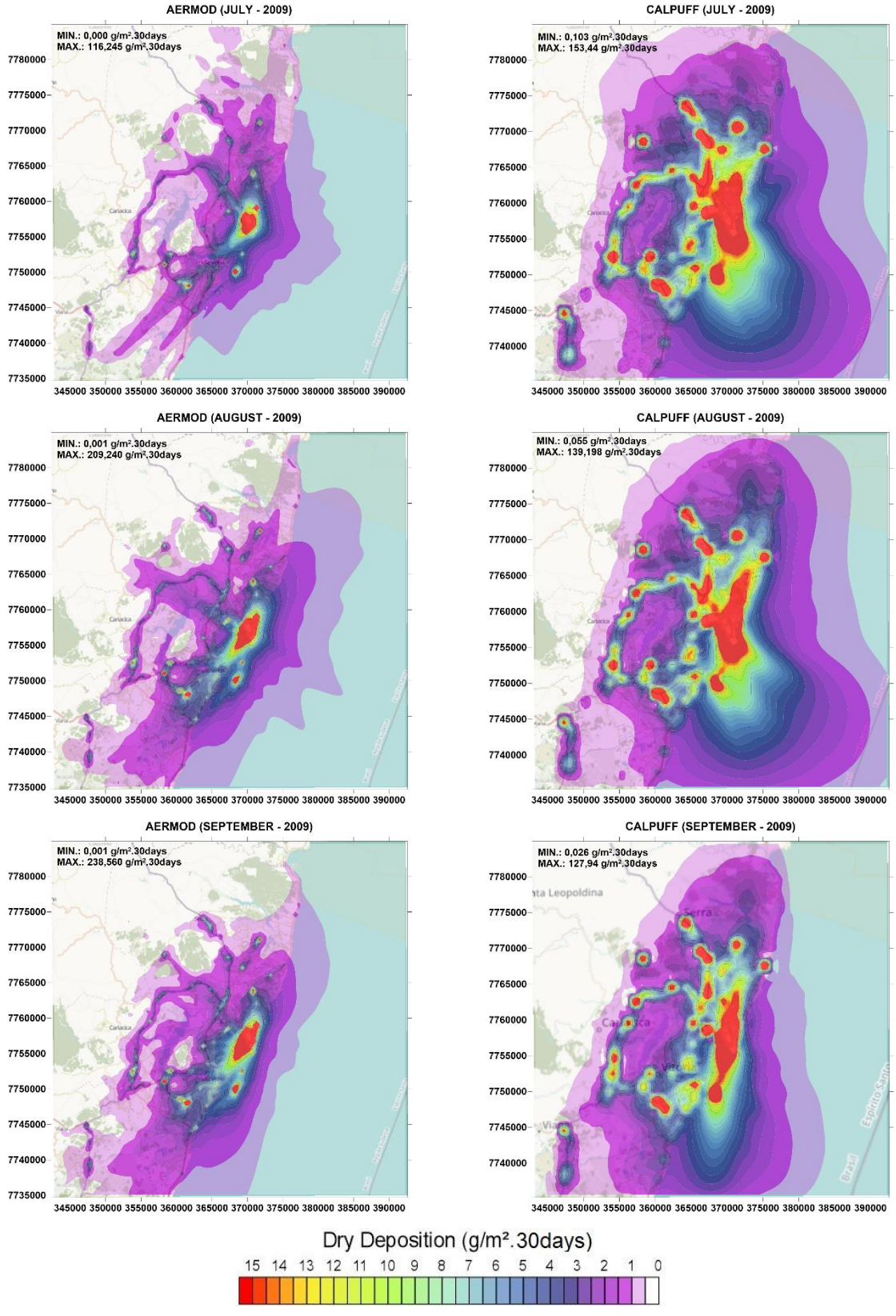

Source: Monticelli (2018).

Figure 16. Monthly averages of dry deposition fluxes modelled by AERMOD (left) and CALPUFF (right) for the study period (continue).

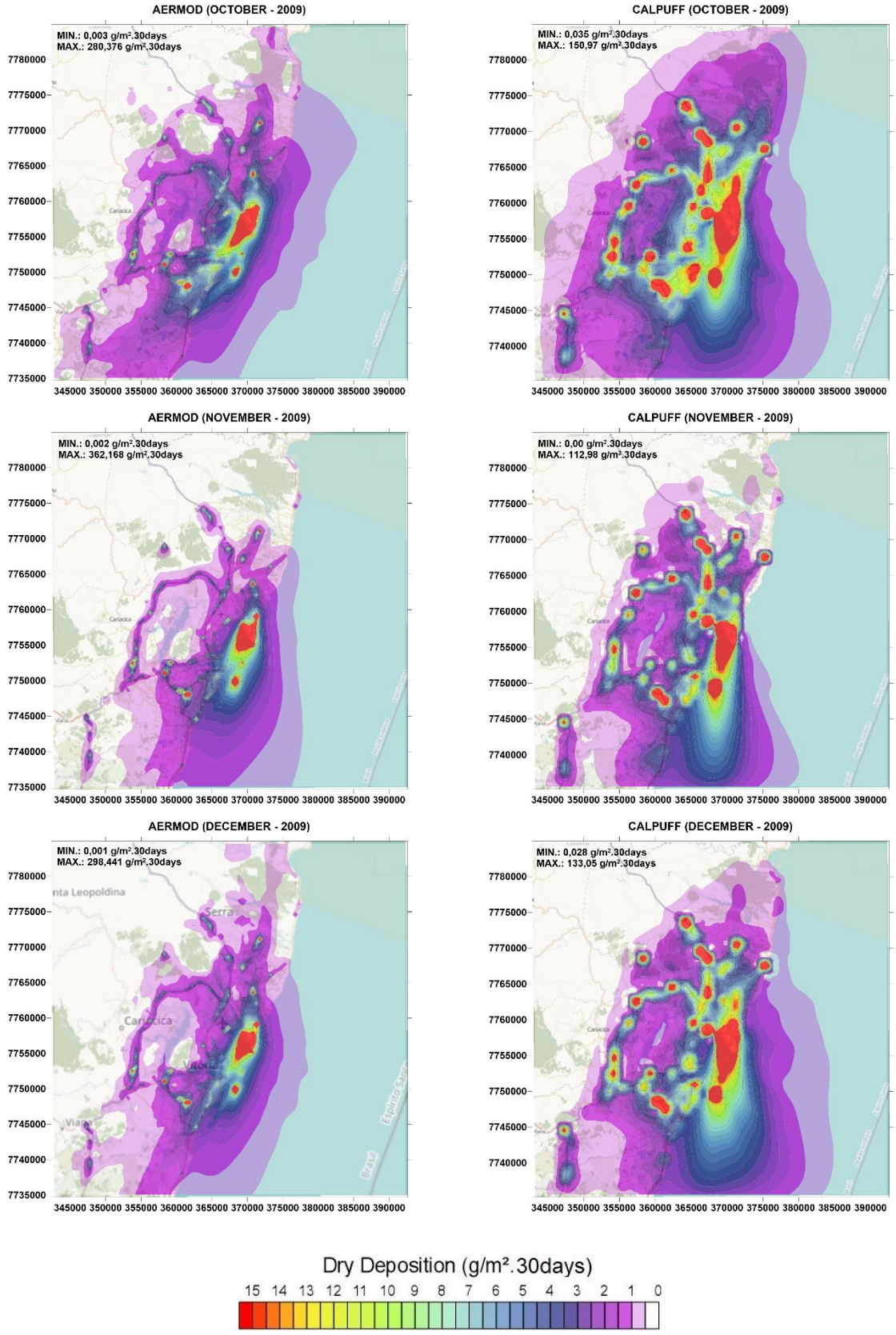

Source: Monticelli (2018).

Figure 16. Monthly averages of dry deposition fluxes modelled by AERMOD (left) and CALPUFF (right) for the study period (final).

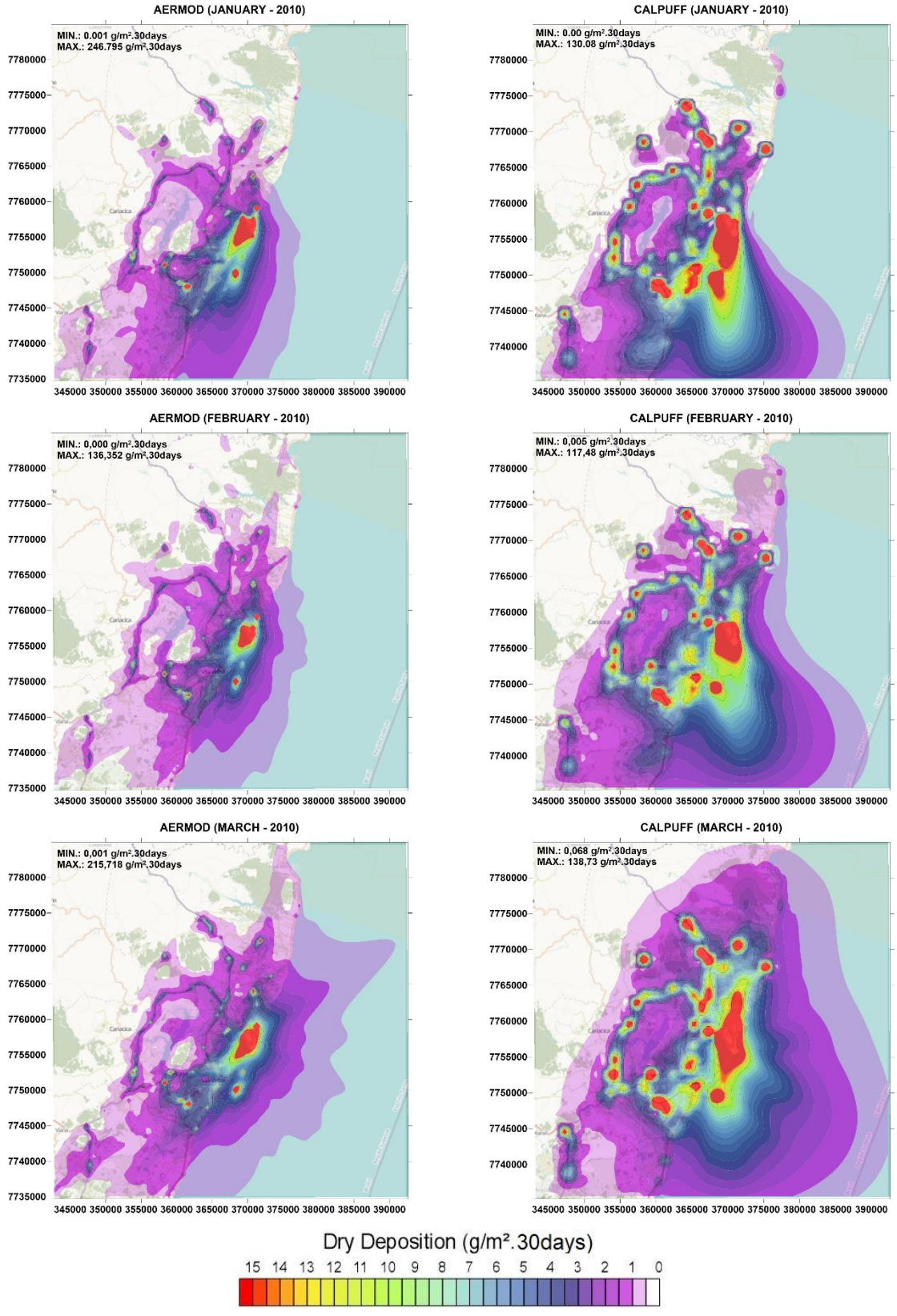

Source: Monticelli (2018).

The statistical parameters used as criteria to define the best-fit model for GVR are those presented in Table 10. In addition, the Weighted Normalized mean square error of the Normalized Ratios (WNNR) and the Fraction Bias analysis using the Robust Highest Concentration (RHC) approach were also employed. Equation 7 presents the WNNR formula and RHC in Equation 8. Because of its stability, RHC favors on top of the average of the 25 highest concentrations, which in this case are the deposition fluxes under evaluation. According to Poli and Cirillo (1993), the WNNR is an alternative to the NMSE, once that the latter is biased toward overestimate.

$$WNNR = \frac{\sum_1^n C_{oi}^2 (1 - e^{-\left|\frac{\ln(C_{pi})}{C_{oi}}\right|})^2}{\overline{C_o}.\sum_1^n e^{-\left|\frac{\ln(C_{pi})}{C_{oi}}\right|}} \quad (Eq.7)$$

$$RHC = x(n) + \left(\bar{x} - x(n)\right)\ln[\frac{3n-1}{2}] \quad (Eq.8)$$

$$FB + RHC = 2[\frac{(RHC_{obs} - RHC_{mea})}{(RHC_{obs} + RHC_{mea})}] \quad (Eq.9)$$

Table 14 summarizes the criteria values obtained for each model. Since there were not many results for comparison, once that particles' deposition measurements takes place every month, it becomes unpractical to apply the statistical parameters of FB and FDS for each monitoring station separately. Thus, all the deposition flux data predicted by AERMOD and CALPUFF compared with observation data will return the best-fit model for the entire domain region rather than a specific location. Afterwards, it is possible to apply the same criteria (with an exception of FB and FDS) for every station.

Table 14. Overall results of the statistical parameters employed

April/2009 to March 2010, GVR	AERMOD	Good fit?	CALPUFF	Good fit?	Best fit?
FB	0.58	✓	-0.22	✓	CALPUFF
FB + RHC	0.43	✓	-0.20	✓	CALPUFF
FDS	0.17	✓	-0.75	✓	AERMOD
WNNR	1.20	X	0.46	✓	CALPUFF
NMSE	1.17	X	0.62	✓	CALPUFF
COC	0.359	X	-0.047	X	AERMOD

Source: Monticelli (2018).

According to USEPA (1992), the Factor Bias (FB) calculation serve as a screening test, which means that it determines whether a competing model achieve the minimum performance standards. Both AERMOD and CALPUFF Factor Bias calculation used the same approach, that is, first with the average of the 25 highest values and then using the RHC factor. For AERMOD, the two cases returned values within the acceptable range (FB = ± 0.67), which indicates that the Eulerian model passed the screening test. However, it also suggests that AERMOD underestimates the deposition flux by a factor of two of FB = 0.58. CALPUFF had an interesting performance as well, with values of FB and FB +RHC within the acceptable range, moreover suggesting that the Lagrangian model overestimates the predictions but only slightly since those two statistics returned a value greater than -0.67. Using only these criteria alone, CALPUFF stands out as the preferred model.

According to Rood (2014), the NMSE indicates the variance of the data analyzed. A NMSE value of one represents that the differences between the observed and predicted records approach in average, and a value of zero indicates perfect match. In this case, AERMOD returned a value of 1.20 corresponding to fair assessment, although it does not approach the average. The Lagrangian model returned a value of NMSE = 0.62 surpassing the Eulerian, thus becoming closer from being suitable. Another statistical parameter employed which CALPUFF had a better result was the WNNR, that gives the same weight to a difference in observed vs. predicted deposition values, being from a under or overestimation (POLI and CIRILO, 1993).

In contrast, the indicator 0.359 COC (AERMOD) against -0.047 COC (CALPUFF) suggests a poor correlation between predictions and observations for the latter, and a weak correlation for AERMOD. On an investigation of the formulas, it became clear that the overestimations of CALPUFF for specific stations 2 and 7 had a major impact in the values revealed at the final comparison.

Next, the author applies the parameters of FB+RHC, COC, NMSE and WNNR to establish a performance of both models for each station separately. Table 15 show results.

Table 15. Results of the statistical parameters employed for each monitoring station

April/2009 to March/2010	*1*	*2*	*3*	*4*	*5*	*6*	*7*	*8*	*SENAC*	*ITALO*
FB+RHC (AERMOD)	1.36	0.66	1.34	1.14	**0.83**	1.00	**-0.12**	1.16	0.74	**0.43**
FB+RHC (CALPUFF)	**0.35**	**-0.64**	**0.42**	**0.15**	1.05	**-0.04**	-1.67	**0.11**	**0.11**	0.85
COC (AERMOD)	-0.63	**0.44**	-0.07	0.33	0.26	-0.09	**0.34**	0.16	0.28	-0.22
COC (CALPUFF)	**-0.72**	0.00	**-0.48**	**0.59**	**-0.61**	**-0.14**	0.22	**-0.51**	**-0.57**	**-0.77**
NMSE (AERMOD)	5.22	**0.84**	1.49	0.29	1.78	1.83	**0.32**	1.39	1.90	0.49
NMSE (CALPUFF)	**0.70**	0.87	**0.20**	**0.04**	**1.14**	**0.32**	1.41	**0.09**	**0.96**	**0.91**
WNNR (AERMOD)	5.22	0.84	1.49	0.29	1.78	1.83	**0.36**	1.39	1.90	0.49
WNNR (CALPUFF)	**0.88**	**0.45**	**0.20**	**0.04**	**1.16**	**0.36**	0.76	**0.07**	**1.13**	**0.91**

Source: Monticelli (2018).

One can see that in agreement with the overall result, CALPUFF had a better prediction behavior for all statistical parameters employed. For RAMQAR 1 to 6, this deduction is almost straightforward. For RAMQAR 7, AERMOD estimations are better, and for SENAC and ITALO, CALPUFF takes the advantage once more.

CALPUFF returned good values for RAMQAR 1 predictions once that the Factor Bias using the RHC is between the intervals of -0.67 to 0.67. The correlation coefficient points out to be strong and the NMSE and its alternative WNNR are closer to one, which indicates that the data averages approach each other.

RAMQAR 2 also favored CALPUFF despite the poor correlation of predictions against observed deposition fluxes. In that sense AERMOD did had a weak correlation as well and the other statistical analysis employed are not as suitable as for the Lagrangian model. The Fraction Bias employing the RHC was still on the acceptable range.

In RAMQAR 3 the NMSE (and WNNR) of CALPUFF results are closer to zero which indicates that predicted and observed data are more similar than for AERMOD (NMSE = WNNR = 1.49). The correlation coefficient supports that, being not high, but fair.

RAMQAR 4 presents the same pattern as the previous station, however with better agreement of deposition fluxes modelled and observed for both models. CALPUFF had its best performance for Enseada among all discrete receptors.

CALPUFF modelled better RAMQAR 5 as well showing a fair COC with NMSE and WNNR pointing out that the averages of predicted and observed deposition approach each other. The FB using RHC indicates that the model tend to under-predictions.

For RAMQAR 6, in all criteria CALPUFF had a superior performance with great numbers for the Fraction Bias (with RHC approach).

AERMOD modelled better RAMQAR 7 (Vila Velha), mainly do it to the overestimations of deposition fluxes from CALPUFF. This becomes notable when analyzing the FB+RHC criteria, which returned a strong negative value for the Lagrangian model. In addition, the values for NMSE and WNNR by AERMOD indicate that the averages of observed and predicted data are near.

RAMQAR 8 had similar construction of results analysis to RAMQAR 4, being the second better performance for CALPUFF among all stations. The COC was fair and the NMSE and WNNR almost 0 (perfect match)

In SENAC (RAMQAR 9), CALPUFF had well fit results. The FB + RHC criterion is it in a high-quality range and the NMSE and WNNR pointing out that the averages of predicted and modelled data approach each other.

Finally, CALPUFF modelled better ITALO (RAMQAR 10) station also with a strong correlation coefficient, NMSE and WNNR indicating agreement of the averages of the predicted and observed data. It only loses to AERMOD in the screening test that favors the Eulerean model.

The Modelled vs. Observed plots are useful to comprehend how close the model was to, properly, predict he experimental results. In Figure one can follow the 1:1 line and get the conclusion that AERMOD in fact had a few predictions close to the real values being the closest 8.61 (AERMOD) compared to 8.56 (Observation) that happened for RAMQAR 7 during March of 2010. Apart from that, the model showed tendencies to underestimate the deposition of particles as confirmed by the statistics.

CALPUFF results shown in Figure 17 points out that between fluxes of 5 and 15 g/m².30days the Lagrangian model had better results, with closer estimations from the1:1 line. Further than that it overestimates, with the highest being 31.54 (CALPUFF) compared to 8.40 (Observation) during January of 2010, in RAMQAR 7. The closest estimation occurred for RAMQAR 6 during July of 2009, in which the prediction given was 6.48 g/m².30days compared to 6.58 g/m².30days observed.

Figure 17. AERMOD and CALPUFF modelled versus observed deposition fluxes.

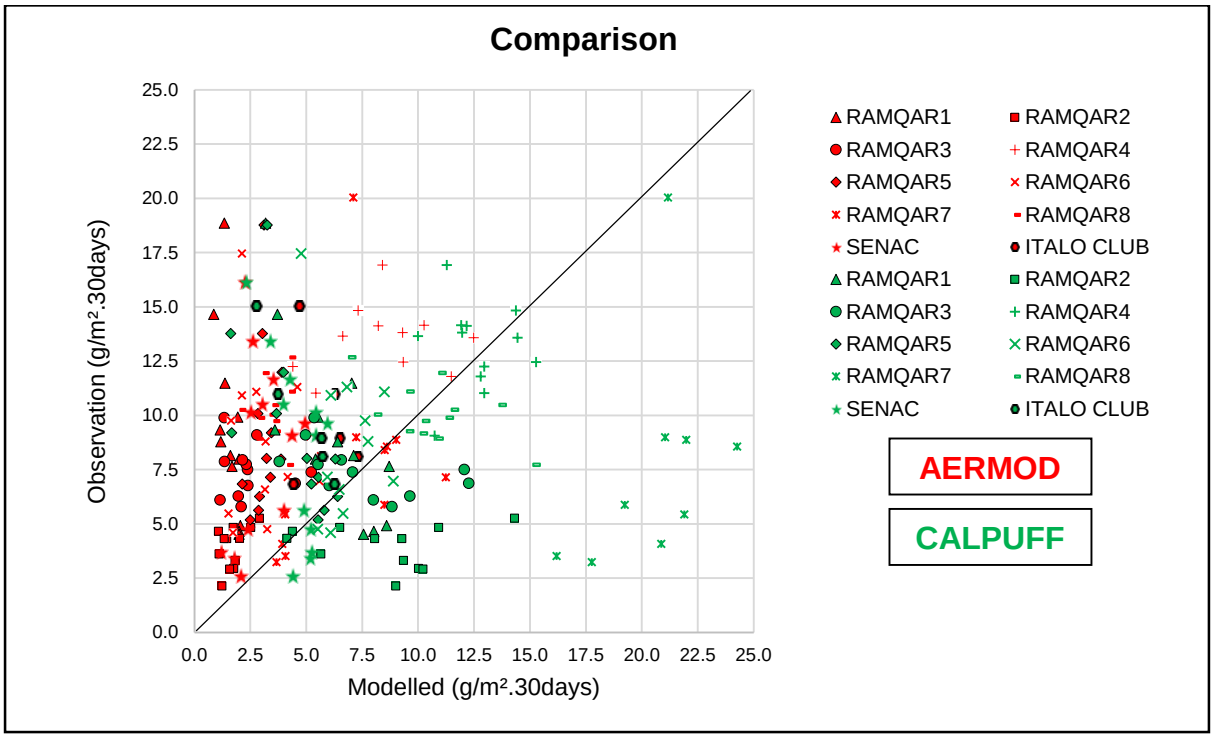

Source: Monticelli (2018).

Figure 18 and 19, below, presents observed versus modelled data plots for each individual station in order to acquire a more elaborated view of the results. From the analysis of those charts, one can conclude that:

a) For RAMQAR 1 to 3, AERMOD underestimated the results while CALPUFF had a mixed performance. In adequacy to the 1:1 line, AERMOD performed better for RAMQAR 2 and CALPUFF to RAMQAR 1. In contrast, RAMQAR 1 had the worst results for AERMOD and RAMQAR 2 for CALPUFF;

b) For RAMQAR 4 to 6, AERMOD underestimated the results while CALPUFF had a mixed performance as well. In adequacy to the 1:1 line, AERMOD and CALPUFF performed better for RAMQAR 4. In contrast, RAMQAR 5 had the worst results for AERMOD and CALPUFF;

c) While AERMOD showed good results for RAMQAR 7, the same does not occur for RAMQAR 8, SENAC and ITALO CLUB. CALPUFF overestimates for the first and move to underestimations towards the latter, being RAMQAR 8 its best performance among this set.

Figure 18. AERMOD and CALPUFF modelled versus observed deposition fluxes for RAMQAR 1 to 6.

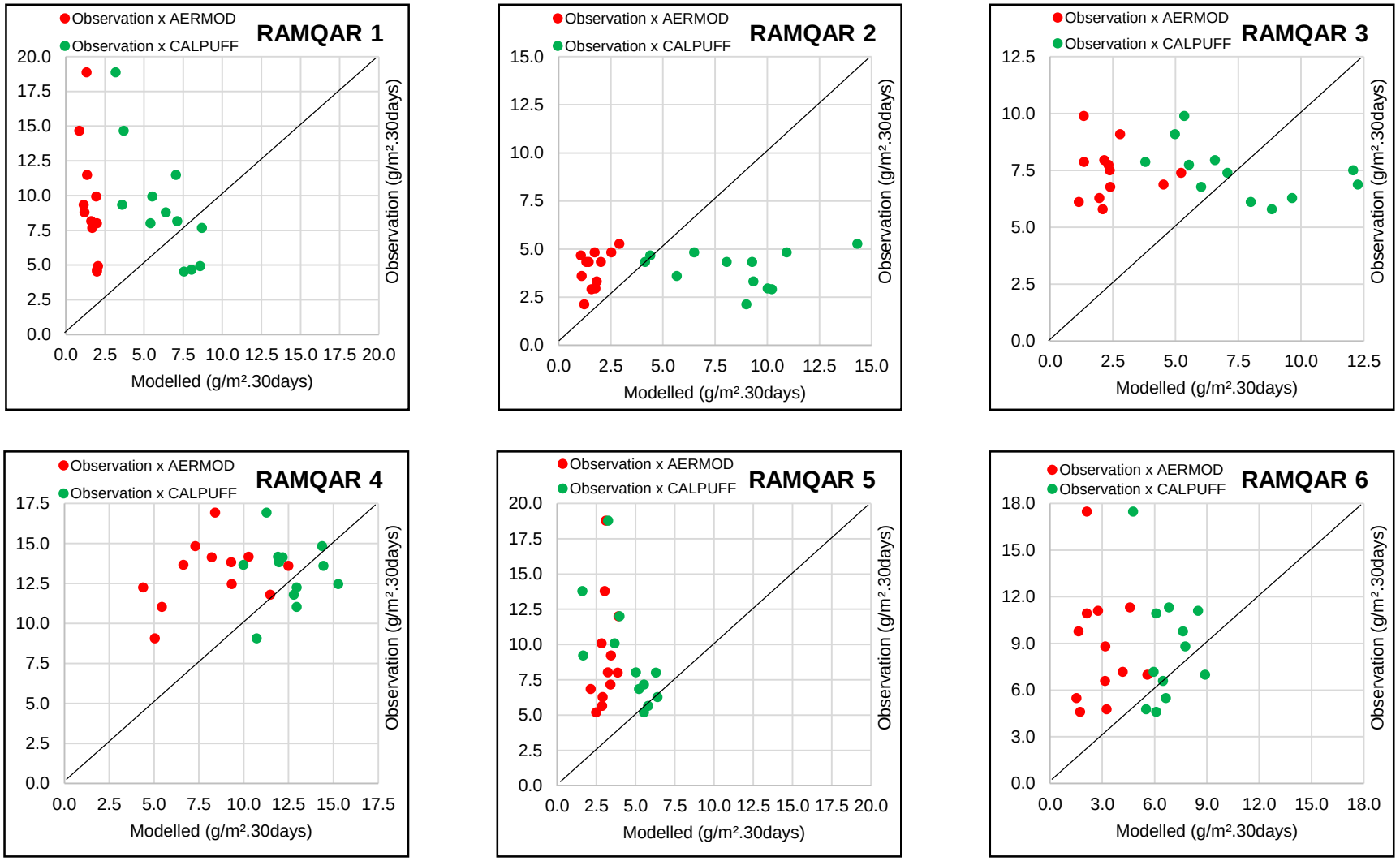

Source: Monticelli (2018).

Figure 19. AERMOD and CALPUFF modelled versus observed deposition fluxes for RAMQAR 7 to 10.

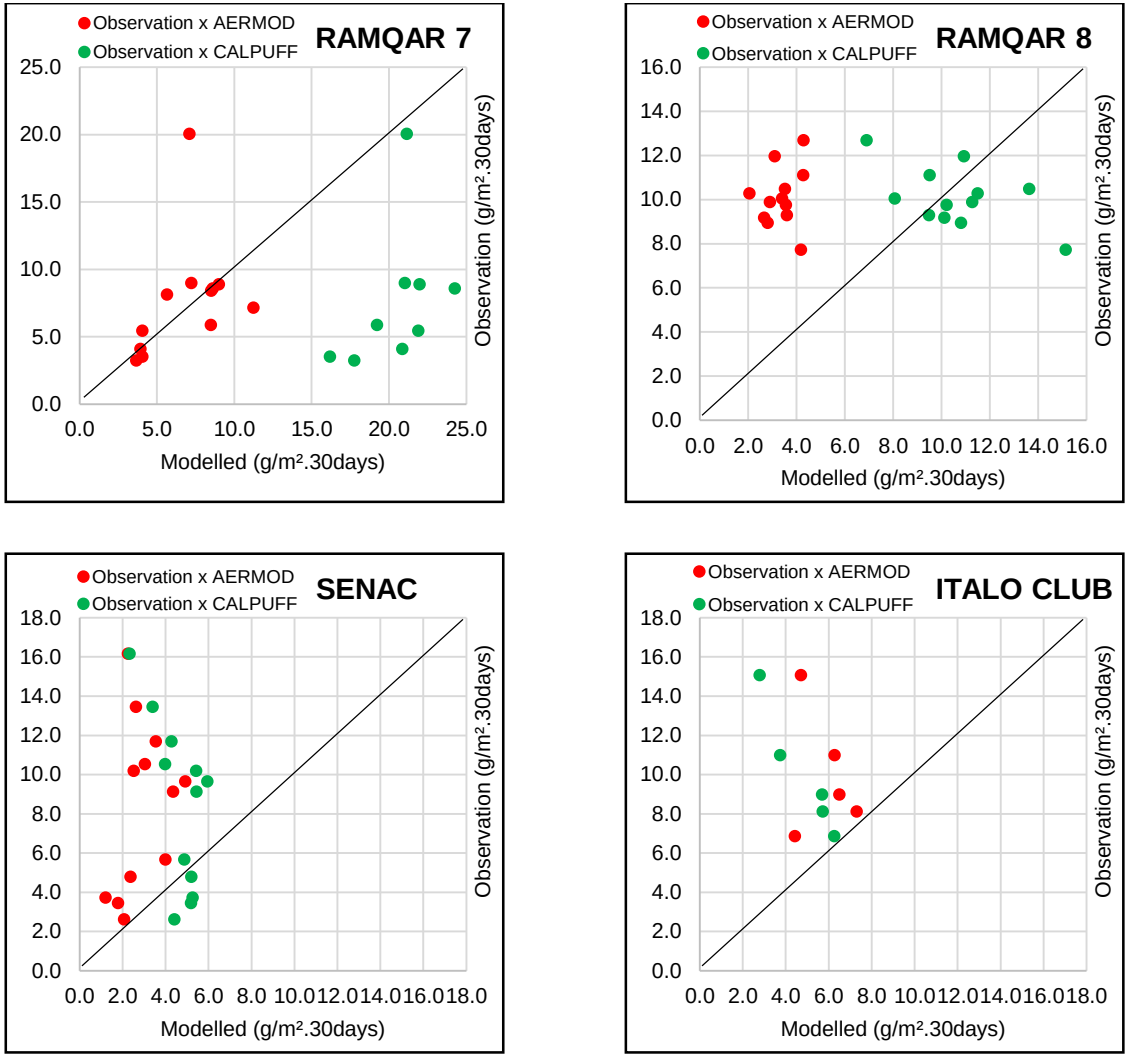

Source: Monticelli (2018).

Next, the data pass through a validation using the Box-Whisker Plot. When analyzing a Box-Whisker Plot it is first necessary to verify the median line at the center of the boxes. For AERMOD, when compared to both the RAMQAR observations and CALPUFF predictions, one conclude that it predicted lower values than those observed or modelled by its competitor. Furthermore, since the same line does not quite cut the box in half, one can infer that data predicted by AERMOD is negatively asymmetric, that is, does not follow a normal distribution. This asymmetry follows CALPUFF results as well. In addition, the number of outliers is significant. Finally, the size of the box indicates the range or variation of data used to construct it. In this matter, CALPUFF had a higher variation than AERMOD.

Figure 20. Box-Whisker Plot of data from AERMOD and CALPUFF.

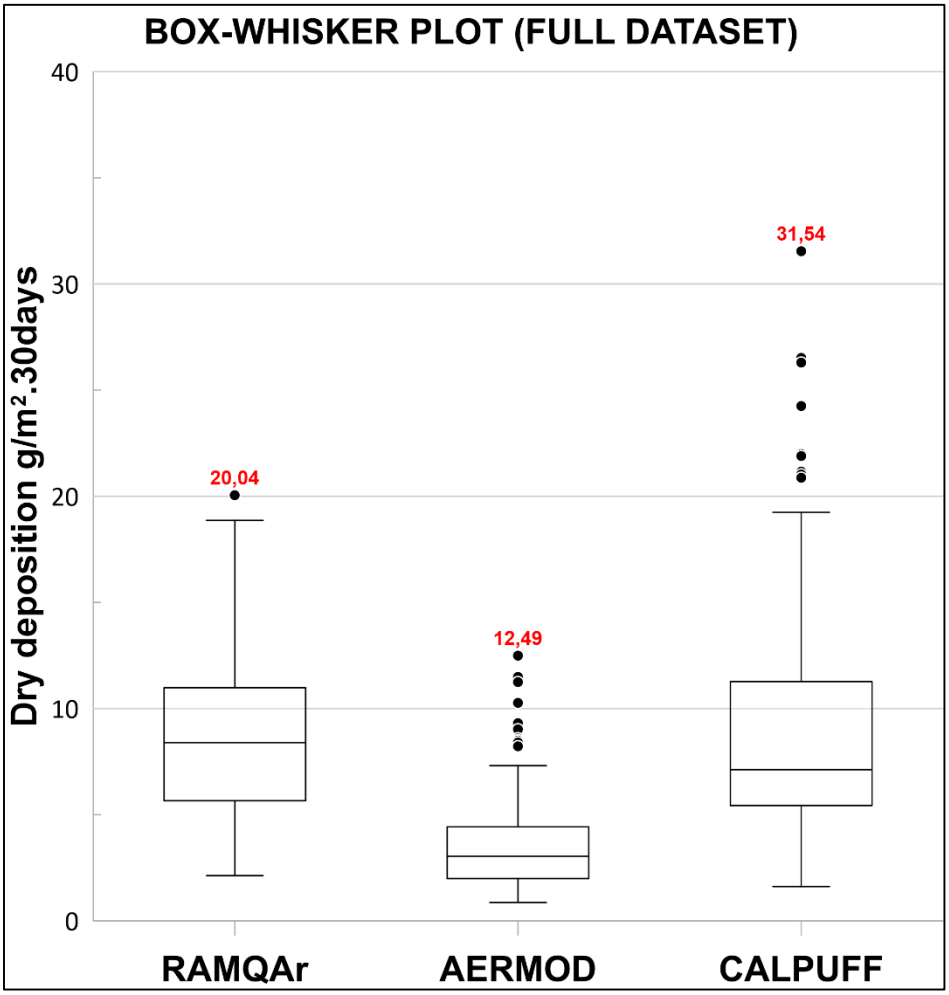

Source: Monticelli (2018).

Following the full dataset chart, are also presented for each RAMQAR station (Figure and 22).

Figure 21. Box-Whisker Plot of data from AERMOD and CALPUFF, for RAMQAR 1 to 6 (a-f).

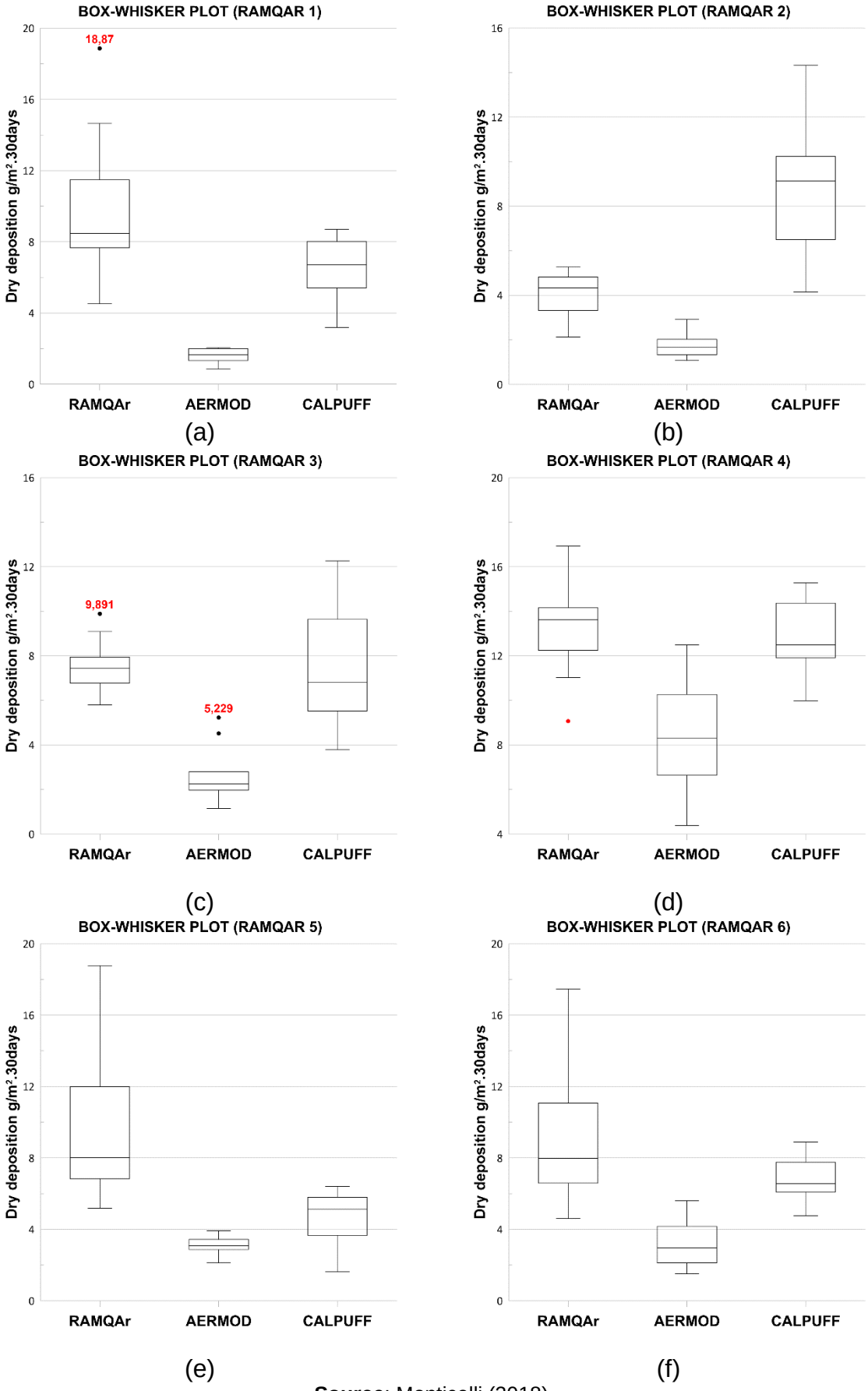

Source: Monticelli (2018).

Figure 22. Box-Whisker Plot of data from AERMOD and CALPUFF, for RAMQAR 7 to 10 (a-d).

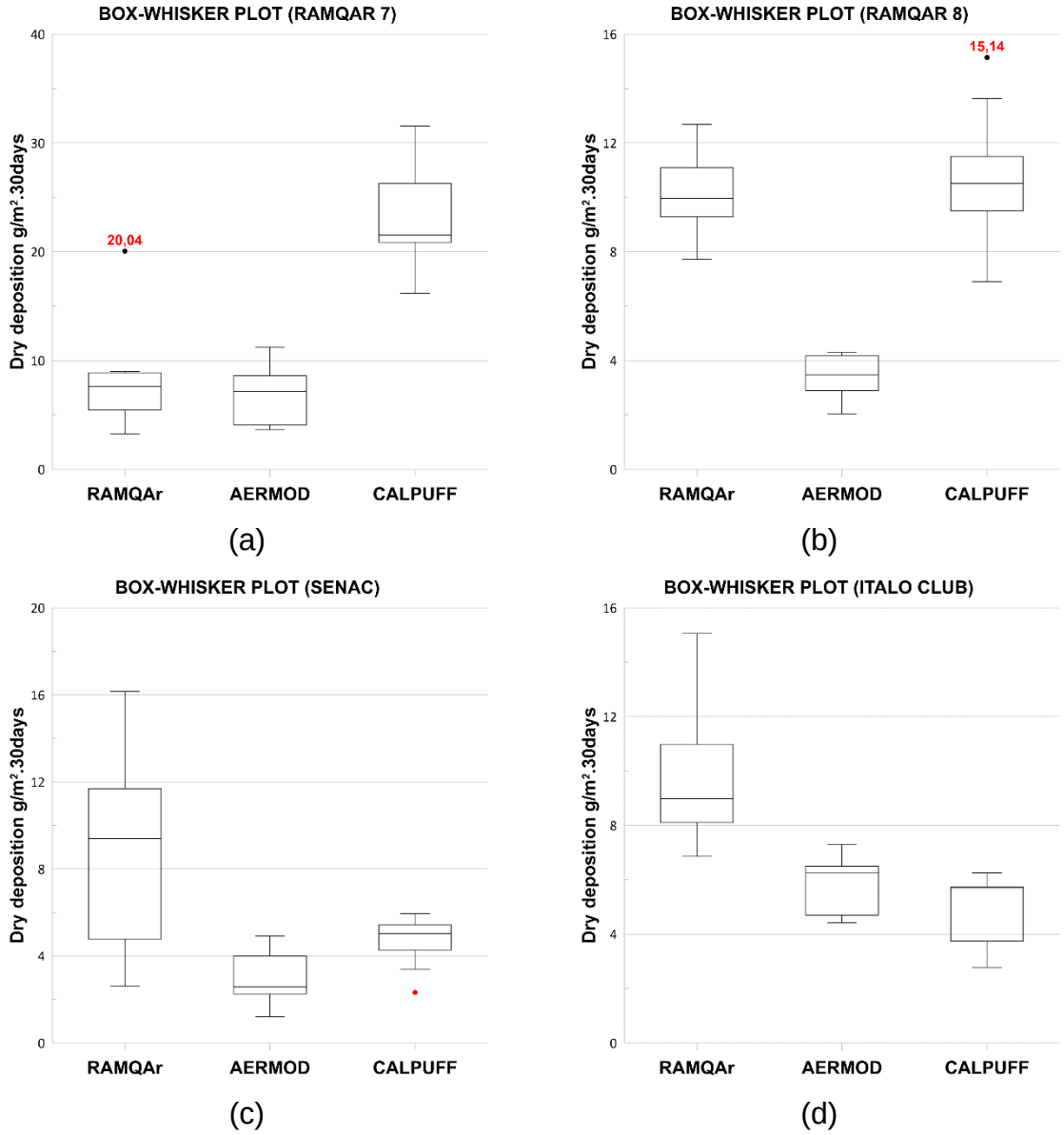

Source: Monticelli (2018).

Adding all the comparisons established during Sections 6.1, one can conclude that overall CALPUFF is the best-fit Gaussian Dispersion Model for modelling dry deposition flux in GVR, under the conditions here presented. Therefore, only the elected model, according with the Methodology given in Section 5, will approach the next section.

6.2 Ungrouping using the dispersion model

As presented in Section 3.4, a source apportionment study conducted via receptor modelling faces some complications regarding model assumptions. In that sense, a major problem is collinearity, a term used to describe the similarity between chemical profiles of sources emission. The CMB Protocol states that:

> *"Source profiles are intended to represent a category of source rather than individual emitters. The number and meaning of these categories is limited by the degree of similarity between the profiles. Mathematically, this similarity is termed "collinearity," which means that two or more of the CMB equations are redundant and the set of equations cannot be solved. (…) When two or more source profiles are "collinear" in a CMB solution, standard errors on source contributions are often very high." (Protocol for Applying and Validating the CMB Model for PM2.5 and VOC, pp 3-1).*

Some authors that faced this problem here mentioned are, Shi et *al.* (2011), Habre, Coull and Koutrakis (2011), Tian et *al.* (2013), Shi et *al.* (2014) and more recently Santos et *al.* (2017).

In the present work, the results from the CMB source apportionment of Santos et *al.* (2017) will be used as a study case for the application of CALPUFF model to overcome the collinearity problem.

Firstly, the sources investigated by Santos et *al.* (2017) are ungrouped. Afterwards, the equations used to integrate the CALPUFF results with those from CMB 8.2 are presented and finally, the validation of CALPUFF model and the new source apportionment results are derived from the proposed methodology.

In Santos *et al.* (2017) the authors grouped sources according to the Table 16.

Table 16. Sources modelled in Santos et al. (2017)

Sources in Santos *et al.* (2017)	**Grouping**
Quarries	Quarries
Civil Construction	Civil Construction
Ressuspension	Ressuspension
Soil	Soil
Sea Breeze	Sea Breeze
Vehicles	Vehicles
Coal	Coal + Coke + Coke Ovens
Siderurgy	Group A: Ore + Pellets + Ovens (Vale)
	Group B: Blast Furnaces + Steelworks + Sintering
	Grupo C: LTQ Ovens + Thermoelectrics
Others	Others
Cement industry	Cement

Source: Monticelli (2018).

In order to assist their source apportionment results, the components (emitters) in Group A, B, C from “Siderurgy” and those grouped as “Coal” had their specific contributions to SPM loadings in GVR estimated by CALPUFF, proved as the preferred model in Section 6.1. The author accomplishes that by removing those sources from CALPUFF runs to see their specific contributions for each receptor at a given month. In Appendix E it is shown the sources considered as belonging to each group in CALPUFF runs.

Equations 10 to 13, developed by the author, describe CALPUFF assessment of source apportionment results.

In Eq. 10 one must use CALPUFF to discover the specific mass contribution (in g/m^2.30days) of an individual source or representative group of sources by subtracting the amount of mass deposited when all sources but the group of interest is modelled from the total amount of mass of deposited particles with all sources modeled.

$$D_{i,j,k} = D_{\forall i,j,k} - D_{\forall i \neg i,j,k} \quad (Eq.10)$$

where, $D_{i,j,k}$ = Contribution to dry deposition (g/m².30days) of source " i" on month "j" in receptor "k", modelled by Dispersion Model; $D_{\forall i,j,k}$ = Contribution to dry deposition (g/m².30days) of all sources " i" on month "j" in receptor "k", modelled by Dispersion Model; $D_{\forall i \neg i,j,k}$ = Contribution to dry deposition (g/m².30days) of all sources minus source " i" on month "j" in receptor "k", modelled by Dispersion Model.

Next, In Eq. 11 one must use CALPUFF results from Eq. 10 to find the total mass contribution for dry deposition of grouped sources from CMB modelling, accordingly with the dispersion model. For instance, the mass contribution of group "Coal" will be the sum of mass contributions of SPM prevenient from all sources that compose such a group.

$$Group\ A \rightarrow T_{j,k}(A) = \sum_{i}^{\forall i \in (A)} D_{i,j,k} \quad (Eq.11)$$

where, $T_{j,k}(A)$ = Total dry deposition (g/m².30days) in Group A (grouped by CMB source apportionment), on month "j" in receptor "k"; $\sum_{i}^{\forall i \in (A)} D_{i,j,k}$ = sum of all individual contributions to dry deposition (g/m².30days) for sources " i" in Group A.

Following this, In Eq.12 one must use CALPUFF results from Eq. 11 to find the total contribution (%) for dry deposition of grouped sources from CMB modelling, accordingly with the dispersion model. The author accomplishes this by dividing a specific mass contribution of an emitter from the total mass of SPM contribution of the group.

$$C_{i,j,k}(A) = \frac{D_{i,j,k}}{T_{j,k}(A)} \quad (Eq.12)$$

where, $T_{j,k}(A)$ = Total dry deposition (g/m².30days) in Group A (grouped by CMB source apportionment), on month "j" in receptor "k"; $C_{i,j,k}(A)$ = Specific dry deposition contribution (%) attributed by Dispersion Model for source " i" onto $T_{j,k}(A)$.

Finally, in Eq. 13 one must use the results from Eq. 12 to find the specific contribution (%) for dry deposition of specific sources amid those grouped by CMB, integrating both models results. The author accomplishes that by a multiplication of contributions.

$$P'_{i,j,k} = \frac{P_{j,k}(A)}{M_{j,k}}.\ C_{i,j,k}(A)\ \ (Eq.13)$$

Where, $P_{j,k}(A)$ = Specific dry deposition contribution (%) attributed by Chemical Mass Balance model to Group A, on month "j" in receptor "k"; $M_{j,k}$ = Total mass explained (%) for Chemical Mass Balance run, on month "j" in receptor "k" and $P'_{i,j,k}$ = New specific dry deposition contribution (%) of source "i" in Group A, on month "j" in receptor "k".

For instance, if "Coal" that is equal to "Coal + Coke + Coke Ovens" emissions, was one of the CMB grouped sources contributors to dry deposition at a given station in a given month. In addition, CALPUFF claims that the mass of SPM contribution of Coal sources was 4 g/m².30days and Coke + Coke Ovens was also 4 g/m².30days. Thus, following Equations 10 to 12 (results expressed through Equations 14 to 19) one agrees that:

$$D_{i,j,k} = D_{\forall i,j,k} - D_{\forall i \neg i,j,k}\ \ (Eq.14)$$

$$D_{coal,1,1} = D_{\forall sources,1,1} - D_{\forall sources-coal,1,1} = 4\ \frac{g}{m^2.month} \quad (Eq.15)$$

$$D_{coke\ and\ coke\ ovens,1,1} = D_{\forall sources,1,1} - D_{\forall sources-coke\ and\ coke\ ovens,1,1}$$
$$= 4\ \frac{g}{m^2.month} \quad (Eq.16)$$

$$Group\ Coal\ \rightarrow\ T_{1,1}(Coal) = \sum_{i}^{\forall i \in (Coal)} D_{i,j,k} = D_{coal,1,1} + D_{coke\ and\ coke\ ovens,1,1}$$
$$= 8\ \frac{g}{m^2.month} \quad (Eq.17)$$

$$C_{coal,1,1}(Coal) = \frac{D_{coal,1,1}}{T_{1,1}(Coal)} = \frac{4}{8} = 50\ \% \quad (Eq.18)$$

$$C_{coke\ and\ coke\ ovens,1,1}(Coal) = \frac{D_{coke\ and\ coke\ ovens,1,1}}{T_{1,1}(Coal)} = \frac{4}{8} = 50\ \% \quad (Eq.19)$$

Now, assuming that also in this month and particular station the source apportionment using the receptor model CMB 8.2 returned a contribution of 88% for the “Coal” grouped sources, with 110% of the mass explained in that run. Since CMB 8.2 faces the problem of collinearity, one can use the results expressed in Eq. 18 and 19, obtained via CALPUFF dispersion model estimations, and generate a new source apportionment through Eq. 13, as shown in Eq. 20 to 22:

$$P'_{i,j,k} = \frac{P_{j,k}(A)}{M_{j,k}}.\ C_{i,j,k}(A) \quad (Eq.20)$$

$$P'_{coal,1,1} = \frac{P_{1,1}(Coal)}{M_{1,1}}.\ C_{coal,1,1}(Coal) \quad (Eq.21)$$

$$P'_{coal,1,1} = \frac{0{,}88}{1{,}1}.\ 0{,}50 = \ 0{,}4\ or\ 40\%\ (Eq.22)$$

The same applies for Coke + Coke ovens emissions that are also part of the CMB grouped sources “Coal”.

Figures 23 to 25 illustrate the sources contribution of four big groups of emitters in the GVR, (1) Traffic lanes, (2) Coal, (3) Siderurgy and (4) Others. This classification follows the grouping done by Santos et *al.* (2017) demonstrated in the previous section.

One can see that in the dispersion model, for the majority of the monitoring stations, the traffic lanes play a major role as contributors for dry deposition, while such behavior does not occur in CMB results. The numeric value of volume sources corresponding to these traffic lanes might be the explanation for such interpretation of CALPUFF. Following this, it is also observable that for the stations where Siderurgy had higher contributions in CMB (Enseada and SENAC), CALPUFF softens the contribution for these emitters, adding more weight to “Others” and “Traffic lanes” groups. In Appedix D one can find the specific contribution values given by each model during the study period.

Figure 23. Results for CMB (left) and CALPUFF (right) source apportionment in monitoring stations RAMQAR 1 (a-b), 3 (c-d) and 4 (e-f).

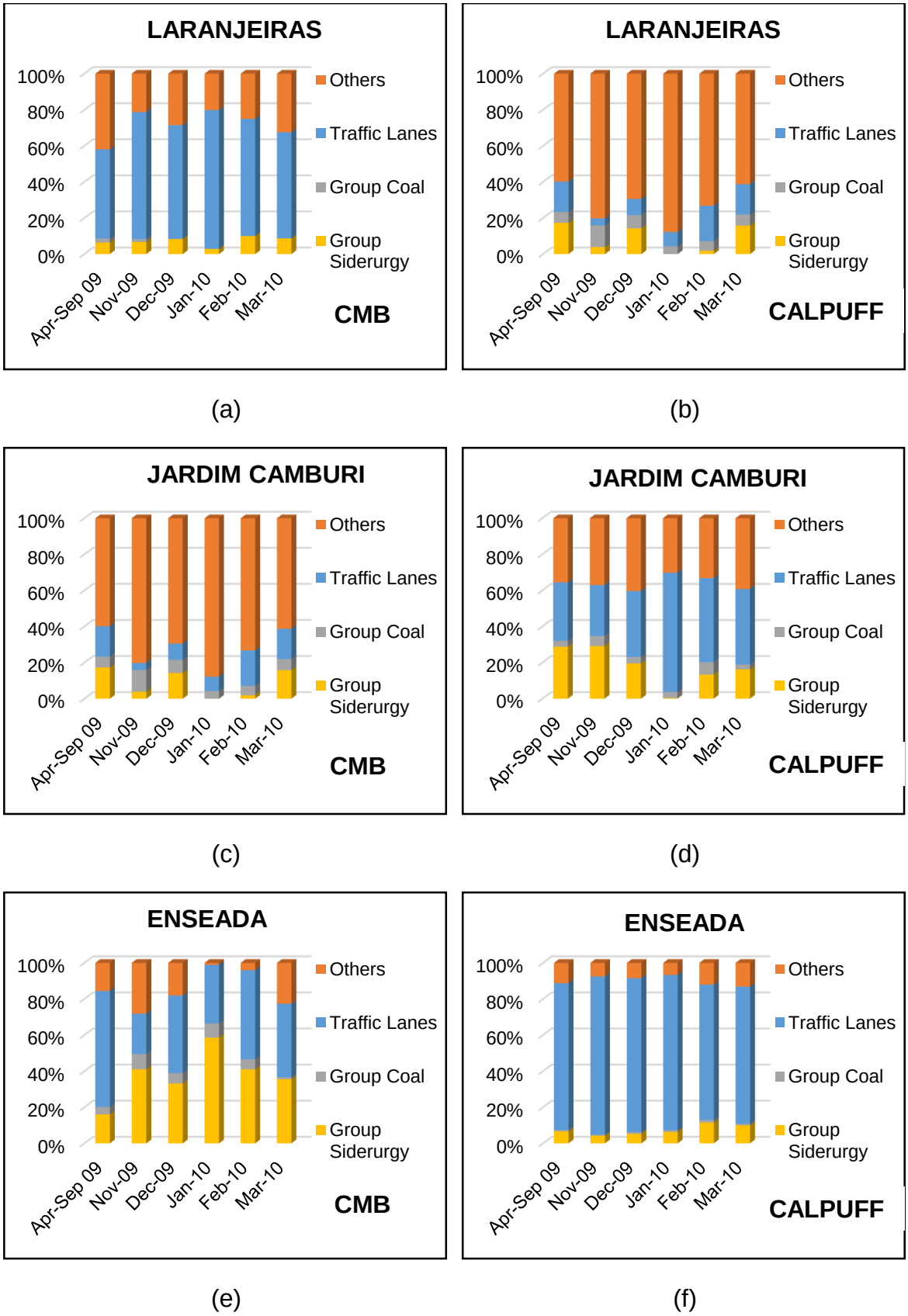

Source: Monticelli (2018).

Figure 24. Results for CMB (left) and CALPUFF (right) source apportionment in monitoring stations RAMQAR 5 (a-b), 6 (c-d) and 7 (e-f).

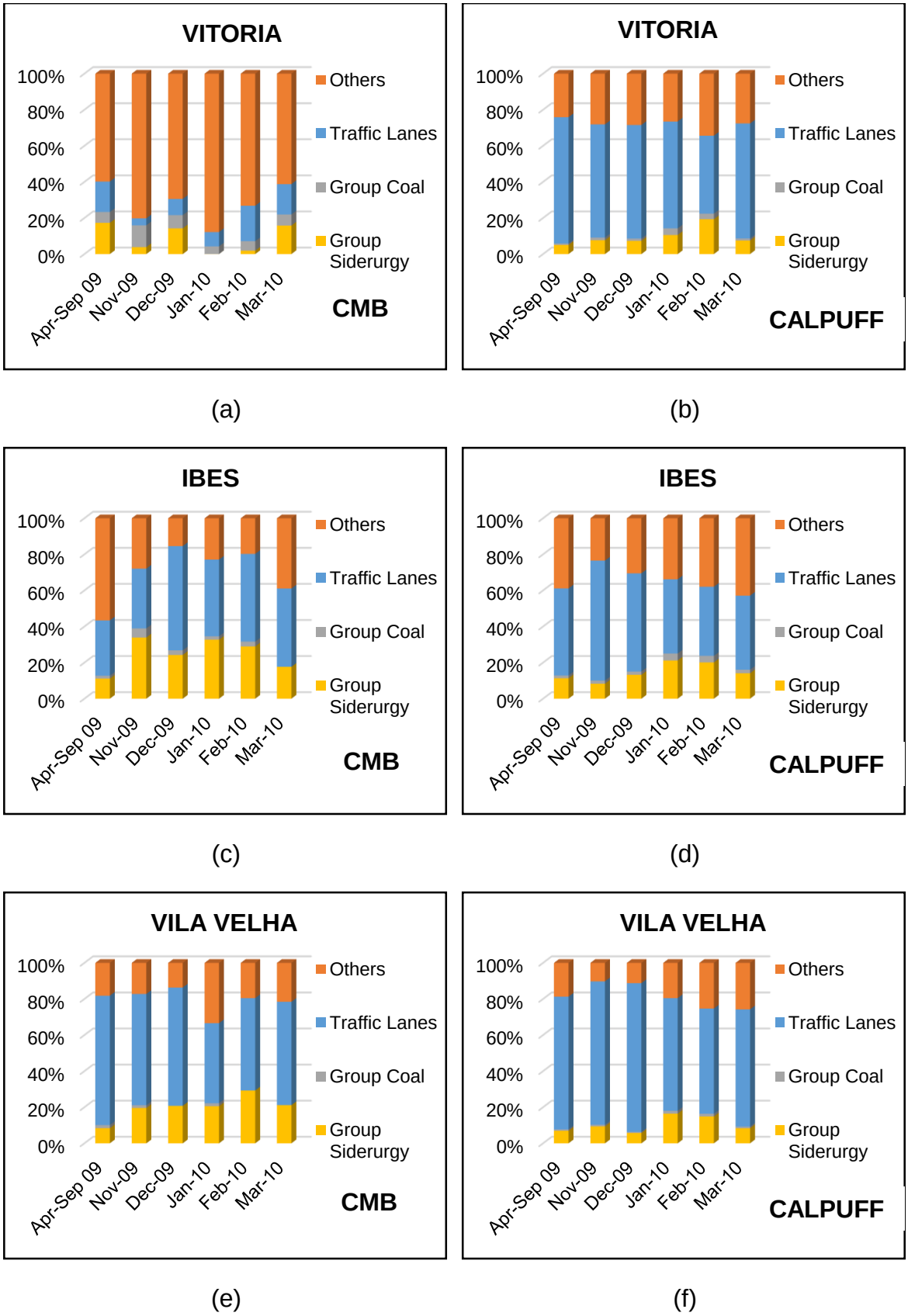

Source: Monticelli (2018).

Figure 25. Results for CMB (left) and CALPUFF (right) source apportionment in monitoring stations RAMQAR 8 (a-b) and 9 (c-d).

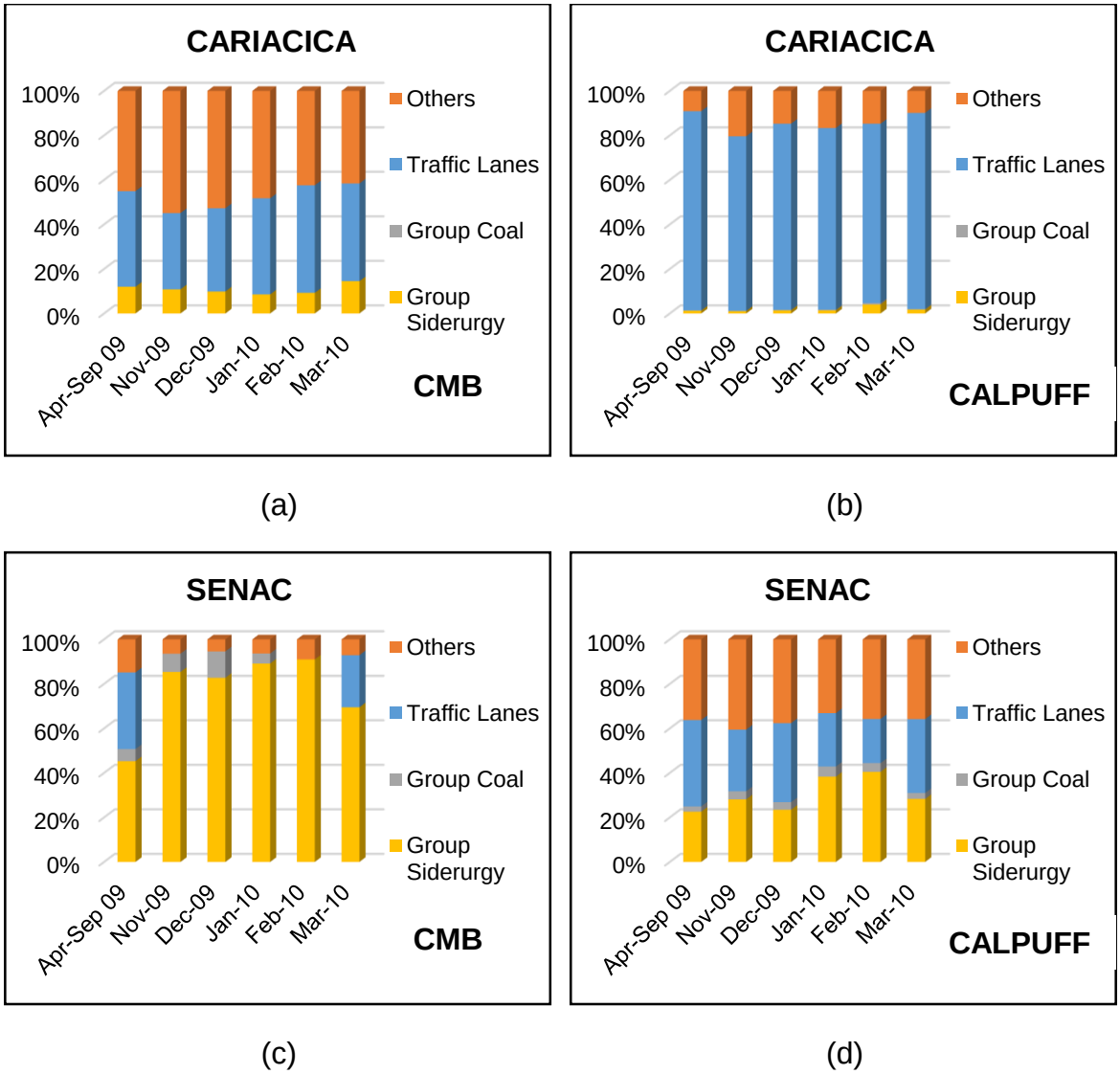

Source: Monticelli (2018).

From the entire collection of emission sources studied (830 total), the author grouped 81 (See Appendix C) to generate new source apportionment results. By ungrouping the sources as shows in Table 16 and applying the Equations 10 to 13 into CMB results show in Figures 26 to 28, it was possible to generate new source apportionments results for the period of April/2009 to March/2010 in GVR as demonstrated by Figures 26 to 28.

Figure 26. Results for CMB (left) and CMB +CALPUFF (right) source apportionment in monitoring stations RAMQAR 1 (a-b), 3 (c-d) and 4 (e-f).

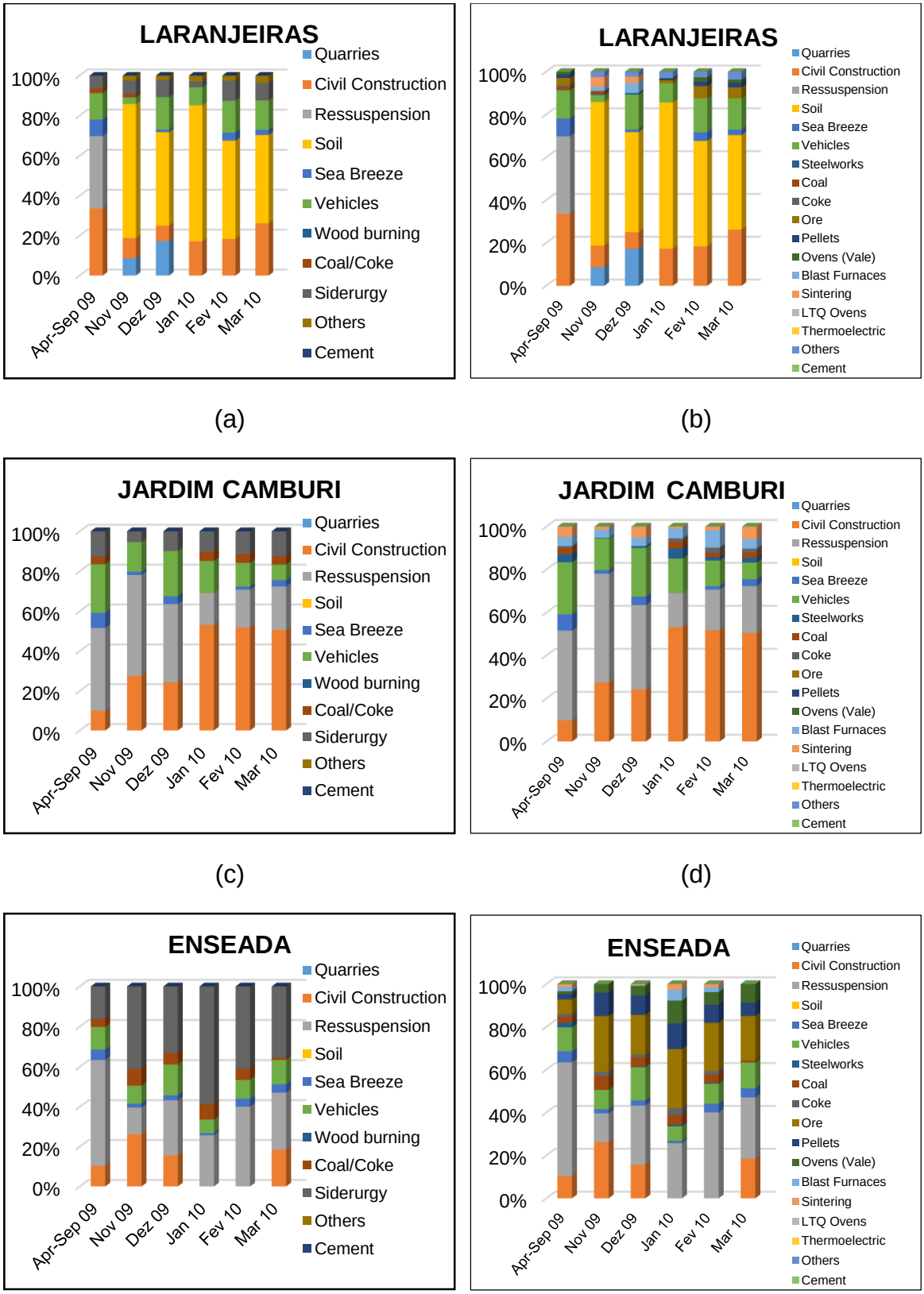

Source: Monticelli (2018).

Figure 27. Results for CMB (left) and CMB +CALPUFF (right) source apportionment in monitoring stations RAMQAR 5 (a-b), 6 (c-d) and 7 (e-f).

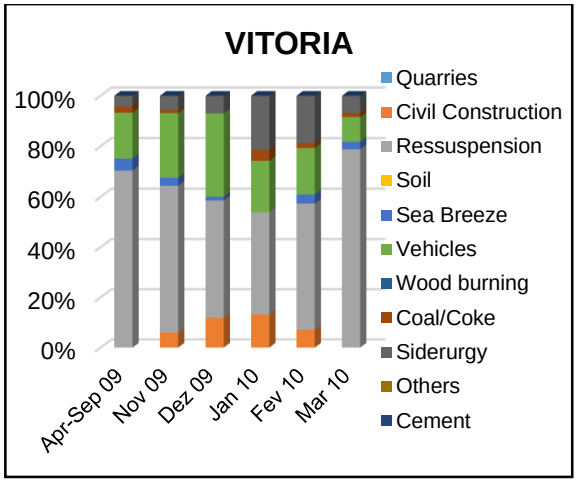

(a)

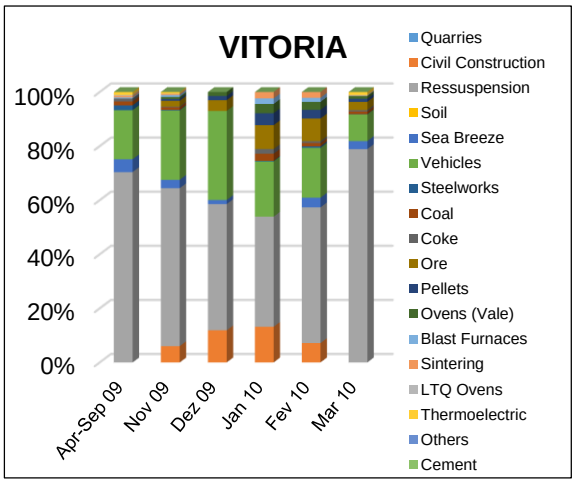

(b)

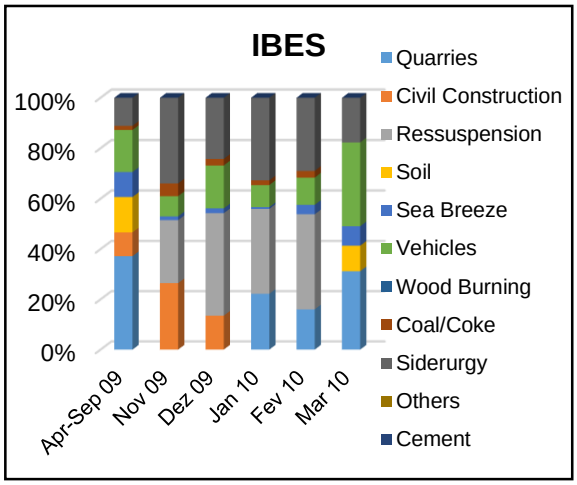

(c)

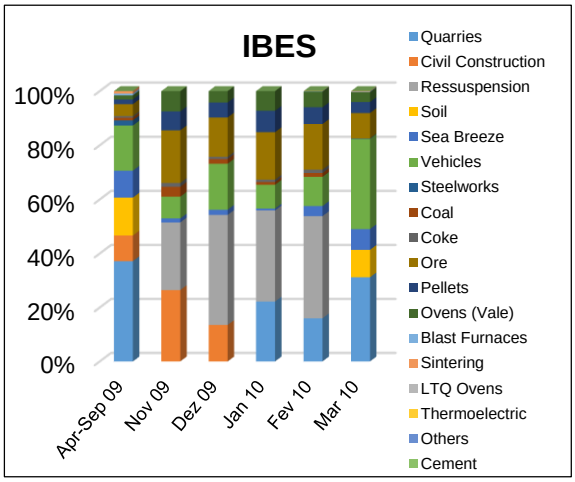

(d)

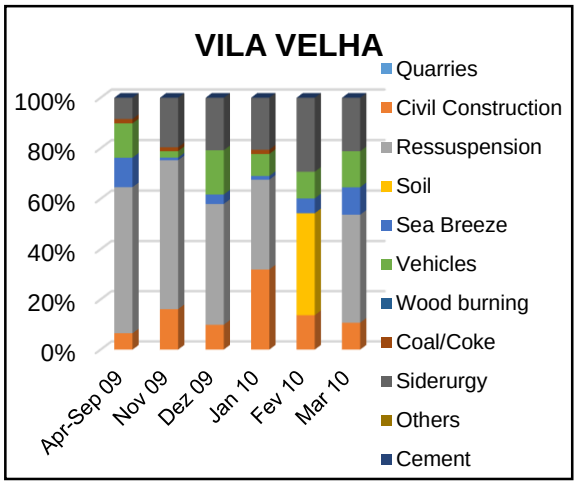

(e)

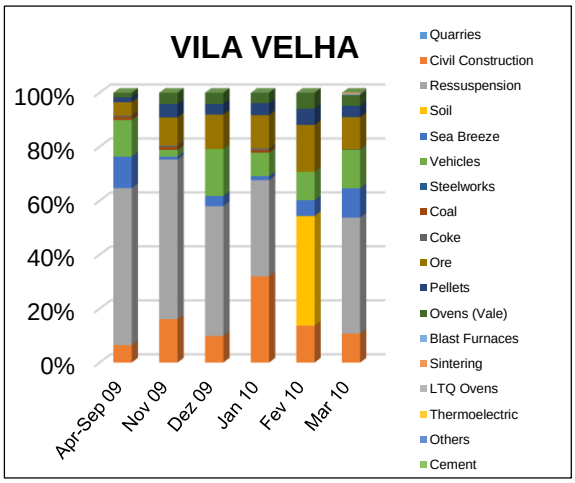

(f)

Source: Monticelli (2018).

Figure 28. Results for CMB (left) and CMB+CALPUFF (right) source apportionment in monitoring stations RAMQAR 8 (a-b) and 9 (c-d).

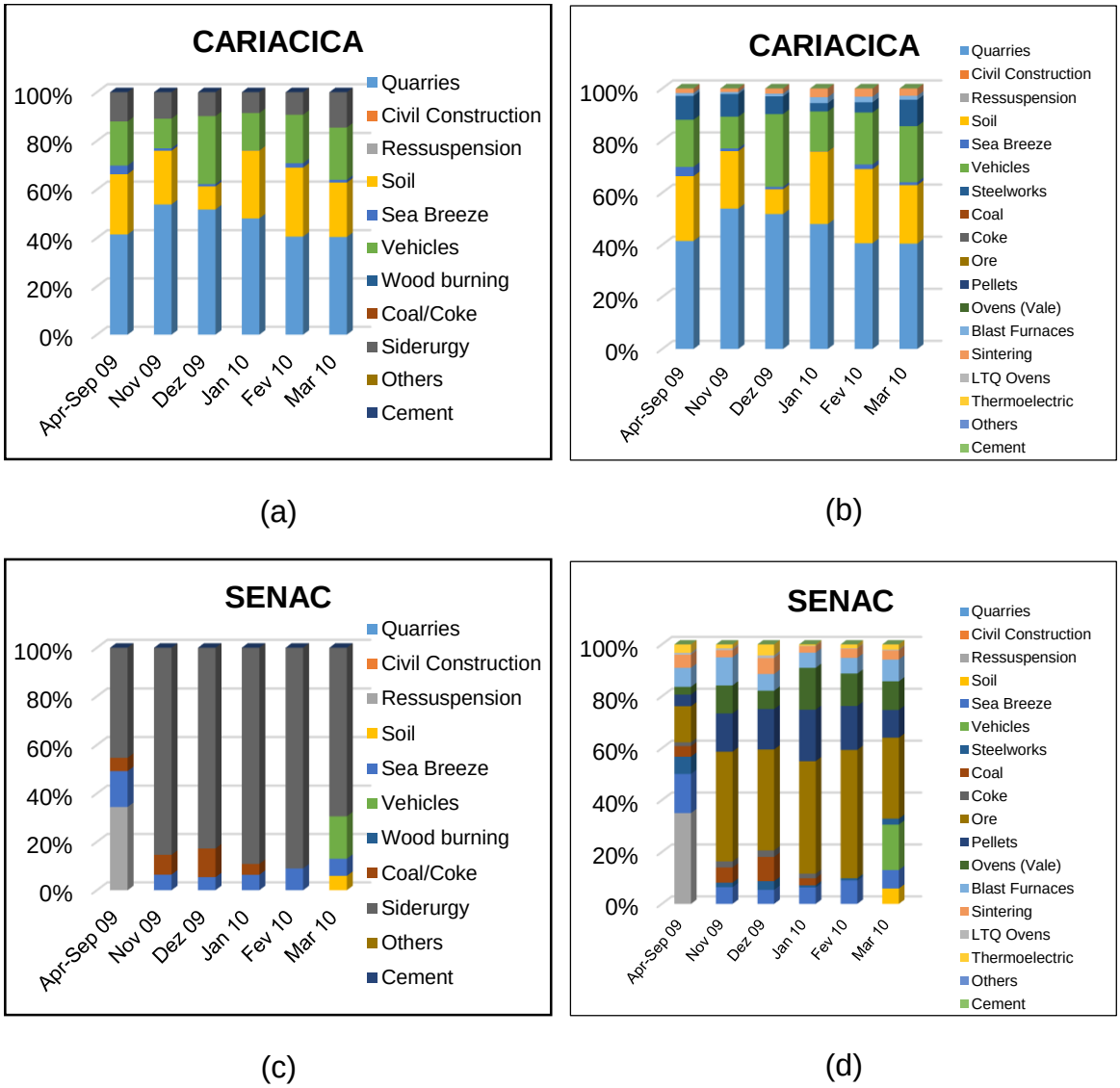

Source: Monticelli (2018).

Appendix E shows in more specifics each contribution in form of tables. The integrated CMB + CALPUFF source apportionment is more notable in RAMQAR 9 SENAC where most of the contributing sources of SPM derive from the Steel industry. For the “Coal” group, emissions related to coal transportation and stock had greater contributions than those related to coke and coke ovens. In Group A, “Ore” sources followed by “Pellets” had major contributions compared to “Ovens”. Moreover, in Group B, Blast Furnaces had a more impact in dry deposition than Sintering and Steelworks. At last, for Group C, the “Thermoelectric” sources presented higher percentages than LTQ Ovens.

7. CONCLUSIONS

This work aimed to compare the use of CALPUFF and AERMOD dispersion models in calculating the particle deposition rate in the GVR and in the aid of the CMB receptor model to identify sources contributions.

The author managed this by first investigating the formulations contained in the CALPUFF and AERMOD manuals to determine particles deposition rate, from that two things befitted notable: (1) both models use the universal formulation for dry deposition as a way to estimate the deposition fluxes, however (2) the resistance model and variables applied are not the same. Together with the distinctions in the Eulerean and Lagragian approach, they contribute to differences in the estimations.

CALPUFF and AERMOD models quantified the dry deposition rate of the particles in the GVR for April/2009 to March/2010, with mainly underestimations by AERMOD and a better adjustment for CALPUFF with a few overestimations.

In a sense, both models had a fair performance following the variations of the deposition fluxes monitored by the RAMQAr stations, when analyzing the Correlation Coefficient (COC). In general and for each station, CALPUFF made better estimations than AERMOD.

At last, the Lagragian model managed to ungroup the sources of Santos et *al.* (2017) from the last SPM report showing that the methodology proposed may be applicable in further investigations of this pollutant. In this sense, the author recommends:

- Exploring the sources contribution to SPM loads in traffic lanes of GVR;
- Upgrade this study with more source apportionment investigations;
- Study the performance of CALPUFF for estimating dry deposition in GVR compared with other models available and;
- Explore the appliance of prognostic meteorological models in CALMET with the purpose of forecast the deposition of SPM in GVR.

REFERENCES

AMERICAN SOCIETY FOR TESTING MATERIALS. ASTM D-1739: **Standard Test Method for Collection and Measurement of Dustfall (Settleable Particulate Matter).** 1998 (re-approved in 2004).

ARYA, S. P. **Air Pollution Meteorology and Dispersion**. [s.l.] Oxford University Press on Demand, 1999.

ASSOCIAÇÃO BARSILEIRA DE NORMAS TÉCNICAS. **ABNT MB-3402: Atmosfera – Determinação da taxa de poeira sedimentável total**, Rio de Janeiro, 1991.

A. SRIVASTAVA, S. G. Source Appointment of Total Suspended Particulate Matter in Coarse and Fine Size Ranges over Delhi, . **Aerosol and Air Quality Research,** v. 8, n. 2, p. 188 –200., 2008.

BALAKRISHNA, G.; PERVEZ, S. Source apportionment of atmospheric dust fallout in an urban-industrial environment in India. **Aerosol and Air Quality Research**, v. 9, n. 3, p. 359–367, 2009.

BOBBINK, R. *et al.* Global assessment of nitrogen deposition effects on terrestrial plant diversity: A synthesis. **Ecological Applications**, v. 20, n. 1, p. 30–59, 2010.

CHEN, L. *et al.* Dry deposition velocity of total suspended particles and meteorological influence in four locations in Guangzhou, China. **Journal of Environmental Sciences**, v. 24, n. 4, p. 632–639, 2012.

CHU, C. C. *et al.* Dry deposition study by using dry deposition plate and water surface sampler in Shalu, central Taiwan. **Environmental Monitoring and Assessment**, v. 146, n. 1–3, p. 441–451, 2008.

COE, J. M.; LINDBERG, S. E. The morphology and size distribution of atmospheric particles deposited on foliage and inert surfaces. **Journal of the Air Pollution Control Association**, v. 37, n. 3, p. 237–243, 1987.

CONTI, M. M. **Caracterização Química E Morfológica De Partículas Sedimentadas Na Região Metropolitana Da Grande Vitória - ES**. [s.l.] Universidade Federal do Espirito Santo (UFES), 2013.

CONTINI, D. *et al.* Application of PMF and CMB receptor models for the evaluation of the contribution of a large coal-fired power plant to PM10concentrations. **Science of the Total Environment**, v. 560–561, p. 131–140, 2016.

DOURADO, H. O. **Modelling odour dispersion in built environments**. [s.l.] Universidade Federal do Espirito Santo, 2013.

DRESSER, A. L.; HUIZER, R. D. CALPUFF and AERMOD Model Validation Study in the Near Field: Martins Creek Revisited. **Journal of the Air & Waste Management Association**, v. 61, n. 6, p. 647–659, 2011.

DUCE, R. A. *et al.* The Atmospheric Input of Trace Species to the World Ocean. **Global Biochemical Cycles**, v. 5, n. 3, p. 193–259, 1991.

ENGELBRECHT, J. P. *et al.* Physical and chemical properties of deposited airborne particulates over the Arabian Red Sea coastal plain. **Atmospheric Chemistry and Physics**, v. 17, n. 18, p. 11467–11490, 2017.

FINLAYSON-PITTS, B. J.; PITTS JR, J. N. **Chemistry of the Upper and Lower Atmosphere**. [s.l.] Academic Press, 2000.

HABRE, R.; COULL, B.; KOUTRAKIS, P. Impact of source collinearity in simulated PM2.5 data on the PMF receptor model solution. **Atmospheric Environment**, v. 45, n. 38, p. 6938–6946, 2011.

HU, M. *et al.* Estimation of size-resolved ambient particle density based on the measurement of aerosol number, mass, and chemical size distributions in the winter in Beijing. **Environmental Science and Technology**, v. 46, n. 18, p. 9941–9947, 2012.

JANE MÉRI SANTOS E NEYVAL COSTA REIS JÚNIOR. **Caracterização e Quantificação De Partículas Sedimentadas Na Região Da Grande Vitória**. Vitoria - ES: [s.n.].

JONSSON, L.; KARLSSON, E.; JÖNSSON, P. Aspects of particulate dry deposition in the urban environment. **Journal of Hazardous Materials**, v. 153, n. 1–2, p. 229–243, 2008.

LEE, H. *et al.* Evaluation of concentrations and source contribution of PM 10 and SO 2 emitted from industrial complexes in Ulsan, Korea: Interfacing of the WRF–CALPUFF modeling tools. **Atmospheric Pollution Research**, v. 5, n. 4, p. 664–676, 2014.

LI, H. W. *et al.* Impacts of hazardous air pollutants emitted from phosphate fertilizer production plants on their ambient concentration levels in the Tampa Bay area. **Air Quality, Atmosphere and Health**, v. 8, n. 5, p. 453–467, 2015.

LIU, J. *et al.* Dry deposition of particulate matter at an urban forest, wetland and lake surface in Beijing. **Atmospheric Environment**, v. 125, p. 178–187, 2016.

MACHADO, M. *et al.* A new methodology to derive settleable particulate matter guidelines to assist policy-makers on reducing public nuisance. **Atmospheric Environment**, v. 182, 2018.

MACHADO, M. *et al.* A new methodology to derive settleable particulate matter guidelines to assist policy-makers on reducing public nuisance. **Atmospheric Environment**, v. 182, p. 242–251, 2018.

PANAS, A. *et al.* Morphology and Elemental Composition of Dustfall Particles Inside Emperor Qin â€™ S Terra-Cotta Warriors and Horses Museum. **Beilstein Journal of Nanotechnology**, v. 5, n. 1, p. 1590–1602, 2014.

PERVEZ, S.; BALAKRISHNA, G.; TIWARI, S. Source apportionment of mercury in

dust fallout at urban residential area of Central India. **Atmospheric Chemistry and Physics Discussions**, v. 9, n. 5, p. 21915–21940, 2009.

PETROFF, A. *et al.* Aerosol dry deposition on vegetative canopies. Part I: Review of present knowledge. **Atmospheric Environment**, v. 42, n. 16, p. 3625–3653, 2008a.

___. Aerosol dry deposition on vegetative canopies. Part II: A new modelling approach and applications. **Atmospheric Environment**, v. 42, n. 16, p. 3654–3683, maio 2008b.

PETROFF, A.; ZHANG, L. Development and validation of a size-resolved particle dry deposition scheme for application in aerosol transport models. **Geoscientific Model Development**, v. 3, n. 2, p. 753–769, 2010.

POLI, A. A; CIRILLO, M. C. On the use of the normalized mean square error in evaluating dispression model performance. **Ae**, v. 27, n. 15, p. 2427–2434, 1993.

PRIYADARSHINI, S.; SHARMA, M.; SINGH, D. Synergy of receptor and dispersion modelling: Quantification of PM10emissions from road and soil dust not included in the inventory. **Atmospheric Pollution Research**, v. 7, n. 3, p. 403–411, 2016.

ROOD, A. S. Performance evaluation of AERMOD, CALPUFF, and legacy air dispersion models using the Winter Validation Tracer Study dataset. **Atmospheric Environment**, v. 89, p. 707–720, 2014.

ROY, D.; SINGH, G.; YADAV, P. Identification and elucidation of anthropogenic source contribution in PM10 pollutant: Insight gain from dispersion and receptor models. **Journal of Environmental Sciences (China)**, v. 48, p. 69–78, 2016.

SAKATA, M.; ASAKURA, K. Atmospheric dry deposition of trace elements at a site on Asian-continent side of Japan. **Atmospheric Environment**, v. 45, n. 5, p. 1075–1083, 2011.

SANTIAGO, A. M. **Simulação Da Camada Limite Planetária Sobre A Região Metropolitana Da Grande Vitória Com O Uso Do Modelo De Mesoescala WRF**. [s.l.] Universidade Federal do Espirito Santo (UFES), 2009.

SANTOS, J. M. *et al.* Source apportionment of settleable particles in an impacted urban and industrialized region in Brazil. **Environmental Science and Pollution Research**, v. 24, n. 27, p. 22026–22039, 2017.

SCIRE, J. S.; STRIMAITIS, D. G.; YAMARTINO, R. J. A User ' s Guide for the CALPUFF Dispersion Model. **Eearth Tech. Inc**, n. January, p. 521, 2000.

SEINFELD, J. H.; WILEY, J. **ATMOSPHERIC From Air Pollution to Climate Change SECOND EDITION**. [s.l: s.n.]. v. 51

SHI, G. L. *et al.* Estimated contributions and uncertainties of PCA/MLR-CMB results: Source apportionment for synthetic and ambient datasets. **Atmospheric Environment**, v. 45, n. 17, p. 2811–2819, 2011.

___. A comparison of multiple combined models for source apportionment, including

the PCA/MLR-CMB, Unmix-CMB and PMF-CMB Models. **Aerosol and Air Quality Research**, v. 14, n. 7, p. 2040–2050, 2014.

SILVA, A. M.; SARNAGLIA, V. D. M. **Estudo Da Qualidade Do Ar Na Região Metropolitana Da Grande Vitória Empregando Um Modelo De Dispersão Atmosférica - CALPUFF**. [s.l.] Universidade Federal do Espirito Santo (UFES), 2010.

TARTAKOVSKY, D.; STERN, E.; BRODAY, D. M. Comparison of dry deposition estimates of AERMOD and CALPUFF from area sources in flat terrain. **Atmospheric Environment**, v. 142, p. 430–432, 2016a.

___. Dispersion of TSP and PM10emissions from quarries in complex terrain. **Science of the Total Environment**, v. 542, p. 946–954, 2016b.

TIAN, Y. Z. *et al.* Effects of collinearity, unknown source and removed factors on the NCPCRCMB receptor model solution. **Atmospheric Environment**, v. 81, p. 76–83, 2013.

TOMAŠEVIĆ, M. *et al.* Characterization of trace metal particles deposited on some deciduous tree leaves in an urban area. **Chemosphere**, v. 61, n. 6, p. 753–760, 2005.

U.S. EPA. **User's Guide for the AMS/EPA Regulatory Model (AERMOD)**, 2015. Disponível em: <https://www3.epa.gov/ttn/scram/dispersion_prefrec.htm#aermod>

US EPA. Haul Road Workgroup Final Report Submission to EPA-OAQPS. p. 22, 2012.

VALLACK, H. W.; SHILLITO, D. E. Suggested guidelines for deposited ambient dust. **Atmospheric Environment**, v. 32, n. 16, p. 2737–2744, 1998.

ZHENG, M. *et al.* Dry and wet deposition of elements in Hong Kong. **Marine Chemistry**, v. 97, n. 1–2, p. 124–139, 2005.

APPENDIX A METEOROLOGICAL CONDITIONS DURING THE STUDY PERIOD

This appendix aims to present the meteorological data for the study period, giving brief comments on the most important variables for the modelling.

Figure 29. Time series of atmospheric pressure.

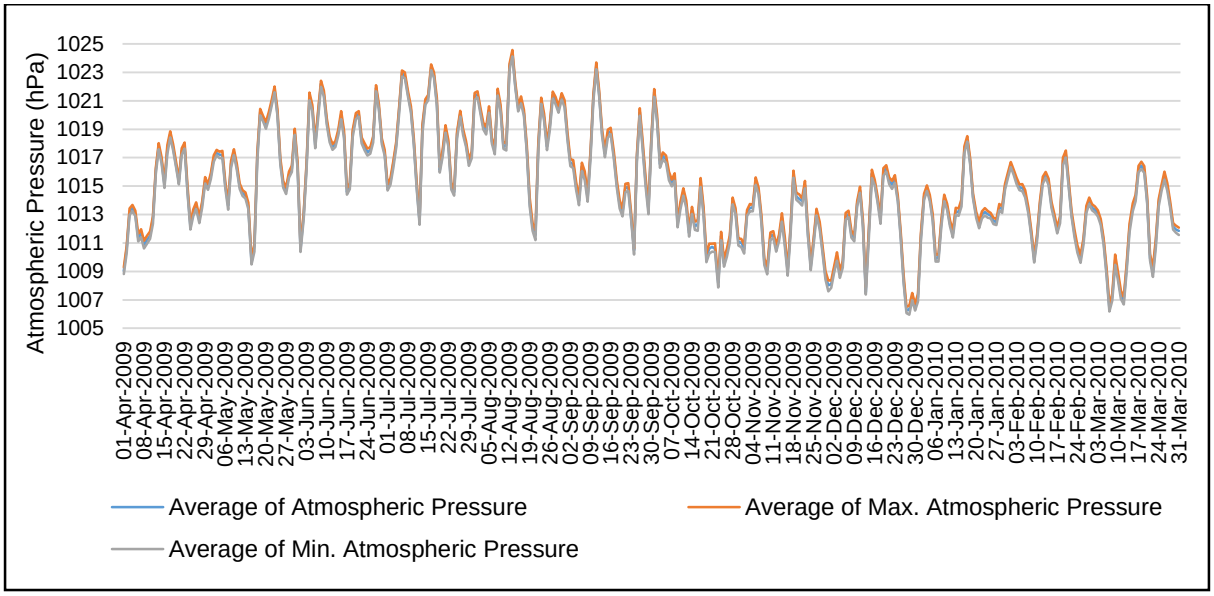

Source: Monticelli (2018).

One can observe from the time series of atmospheric pressure that, in average, there was a considerable drop from October 14th of 2009 forward, having the lowest value in December/2009.

Figure 30. Time series of wind speed.

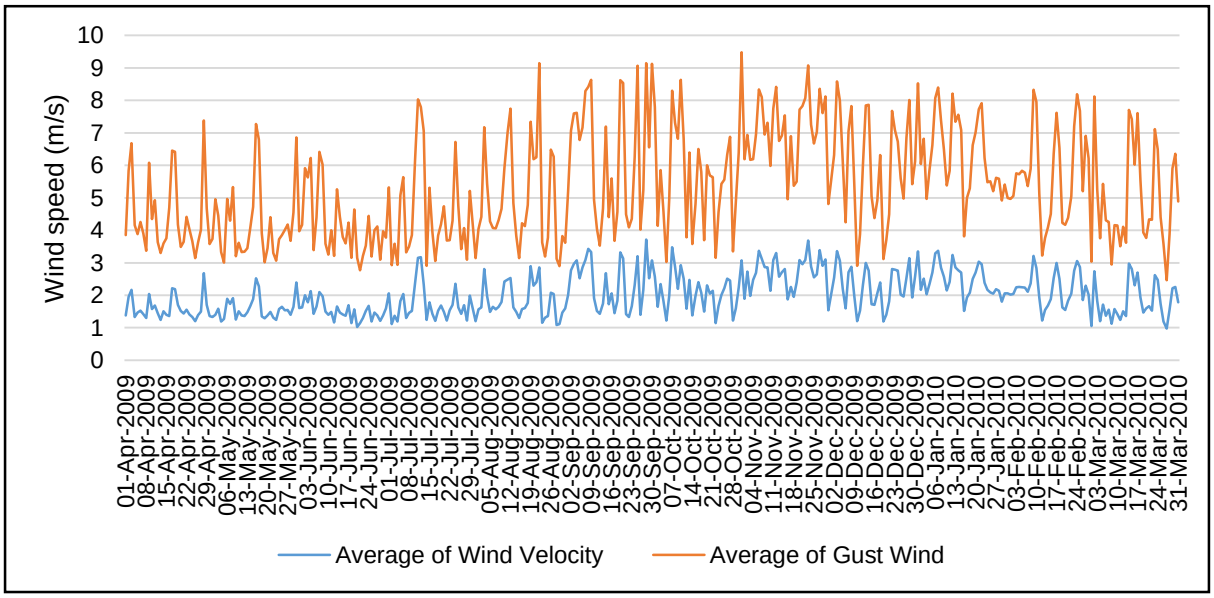

Source: Monticelli (2018).

For the wind speed there is a time series consistency, having the speed values always lower than 4m/s but higher than 1m/s. Accordingly with the Beaufort scale, the predominance of winds in GVR during 2009 – 2010 were Light air (0,3 – 1,5m/s), Light breeze (1,6 – 3,3m/s) and Gentle breeze (3,4 – 5,5m/s).

Figure 31. Time series of solar radiation.

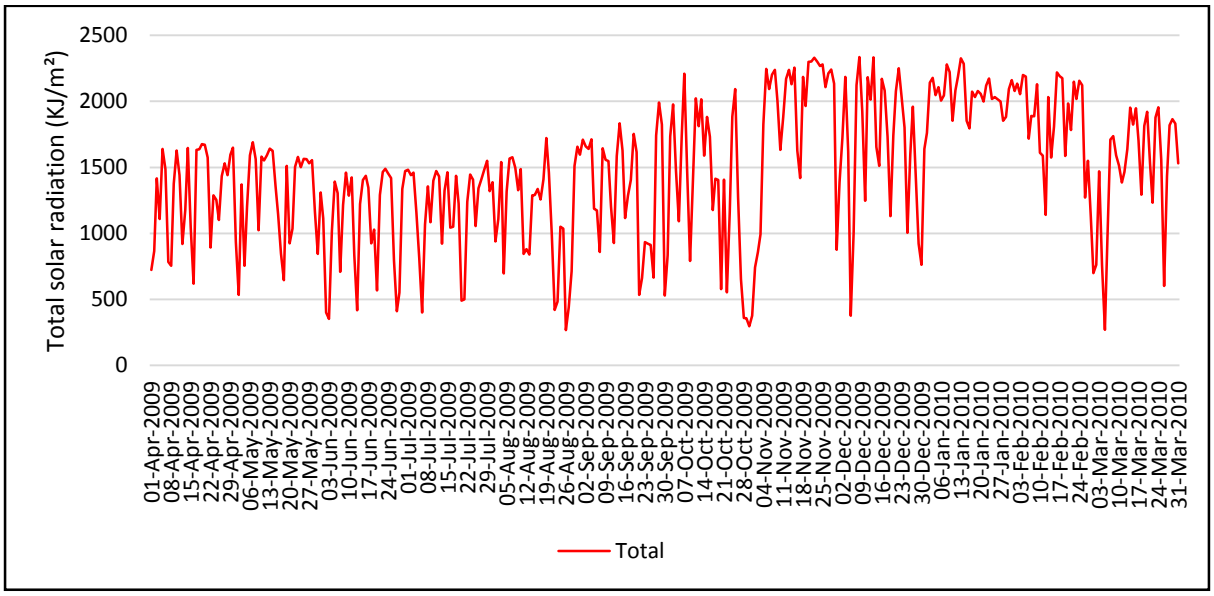

Source: Monticelli (2018).

The amount of solar radiation changes abruptly which could be related to the highest precipitation events in GVR during April/2009 to March/2010. In addition, one can perceive that during autumn/winter (April – August) the solar radiation income is lower than on spring/summer (October – March).

Figure 32. Time series of precipitation.

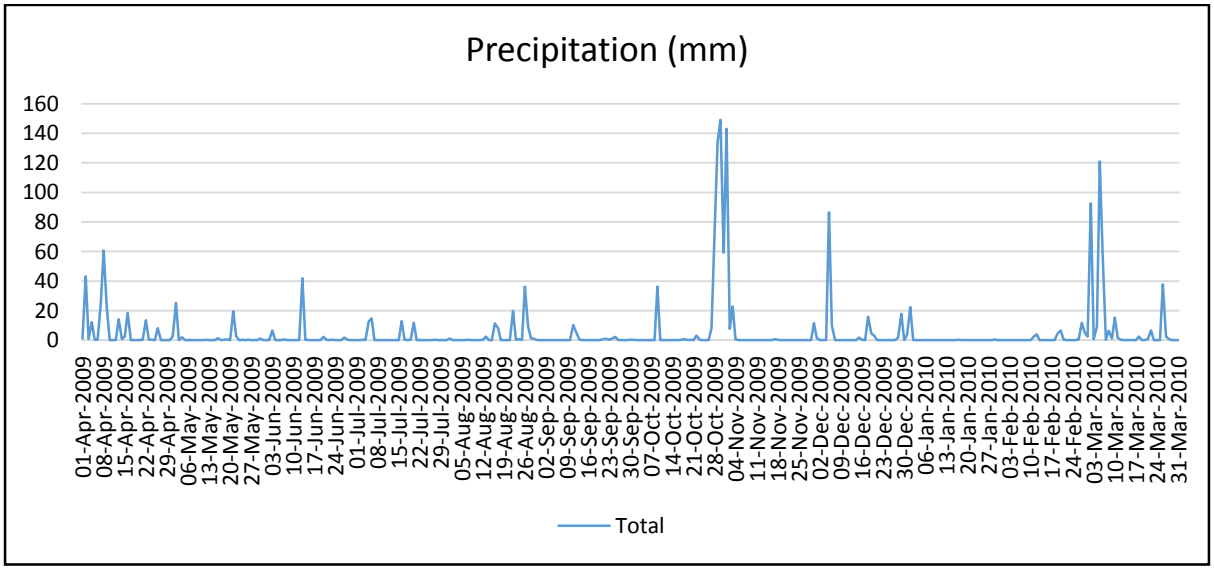

Source: Monticelli (2018).

As quoted in Santos et *al.* (2017) the GVR present a dry season (April – August) and a wet season (October – March) which is clearly notable in the time series of precipitation, being the highest even in October of 2009.

Figure 33. Time series of temperature.

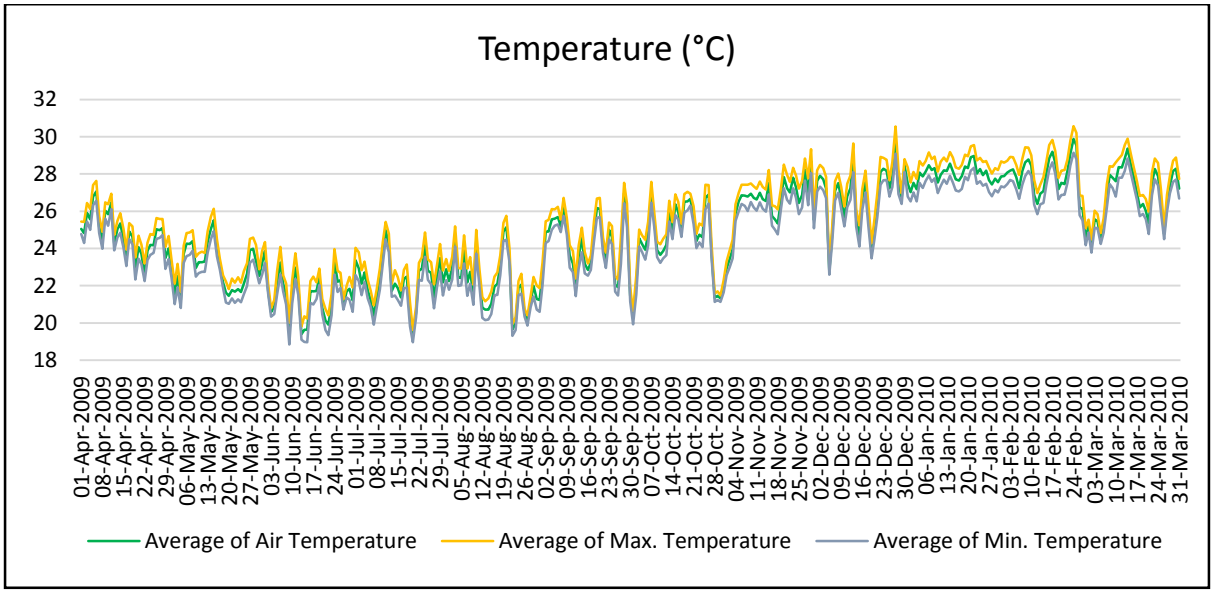

Source: Monticelli (2018).

The average air temperature follows the same pattern as the total solar radiation, having an increase after August/2009. The highest value of the time series happened in December/2009.

Figure 34. Time series of relative humidity.

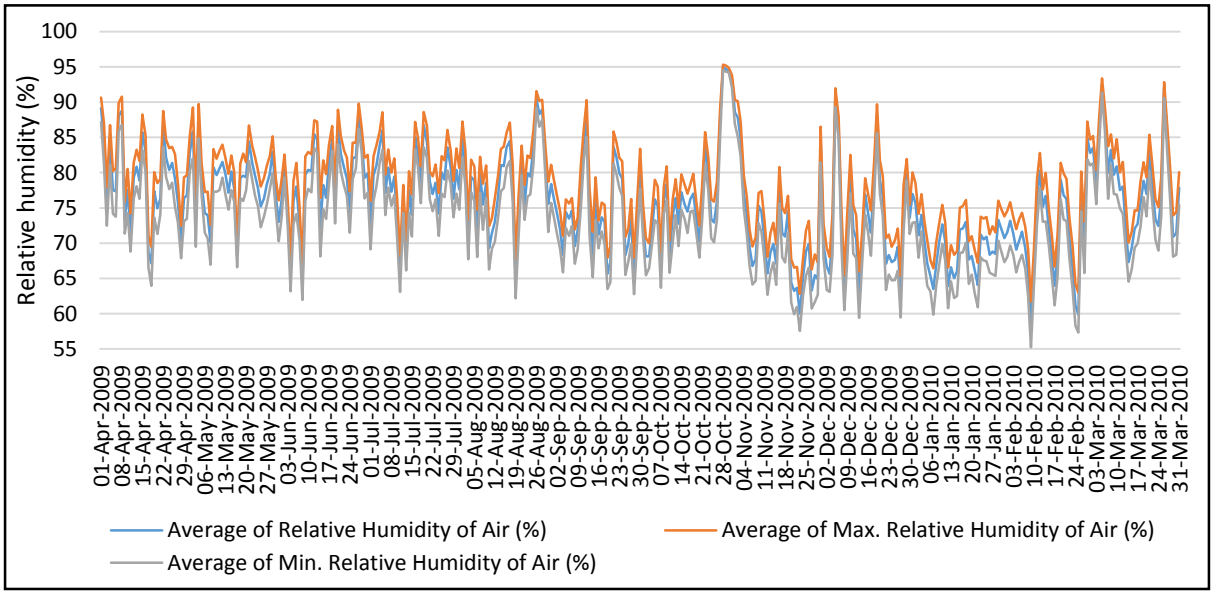

Source: Monticelli (2018).

The times series of relative humidity has its peaks during the months of high precipitation events and went near 55% during February/2010.

Figure 35. Average cloud cover baseline height variation.

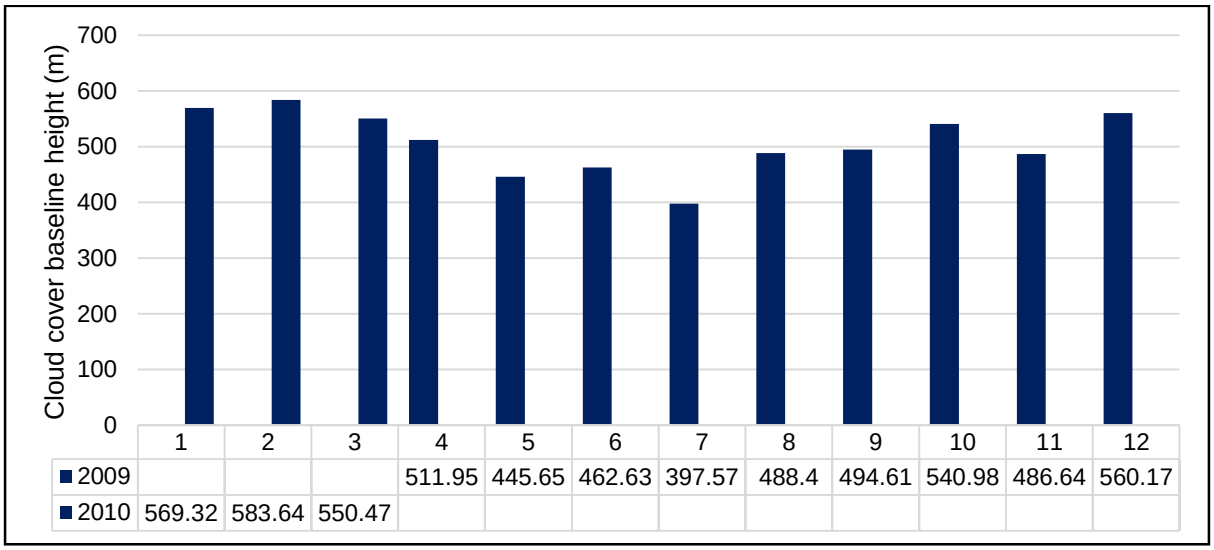

Source: Monticelli (2018).

The monthly average cloud cover baseline height varied between 397,57m (in July/2009) to 583,64m (February/2010). The lowest values happened during the winter and the highest during summer in the region. This can be explained by the planetary boundary layer behavior during warm and cold seasons.

Figure 36. Average cloud cover variation.

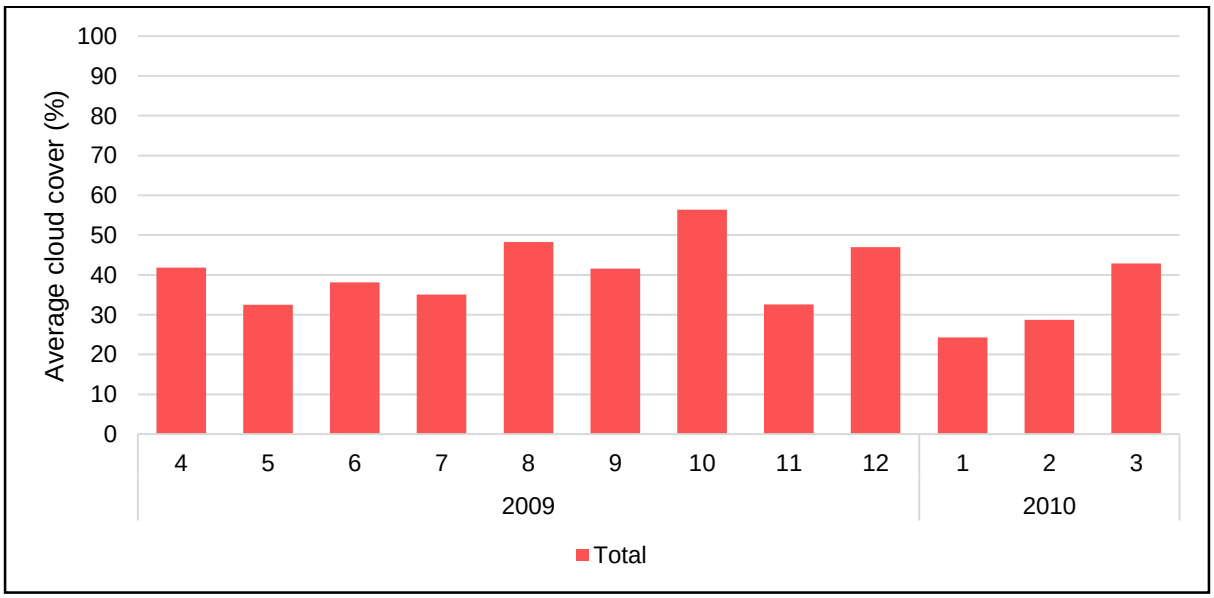

Source: Monticelli (2018).

Regarding the monthly average cloud cover variation during April/2019 to March/2010 one can observe that the month with the highest precipitation event (October/2009) had the highest average cloud cover (56%).

Figure 37. Wind rose.

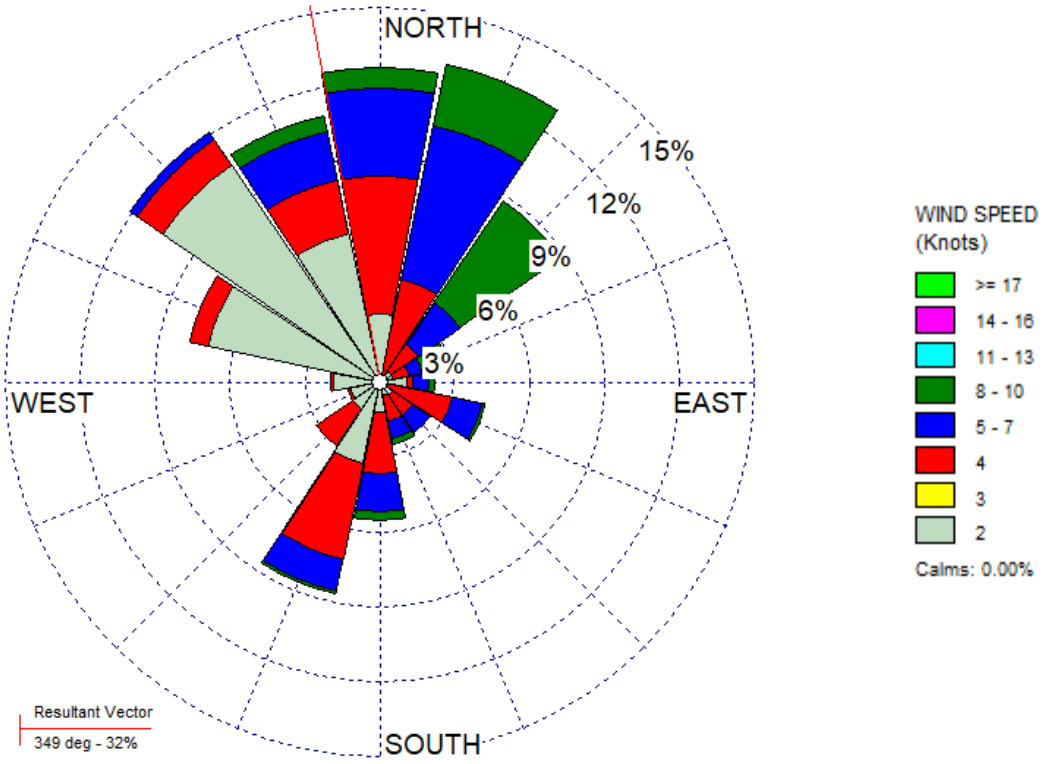

Source: Monticelli (2018).

The annual wind rose agrees with the expected behavior of the region, having the strongest and common winds coming from the N-NE directions, having also register winds coming from the S-SW directions related to the months of April/2009 to August/2009.

APPENDIX B LEGISLATION CONCERNING DRY DEPOSITION

The quantification of deposition flux of Settleable Particulate Matter (SPM) relies on the sum of particles' mass deposited by a unit of area over time. It is therefore, expressed in terms of mg/m^2/day or g/m^2/30 days, usually. Due to the relatively small area of many collectors, sampling often takes 30 days in order to collect a considerable amount of material for further analysis. The issue with this methodology is that the approach by the mean value may misrepresent the highest and lowest rates for some specific days (CONTI, 2013).

Table 17 shows some references (standards) gathered in the literature and countries as well as states' legislations for the deposition flux of SPM, updated from Machado, et *al.* (2018).

Table 17. National and International legislation for deposition flux of SPM

Country	Average time	Standard (mg/m^2/days)	Standard (g/m^2/30days)
SOUTH AFRICA	Monthly (residential areas)	600	18
	Monthly (non-residential areas)	1200	36
GERMANY	Annual	350	10.5
ARGENTINA	Annual	333	10
➢ Buenos Aires	Monthly	33.3	1[(a)]
BRAZIL			
➢ Espírito Santo	Monthly	466.2	14
➢ Minas Gerais	Monthly (industrial area)	333	10
	Monthly (residential and commercial area)	166.5	5
CANADA			
➢ Alberta	Monthly (residential and recreational area)	176.6	5.3
	Monthly (commercial and industrial areas)	526.6	15.8
➢ Newfoundland	Annual	12[(b)]	0.3
	Monthly	280	7[(c)]
➢ Ontario	Annual	12[(b)]	0.3
	Monthly	280	7[(c)]

Legend: (a) 98% percentile; (b) presented in the legislation as 4.6 g/m^2 in 1 year; (c) presented in the legislation as 7 g/m^2 in 30 days.

Source: Updated from Machado et *al.* (2018)

In Great Britain, there was no legislation for SPM, though standards for atmospheric $PM_{2.5}$ and PM_{10} exist. Vallack and Shillito (1998) proposed guidelines for ambient

deposited dust based on the background levels normally observed and the *"likelihood of complain approach".*

Finland and Spain provided no legislation regarding SPM. However, the *"Government Decree on air quality"* and/or *"European Union's Air Quality Framework Directive"* regulates PM_{10} and $PM_{2.5}$. Vallack and Shillito (1998) provided values for it in their study as well.

Although Vallack and Shillito (1998) provided two standards for SPM in Western Australia, the author obtained no mention towards a legislation regarding this pollutant. The value of 133mg/m^2/days was take into account when first perceived the loss of amenity and the value of 333mg/m^2/days when occurred an unacceptable reduction in air quality. Further, the *"Department of the Environmental and Energy"* of Australia set in June of 1998 the *"National Environment and Protection Measure for Ambient Air Quality"* which the States and Territories agreed to follow. The standards present in the document relate to six criteria air pollutants: CO, NO_2, photochemical oxidants, SO_2, Pb and particles with no mention to SPM.

German legislation for dust deposition is the *"First General Administrative Regulation Pertaining the Federal Immission Control Act"* and accounts for non-Hazardous Dust. It states that a permit may not be refused if the installation exceeds the limit value, only in the case that the additional load surpass 10.5mg/(m^2.day). In additional to the deposition standard present in Table 17, the German legislation comply with different deposition values for heavy metals, expressed in Table 18.

Table 18. German legislation for deposition fluxes of heavy metals.

Substance/Group of Substances	Allowed deposition in µg/(m^2.day)	Averaging Period
Arsenic (Ar)	4	Annual
Lead (Pb)	100	Annual
Cadmium (Cd)	2	Annual
Nickel (Ni)	15	Annual
Mercury (Hg)	1	Annual
Thallium (Tl)	2	Annual

Source: Gemeinsames Ministerialblatt, GMBl. p. 511 (2002).

Argentina's *National Law 20.284/1973* regarding atmospheric contamination set methods for sampling and analysis of SPM. The amount of pollutant present in the atmosphere pronounces the situation in which the population is at risk. While for some pollutants (CO - ppm, NOx – ppm, SO_2 – ppm, O_3 – ppm, TSP – mg/m^3) each situation (Alert, Alarm, Emergency) are clearly defined (higher concentrations indicate higher risk), for SPM the same value is adopted for all.

In Brazil, the national legislation "*CONAMA 03/1990"* does not declare any standard for SPM. However, some States like Espírito Santo (ES) and Minas Gerais (MG), through "*Decreto № 3463-R/2013"* and "*COPAM № 01/1981"*, had their own standards regulated. Specifically for ES, the pollutants thresholds are in accord with the goals desired. There are a number of 3 (three) intermediary objectives and 1 (one) final objective. For SPM, the value of $14g/m^2/30days$ represent the first objective, and the next goals will be stablished after the publication of the *Strategic Plan of Air Quality* (*PEQAr – portuguese*).

Canada presented no legislation regarding dustfall of any kind. However, some provinces (see Table 17) had their own ambient air quality regulations, namely: *Alberta Environmental Protection and Enhancement Act (EPEA), Ontario's Ambient Air Quality Criteria and Newfoundland and Labrador Regulation 39/04*. Although Vallack and Shillito (1998) provided values for Manitoba province, there are no current legislation according to the recent *Ambient Air Quality Criteria of Manitoba*, updated in July 2005.

Vallack and Shillito (1998) also presented ambient air quality standards for a group of States in USA, yet, after the NAAQS (*New Ambient Air Quality Standards*) adopted by the Environmental Protection Agency of USA, those standards became outdated.

South Africa recently (2013) adopted standards for Settleable Particulate Matter through the *Air Quality Act 39 of 2004, National Dust Control Regulations*. Accordingly with this document, it is allowed two exceedances from the values presented in Table 17, as long as they don't occur in sequential months.

APPENDIX C SOURCES CONSIDERED IN CALPUFF SOURCE APPORTIONEMNT RUNS

- GROUP “CARVAO”

Coal:

Source ID	Fonte Emissora	Empresa	UTM X	UTM Y
S73	Fugitivas Carregamento de Carvão nos Fornos de Coque	Arcelor Mittal Tubarão	371458	7760116
S78	Pátio de Carvão (empilhamento/ manuseio)	Arcelor Mittal Tubarão	372273	7759820
S88	Pontos de Transferência do Pátio de Carvão	Arcelor Mittal Tubarão	371871	7759521
S178	Pátio de Carvão	Vale	371137	7758852
S185	Píer de Carvão	Vale	370855	7755185
S205	Recebimento do Silo de Carvão 3A106 - Usina 3	Vale	369310	7758008
S206	Recebimento do Silo de Carvão 4A106 - Usina 4	Vale	369313	7758001
S207	Recebimento do Silo de Carvão 5SL4 - Usinas 5 e 6	Vale	370296	7757260
S208	Recebimento do Silo de Carvão 7A1F - Usina 7	Vale	370400	7757332
S209	Recebimento do Silo de Carvão AZ106 - Usinas 1 e 2	Vale	369307	7758016
S235	Transferências - Pátio de Carvão	Vale	370985	7758165
S242	Transferências - Píer de Carvão	Vale	371184	7755286
S622	Carregamento de Carvão	Sol Coqueria	371034	7762596
S626	Pátio de Carvão	Sol Coqueria	371200	7762172
S628	Transferência de Carvão	Sol Coqueria	371124	7762273
S690	Movimentação de Carvão Mineral	Unibrás	371474	7771051
S691	Pilha de Carvão Mineral	Unibrás	371691	7771104

Coke:

Source ID	Fonte Emissora	Empresa	UTM X	UTM Y
S09	Chaminé 1 da Coqueria	Arcelor Mittal Tubarão	371374	7760232
S10	Chaminé 2 da Coqueria	Arcelor Mittal Tubarão	371535	7760122
S624	Desenfornamento de Coque	Sol Coqueria	371034	7762596
S623	Chaminé Principal	Sol Coqueria	371473	7762433
S36	F. Mangas da Planta de Combustíveis - Coque e Antracito	Arcelor Mittal Tubarão	371089	7759989
S38	F. Mangas do Desenfornamento de Coque	Arcelor Mittal Tubarão	371267	7760173
S41	F. Mangas do Laboratório Coqueria	Arcelor Mittal Tubarão	371753	7760194
S57	F. Mangas Sistema 1 do Trat. de Coque	Arcelor Mittal Tubarão	371217	7760354
S58	F. Mangas Sistema 10 do Trat. de Coque	Arcelor Mittal Tubarão	371293	7760188
S59	F. Mangas Sistema 11 do Trat. de Coque	Arcelor Mittal Tubarão	370996	7760093
S61	F. Mangas Sistema 2 do Trat. de Coque	Arcelor Mittal Tubarão	371089	7760128
S63	F. Mangas Sistema 3 do Trat. de Coque	Arcelor Mittal Tubarão	371107	7760190
S64	F. Mangas Sistema 5 do Trat. de Coque	Arcelor Mittal Tubarão	370934	7760170
S65	F. Mangas Sistema 6 do Trat. de Coque	Arcelor Mittal Tubarão	370873	7760218
S66	F. Mangas Sistema 9 do Trat. de Coque	Arcelor Mittal Tubarão	371180	7760295
S87	Pontos de Transferência da Coqueria	Arcelor Mittal Tubarão	371281	7760460
S625	Manuseio de Coque	Sol Coqueria	371378	7762116
S73	Fugitivas Carregamento de Carvão nos Fornos de Coque	Arcelor Mittal Tubarão	371458	7760116
S74	Fugitivas Desenfornamento de Coque	Arcelor Mittal Tubarão	371430	7760108
S75	Fugitivas Portas das Baterias de Coque	Arcelor Mittal Tubarão	371407	7760153

- GROUP A:

Ore:

Source ID	Emission Source	Industry	UTM X	UTM Y
S179	Pátio de Finos - Terminal de Minérios	Vale	370116	7756800
S182	Pátio de Granulados - Terminal de Minérios	Vale	369892	7756722
S186	Píer do Terminal de Minérios	Vale	369608	7756235
S236	Transferências - Pátio de Finos (Terminal de Minérios)	Vale	370550	7756645
S237	Transferências - Pátio de Granulados (Terminal de Minérios)	Vale	369889	7757032
S243	Transferências - Terminal de Minérios	Vale	369962	7756042

Pellets:

Source ID	Emission Source	Industry	UTM X	UTM Y
S83	Pilhas Pátio de Minérios/Fundentes/Pelotas/Antracito	Arcelor Mittal Tubarão	370984	7759994
S93	PT's_Pátios de Minérios/Fundentes/Pelotas/Antracito	Arcelor Mittal Tubarão	371086	7759689
S183	Pátio de Pelotas - Usinas de 1 a 4	Vale	369347	7757690
S184	Pátio de Pelotas - Usinas de 5 a 7	Vale	370453	7757744
S238	Transferências - Pátio de Pelotas (Usinas 1 a 4)	Vale	369502	7757587
S239	Transferências - Pátio de Pelotas (Usinas 5 a 7)	Vale	370639	7757525

Ovens (Vale):

Source ID	Emission Source	Industry	UTM X	UTM Y
S172	Entr/Saída Forno, Peneiramento, Cam Forram. P0/P1 - Usina 1	Vale	369466	7757933
S173	Entrada e Saída do Forno, Peneiramento - Usina 3	Vale	369396	7757941
S174	Entrada Forno, Peneiramento e Camada de Forramento - Usina 2	Vale	369485	7757963

- GROUP B:

Blast Furnaces:

Source ID	Emission Source	Industry	UTM X	UTM Y
S16	Chaminé dos Regeneradores AF1	Arcelor Mittal Tubarão	370697	7760328
S17	Chaminé dos Regeneradores AF2	Arcelor Mittal Tubarão	370649	7760195
S18	Chaminé dos Regeneradores AF3	Arcelor Mittal Tubarão	370297	7760111
S23	F. Mangas da Casa de Corrida - AF2	Arcelor Mittal Tubarão	370541	7760267
S24	F. Mangas da Casa de Corrida 1 - AF1	Arcelor Mittal Tubarão	370615	7760522
S25	F. Mangas da Casa de Corrida 1 - AF3	Arcelor Mittal Tubarão	370383	7760206
S26	F. Mangas da Casa de Corrida 2 - AF1	Arcelor Mittal Tubarão	370721	7760555
S27	F. Mangas da Casa de Corrida 2 - AF3	Arcelor Mittal Tubarão	370357	7760204
S55	F. Mangas Silos de Retorno AF2	Arcelor Mittal Tubarão	370805	7759944
S56	F. Mangas Sistema 1 - Abastecimento AF3	Arcelor Mittal Tubarão	371067	7759937
S60	F. Mangas Sistema 2 - Abastecimento AF3	Arcelor Mittal Tubarão	370953	7759970
S62	F. Mangas Sistema 3 - Abastecimento AF3	Arcelor Mittal Tubarão	370795	7759924
S67	F. Mangas Stock House - AF1	Arcelor Mittal Tubarão	371048	7760351
S68	F. Mangas Stock House - Coque - AF2	Arcelor Mittal Tubarão	370767	7759938
S69	F. Mangas Stock House - Coque - AF3	Arcelor Mittal Tubarão	370711	7759960
S70	F. Mangas Stock House - Sinter - AF2	Arcelor Mittal Tubarão	370762	7759966
S71	F. Mangas Stock House - Sinter - AF3	Arcelor Mittal Tubarão	370686	7759931
S72	F. Mangas Transf. Matérias Primas - AF2	Arcelor Mittal Tubarão	370929	7760147

Steelworks:

Source ID	Emission Source	Industry	UTM X	UTM Y
S05	Chaminé do Filtro de Manga do Despoeiramento da Aciaria	Arcelor Mittal Cariacica	357973	7749438
S76	Fugitivas Sistemas Secundários Aciaria	Arcelor Mittal Tubarão	370556	7761129
S94	Topo Aciaria	Arcelor Mittal Tubarão	370422	7761125
S49	F. Mangas Secundário 1	Arcelor Mittal Tubarão	370537	7760938

Sintering:

Source ID	Emission Source	Industry	UTM X	UTM Y
S37	F. Mangas de Matérias Primas da Sinter	Arcelor Mittal Tubarão	370982	7760210
S89	Pontos de Transferências Sinterização	Arcelor Mittal Tubarão	371070	7760127
S91	Precipitador Eletrostático Principal	Arcelor Mittal Tubarão	371409	7759895
S92	Precipitador Eletrostático Secundário	Arcelor Mittal Tubarão	371080	7760058

- GROUP C:

LTQ Ovens:

Source ID	Emission Source	Industry	UTM X	UTM Y
S13	Chaminé do Forno de Reaquecimento de Placas	Arcelor Mittal Tubarão	370289	7761533

Thermoelectric:

Source ID	Emission Source	Industry	UTM X	UTM Y
S11	Chaminé das Centrais Termelétricas 1 e 2	Arcelor Mittal Tubarão	371217	7760553
S12	Chaminé das Centrais Termelétricas 3 e 4	Arcelor Mittal Tubarão	371266	7760610

APPENDIX D SOURCE APPORTIONMENT OF CMB AND CALPUFF

RAMQAR 1 - LARANJEIRAS

CALPUFF	Apr-Sep 09	Nov-09	Dec-09	Jan-10	Feb-10	Mar-10
Traffic Lanes	16.89%	3.87%	8.96%	7.92%	19.67%	16.79%
Others	59.77%	80.18%	69.44%	87.79%	73.19%	61.23%
Group Coal	6.00%	12.09%	7.31%	4.26%	5.25%	6.13%
Group Siderurgy	17.33%	3.86%	14.29%	0.03%	1.89%	15.84%
CMB	**Apr-Sep 09**	**Nov-09**	**Dec-09**	**Jan-10**	**Feb-10**	**Mar-10**
Traffic Lanes	49.40%	70.37%	63.01%	76.97%	65.01%	58.81%
Others	41.90%	21.28%	28.56%	20.13%	24.97%	32.48%
Group Coal	2.31%	1.63%	0.00%	0.00%	0.00%	0.00%
Group Siderurgy	6.39%	6.72%	8.43%	2.90%	10.01%	8.72%

RAMQAR 3 – JARDIM CAMBURI

CALPUFF	Apr-Sep 09	Nov-09	Dec-09	Jan-10	Feb-10	Mar-10
Traffic Lanes	32.37%	28.25%	36.52%	66.10%	46.62%	41.86%
Others	35.52%	37.02%	40.31%	30.15%	33.13%	39.20%
Group Coal	3.28%	5.55%	3.62%	3.41%	6.87%	2.70%
Group Siderurgy	28.83%	29.18%	19.55%	0.35%	13.37%	16.24%
CMB	**Apr-Sep 09**	**Nov-09**	**Dec-09**	**Jan-10**	**Feb-10**	**Mar-10**
Traffic Lanes	16.89%	3.87%	8.96%	7.92%	19.67%	16.79%
Others	59.77%	80.18%	69.44%	87.79%	73.19%	61.23%
Group Coal	6.00%	12.09%	7.31%	4.26%	5.25%	6.13%
Group Siderurgy	17.33%	3.86%	14.29%	0.03%	1.89%	15.84%

RAMQAR 4 - ENSEADA

CALPUFF	Apr-Sep 09	Nov-09	Dec-09	Jan-10	Feb-10	Mar-10
Traffic Lanes	81.37%	87.64%	85.39%	86.03%	75.08%	75.93%
Others	11.21%	7.54%	8.42%	6.62%	12.00%	13.13%
Group Coal	0.82%	0.60%	0.86%	1.02%	1.44%	0.96%
Group Siderurgy	6.60%	4.22%	5.33%	6.32%	11.48%	9.98%
CMB	**Apr-Sep 09**	**Nov-09**	**Dec-09**	**Jan-10**	**Feb-10**	**Mar-10**
Traffic Lanes	64.23%	22.40%	43.06%	32.50%	49.39%	40.73%
Others	15.56%	28.13%	18.07%	1.08%	4.01%	22.62%
Group Coal	4.17%	8.46%	5.74%	7.78%	5.62%	1.14%
Group Siderurgy	16.05%	41.01%	33.14%	58.64%	40.97%	35.51%

RAMQAR 5 - VITORIA

CALPUFF	Apr-Sep 09	Nov-09	Dec-09	Jan-10	Feb-10	Mar-10
Traffic Lanes	70.02%	62.75%	62.96%	59.23%	43.21%	63.77%
Others	24.13%	28.10%	28.43%	26.52%	34.37%	27.58%
Group Coal	0.78%	1.46%	1.27%	3.69%	3.09%	1.14%
Group Siderurgy	5.07%	7.69%	7.34%	10.57%	19.34%	7.52%
CMB	**Apr-Sep 09**	**Nov-09**	**Dec-09**	**Jan-10**	**Feb-10**	**Mar-10**
Traffic Lanes	16.89%	3.87%	8.96%	7.92%	19.67%	16.79%
Others	59.77%	80.18%	69.44%	87.79%	73.19%	61.23%
Group Coal	6.00%	12.09%	7.31%	4.26%	5.25%	6.13%
Group Siderurgy	17.33%	3.86%	14.29%	0.03%	1.89%	15.84%

RAMQAR 6 - IBES

CALPUFF	Apr-Sep 09	Nov-09	Dec-09	Jan-10	Feb-10	Mar-10
Traffic Lanes	48.22%	66.50%	54.42%	41.15%	38.33%	41.06%
Others	38.88%	23.46%	30.50%	33.80%	37.93%	42.87%
Group Coal	1.53%	1.74%	1.84%	3.84%	3.65%	1.94%
Group Siderurgy	11.37%	8.30%	13.24%	21.21%	20.09%	14.13%
CMB	**Apr-Sep 09**	**Nov-09**	**Dec-09**	**Jan-10**	**Feb-10**	**Mar-10**
Traffic Lanes	30.66%	33.11%	57.76%	42.51%	48.64%	43.40%
Others	56.59%	27.92%	15.42%	22.89%	19.73%	38.92%
Group Coal	1.62%	5.02%	2.58%	1.88%	2.67%	0.00%
Group Siderurgy	11.13%	33.95%	24.25%	32.72%	28.97%	17.68%

RAMQAR 7 – VILA VELHA

CALPUFF	Apr-Sep 09	Nov-09	Dec-09	Jan-10	Feb-10	Mar-10
Traffic Lanes	73.55%	79.52%	82.42%	62.47%	58.34%	64.97%
Others	18.70%	10.23%	11.21%	19.54%	25.29%	25.74%
Group Coal	0.78%	0.89%	0.64%	1.55%	1.45%	0.92%
Group Siderurgy	6.96%	9.37%	5.73%	16.44%	14.92%	8.37%
CMB	**Apr-Sep 09**	**Nov-09**	**Dec-09**	**Jan-10**	**Feb-10**	**Mar-10**
Traffic Lanes	71.71%	61.66%	65.57%	44.37%	51.15%	57.28%
Others	18.16%	17.20%	13.64%	33.39%	19.55%	21.56%
Group Coal	1.72%	1.56%	0.00%	1.66%	0.00%	0.00%
Group Siderurgy	8.41%	19.58%	20.78%	20.58%	29.29%	21.17%

RAMQAR 8 - CARIACICA

CALPUFF	Apr-Sep 09	Nov-09	Dec-09	Jan-10	Feb-10	Mar-10
Traffic Lanes	89.48%	78.43%	83.66%	81.62%	80.54%	88.13%
Others	9.10%	20.39%	14.73%	16.67%	14.75%	9.88%
Group Coal	0.18%	0.15%	0.22%	0.30%	0.67%	0.25%
Group Siderurgy	1.24%	1.03%	1.39%	1.41%	4.03%	1.73%
CMB	**Apr-Sep 09**	**Nov-09**	**Dec-09**	**Jan-10**	**Feb-10**	**Mar-10**
Traffic Lanes	42.94%	34.24%	37.41%	43.21%	48.33%	43.90%
Others	45.05%	54.90%	52.75%	48.25%	42.41%	41.58%
Group Coal	0.00%	0.00%	0.00%	0.00%	0.00%	0.00%
Group Siderurgy	12.01%	10.85%	9.84%	8.54%	9.26%	14.51%

RAMQAR 9 – SENAC

CALPUFF	Apr-Sep 09	Nov-09	Dec-09	Jan-10	Feb-10	Mar-10
Traffic Lanes	38.82%	27.69%	35.53%	23.95%	19.84%	33.23%
Others	36.22%	40.57%	37.60%	33.16%	35.74%	35.80%
Group Coal	2.39%	3.63%	3.40%	4.59%	3.96%	2.66%
Group Siderurgy	22.57%	28.12%	23.47%	38.30%	40.46%	28.32%
CMB	**Apr-Sep 09**	**Nov-09**	**Dec-09**	**Jan-10**	**Feb-10**	**Mar-10**
Traffic Lanes	34.40%	0.00%	0.00%	0.00%	0.00%	23.42%
Others	14.86%	6.43%	5.39%	6.35%	9.00%	7.10%
Group Coal	5.47%	8.19%	11.86%	4.52%	0.00%	0.00%
Group Siderurgy	45.27%	85.37%	82.75%	89.13%	91.00%	69.48%

APPENDIX E SOURCE APPORTIONMENT OBTAINED USING THE METHODOLOGY PROPOSED IN THIS WORK

- RAMQAR 1 (LARANJEIRAS):

SOURCES	Apr-Sep 09	Nov 09	Dez 09	Jan 10	Fev 10	Mar 10
Quarries	0.00%	8.68%	17.24%	0.00%	0.00%	0.00%
Civil Construction	33.59%	10.08%	7.80%	17.28%	18.43%	26.24%
Ressuspension	36.24%	0.00%	0.00%	0.00%	0.00%	0.00%
Soil	0.00%	67.06%	46.76%	68.33%	49.24%	44.15%
Sea Breeze	8.31%	0.00%	1.24%	0.00%	4.01%	2.55%
Vehicles	13.17%	3.27%	16.26%	9.03%	15.88%	14.65%
Steelworks	0.00%	0.29%	0.75%	0.00%	0.00%	0.00%
Coal	1.50%	1.37%	0.00%	0.00%	0.00%	0.00%
Coke	0.77%	0.27%	0.00%	0.00%	0.00%	0.00%
Ore	3.50%	0.00%	0.00%	1.36%	5.74%	5.10%
Pellets	1.71%	0.00%	0.00%	0.78%	2.00%	2.18%
Ovens (Vale)	1.20%	0.00%	0.00%	0.28%	2.12%	1.44%
Blast Furnaces	0.00%	1.90%	4.68%	0.00%	0.00%	0.00%
Sintering	0.00%	4.58%	2.97%	0.00%	0.00%	0.00%
LTQ Ovens	0.00%	0.00%	0.00%	0.00%	0.00%	0.00%
Thermoelectrics	0.00%	0.00%	0.00%	0.00%	0.00%	0.00%
Others	0.00%	2.50%	2.28%	2.95%	2.57%	3.68%
Cement	0.00%	0.00%	0.00%	0.00%	0.00%	0.00%
Total (%)	**100.00%**	**100.00%**	**100.00%**	**100.00%**	**100.00%**	**100.00%**

- RAMQAR 3 (JARDIM CAMBURI):

SOURCES	Apr-Sep 09	Nov 09	Dez 09	Jan 10	Fev 10	Mar 10
Quarries	0.00%	0.00%	0.00%	0.00%	0.00%	0.00%
Civil Construction	9.85%	27.51%	24.25%	53.18%	51.84%	50.53%
Ressuspension	41.73%	50.57%	39.22%	15.85%	18.87%	21.79%
Soil	0.00%	0.00%	0.00%	0.00%	0.00%	0.00%
Sea Breeze	7.57%	1.66%	3.95%	0.00%	1.62%	3.20%
Vehicles	24.28%	14.79%	22.67%	16.12%	11.86%	7.74%
Steelworks	3.70%	0.28%	0.89%	4.73%	1.64%	2.18%
Coal	2.77%	0.00%	0.00%	3.05%	2.03%	2.52%
Coke	1.02%	0.00%	0.00%	1.61%	2.39%	1.75%
Ore	0.00%	0.00%	0.00%	0.00%	0.00%	0.00%
Pellets	0.00%	0.00%	0.00%	0.00%	0.00%	0.00%
Ovens (Vale)	0.00%	0.00%	0.00%	0.00%	0.00%	0.00%
Blast Furnaces	4.31%	3.76%	3.89%	4.69%	7.99%	4.42%
Sintering	4.77%	1.44%	5.11%	0.77%	1.75%	5.87%
LTQ Ovens	0.00%	0.00%	0.00%	0.00%	0.00%	0.00%
Thermoelectrics	0.00%	0.00%	0.00%	0.00%	0.00%	0.00%
Others	0.00%	0.00%	0.00%	0.00%	0.00%	0.00%
Cement	0.00%	0.00%	0.00%	0.00%	0.00%	0.00%
Total (%)	**100.00%**	**100.00%**	**100.00%**	**100.00%**	**100.00%**	**100.00%**

- RAMQAR 4 (ENSEADA):

SOURCES	Apr-Sep 09	Nov 09	Dez 09	Jan 10	Fev 10	Mar 10
Quarries	0.00%	0.00%	0.00%	0.00%	0.00%	0.00%
Civil Construction	10.39%	26.21%	15.62%	0.00%	0.00%	18.40%
Ressuspension	52.98%	13.42%	27.61%	25.67%	40.04%	28.64%
Soil	0.00%	0.00%	0.00%	0.00%	0.00%	0.00%
Sea Breeze	5.17%	1.94%	2.44%	1.07%	4.01%	4.21%
Vehicles	11.26%	9.00%	15.45%	6.82%	9.36%	12.06%
Steelworks	2.07%	0.00%	0.24%	0.71%	0.39%	0.00%
Coal	2.91%	6.47%	4.34%	4.46%	3.84%	0.81%
Coke	1.26%	1.96%	1.41%	3.33%	1.75%	0.37%
Ore	6.74%	26.05%	18.49%	27.51%	22.51%	20.61%
Pellets	2.43%	10.92%	9.03%	12.06%	8.43%	6.18%
Ovens (Vale)	1.44%	4.04%	4.55%	10.64%	5.90%	8.71%
Blast Furnaces	1.92%	0.00%	0.36%	5.09%	2.23%	0.00%
Sintering	1.44%	0.00%	0.46%	2.63%	1.53%	0.00%
LTQ Ovens	0.00%	0.00%	0.00%	0.00%	0.00%	0.00%
Thermoelectrics	0.00%	0.00%	0.00%	0.00%	0.00%	0.00%
Others	0.00%	0.00%	0.00%	0.00%	0.00%	0.00%
Cement	0.00%	0.00%	0.00%	0.00%	0.00%	0.00%
Total (%)	**100.00%**	**100.00%**	**100.00%**	**100.00%**	**100.00%**	**100.00%**

- RAMQAR 5 (VITORIA CITY CENTER):

SOURCES	Apr-Sep 09	Nov 09	Dez 09	Jan 10	Fev 10	Mar 10
Quarries	0.00%	0.00%	0.00%	0.00%	0.00%	0.00%
Civil Construction	0.00%	6.02%	11.88%	13.19%	7.18%	0.00%
Ressuspension	70.39%	58.41%	46.68%	40.72%	50.18%	78.89%
Soil	0.00%	0.00%	0.00%	0.00%	0.00%	0.00%
Sea Breeze	4.76%	3.10%	1.49%	0.00%	3.58%	2.99%
Vehicles	18.14%	25.66%	32.96%	20.43%	18.45%	9.81%
Steelworks	1.78%	0.20%	0.00%	0.23%	0.53%	0.12%
Coal	1.42%	0.96%	0.00%	2.61%	1.22%	0.98%
Coke	1.09%	0.28%	0.00%	1.75%	0.70%	0.54%
Ore	0.00%	2.11%	3.97%	8.81%	8.35%	3.01%
Pellets	0.00%	0.69%	1.54%	4.44%	3.20%	1.16%
Ovens (Vale)	0.00%	0.73%	1.47%	3.43%	2.95%	1.01%
Blast Furnaces	0.42%	0.70%	0.00%	2.03%	1.52%	0.06%
Sintering	0.58%	0.43%	0.00%	2.37%	2.14%	0.08%
LTQ Ovens	0.30%	0.09%	0.00%	0.00%	0.00%	0.21%
Thermoelectrics	1.14%	0.61%	0.00%	0.00%	0.00%	1.13%
Others	0.00%	0.00%	0.00%	0.00%	0.00%	0.00%
Cement	0.00%	0.00%	0.00%	0.00%	0.00%	0.00%
Total (%)	**100.00%**	**100.00%**	**100.00%**	**100.00%**	**100.00%**	**100.00%**

- RAMQAR 6 (IBES):

SOURCES	Apr-Sep 09	Nov 09	Dez 09	Jan 10	Fev 10	Mar 10
Quarries	37.18%	0.00%	0.00%	22.20%	16.00%	31.21%
Civil Construction	9.50%	26.44%	13.51%	0.00%	0.00%	0.00%
Ressuspension	0.00%	25.08%	40.78%	33.77%	37.85%	0.00%
Soil	14.01%	0.00%	0.00%	0.00%	0.00%	10.16%
Sea Breeze	9.93%	1.47%	1.91%	0.70%	3.73%	7.71%
Vehicles	16.66%	8.02%	17.00%	8.75%	10.79%	33.24%
Steelworks	1.90%	0.00%	0.00%	0.00%	0.02%	0.20%
Coal	0.98%	3.66%	1.74%	1.04%	1.39%	0.00%
Coke	0.59%	1.40%	0.81%	0.88%	1.25%	0.00%
Ore	4.42%	19.44%	14.52%	17.52%	16.83%	9.38%
Pellets	1.72%	6.98%	5.54%	7.89%	6.21%	4.07%
Ovens (Vale)	1.51%	7.50%	4.20%	7.26%	5.77%	3.66%
Blast Furnaces	0.67%	0.00%	0.00%	0.00%	0.08%	0.17%
Sintering	0.91%	0.00%	0.00%	0.00%	0.09%	0.20%
LTQ Ovens	0.00%	0.00%	0.00%	0.00%	0.00%	0.00%
Thermoelectrics	0.00%	0.00%	0.00%	0.00%	0.00%	0.00%
Others	0.00%	0.00%	0.00%	0.00%	0.00%	0.00%
Cement	0.00%	0.00%	0.00%	0.00%	0.00%	0.00%
Total (%)	**100.00%**	**100.00%**	**100.00%**	**100.00%**	**100.00%**	**100.00%**

- RAMQAR 7 (VILA VELHA):

SOURCES	Apr-Sep 09	Nov 09	Dez 09	Jan 10	Fev 10	Mar 10
Quarries	0.00%	0.00%	0.00%	0.00%	0.00%	0.00%
Civil Construction	6.51%	16.11%	9.89%	31.93%	13.71%	10.70%
Ressuspension	58.15%	59.13%	48.07%	35.66%	0.00%	43.04%
Soil	0.00%	0.00%	0.00%	0.00%	40.60%	0.00%
Sea Breeze	11.66%	1.08%	3.75%	1.47%	5.84%	10.86%
Vehicles	13.57%	2.51%	17.48%	8.72%	10.56%	14.24%
Steelworks	0.00%	0.00%	0.00%	0.00%	0.00%	0.13%
Coal	1.21%	0.98%	0.00%	0.96%	0.00%	0.00%
Coke	0.49%	0.57%	0.00%	0.67%	0.00%	0.00%
Ore	4.92%	10.47%	12.70%	12.26%	17.34%	12.00%
Pellets	1.83%	4.96%	3.98%	4.44%	5.97%	4.19%
Ovens (Vale)	1.66%	4.18%	4.12%	3.88%	5.97%	4.06%
Blast Furnaces	0.00%	0.00%	0.00%	0.00%	0.00%	0.36%
Sintering	0.00%	0.00%	0.00%	0.00%	0.00%	0.44%
LTQ Ovens	0.00%	0.00%	0.00%	0.00%	0.00%	0.00%
Thermoelectrics	0.00%	0.00%	0.00%	0.00%	0.00%	0.00%
Others	0.00%	0.00%	0.00%	0.00%	0.00%	0.00%
Cement	0.00%	0.00%	0.00%	0.00%	0.00%	0.00%
Total (%)	**100.00%**	**100.00%**	**100.00%**	**100.00%**	**100.00%**	**100.00%**

- RAMQAR 8 (CARIACICA):

SOURCES	Apr-Sep 09	Nov 09	Dez 09	Jan 10	Fev 10	Mar 10
Quarries	41.48%	53.92%	51.83%	47.98%	40.61%	40.47%
Civil Construction	0.00%	0.00%	0.00%	0.00%	0.00%	0.00%
Ressuspension	0.00%	0.00%	0.00%	0.00%	0.00%	0.00%
Soil	24.84%	22.05%	9.49%	27.82%	28.43%	22.42%
Sea Breeze	3.57%	1.00%	0.94%	0.13%	1.82%	1.13%
Vehicles	18.10%	12.20%	27.94%	15.26%	19.92%	21.50%
Steelworks	9.17%	8.70%	6.79%	3.20%	3.91%	10.16%
Coal	0.00%	0.00%	0.00%	0.00%	0.00%	0.00%
Coke	0.00%	0.00%	0.00%	0.00%	0.00%	0.00%
Ore	0.00%	0.00%	0.00%	0.00%	0.00%	0.00%
Pellets	0.00%	0.00%	0.00%	0.00%	0.00%	0.00%
Ovens (Vale)	0.00%	0.00%	0.00%	0.00%	0.00%	0.00%
Blast Furnaces	1.08%	0.79%	1.05%	2.26%	2.16%	1.52%
Sintering	1.75%	1.34%	1.97%	3.34%	3.14%	2.79%
LTQ Ovens	0.00%	0.00%	0.00%	0.00%	0.00%	0.00%
Thermoelectrics	0.00%	0.00%	0.00%	0.00%	0.00%	0.00%
Others	0.00%	0.00%	0.00%	0.00%	0.00%	0.00%
Cement	0.00%	0.00%	0.00%	0.00%	0.00%	0.00%
Total (%)	**100.00%**	**100.00%**	**100.00%**	**100.00%**	**100.00%**	**100.00%**

- RAMQAR 9 (SENAC):

SOURCES	Apr-Sep 09	Nov 09	Dez 09	Jan 10	Fev 10	Mar 10
Quarries	0.00%	0.00%	0.00%	0.00%	0.00%	0.00%
Civil Construction	0.00%	0.00%	0.00%	0.00%	0.00%	0.00%
Ressuspension	34.97%	0.00%	0.00%	0.00%	0.00%	0.00%
Soil	0.00%	0.00%	0.00%	0.00%	0.00%	5.93%
Sea Breeze	15.10%	6.44%	5.39%	6.35%	9.00%	7.10%
Vehicles	0.00%	0.00%	0.00%	0.00%	0.00%	17.51%
Steelworks	6.64%	1.74%	3.34%	0.78%	0.85%	2.30%
Coal	4.09%	5.85%	9.38%	2.74%	0.00%	0.00%
Coke	1.46%	2.35%	2.50%	1.78%	0.00%	0.00%
Ore	13.89%	42.25%	38.89%	43.33%	49.47%	31.20%
Pellets	4.51%	14.76%	15.59%	19.84%	16.95%	10.71%
Ovens (Vale)	2.97%	10.80%	7.08%	16.16%	12.49%	11.02%
Blast Furnaces	7.33%	10.86%	6.43%	5.83%	6.07%	8.36%
Sintering	5.03%	2.65%	6.13%	2.50%	3.48%	3.48%
LTQ Ovens	0.76%	0.77%	1.06%	0.15%	0.23%	0.38%
Thermoelectrics	3.24%	1.52%	4.21%	0.55%	1.46%	2.01%
Others	0.00%	0.00%	0.00%	0.00%	0.00%	0.00%
Cement	0.00%	0.00%	0.00%	0.00%	0.00%	0.00%
Total (%)	**100.00%**	**100.00%**	**100.00%**	**100.00%**	**100.00%**	**100.00%**

Table 19. Ungrouped contributions for RAMQAR stations 1 and 3.

RAMQAR 1 LARNJEIRAS	COAL[1]	COAL / COKE[2]	GROUP A[1]	ORE / PELLETS / OVENS[2]	GROUP B[1]	BLAST FURNACES/ SINTERING / STEELWORKS[2]	GROUP C[1]	LTQ OVENS / THERMOELECTRICS[2]
04/09 – 09/09	2.31%	1.50% / 0.77%	6.39%	3.50% / 1.71% / 1.20%	-	-	-	-
11/09	1.63%	1.37% / 0.27%	-	-	6.72%	1.90% / 4.58% / 0.29%	-	-
12/09	-	-	-	-	8.43%	4.68% / 2.97% / 0.75%	-	-
01/10	-	-	2.90%	1.36% / 0.78% / 0.28%	-	-	-	-
02/10	-	-	10.01%	5.74% / 2.00% / 2.12%	-	-	-	-
03/10	-	-	8.72%	5.10% / 2.18% / 1.44%	-	-	-	-
RAMQAR 3 J. CAMBURI	**COAL[1]**	**COAL / COKE[2]**	**GROUP A[1]**	**ORE / PELLETS / OVENS[2]**	**GROUP B[1]**	**BLAST FURNACES/ SINTERING / STEELWORKS[2]**	**GROUP C[1]**	**LTQ OVENS / THERMOELECTRICS[2]**
04/09 – 09/09	3.77%	2.72% / 1.02%	-	-	12.72%	4.31% / 4.77% / 3.70%	-	-
11/09	-	-	-	-	5.47%	3.76% / 1.44% / 0.28%	-	-
12/09	-	-	-	-	9.89%	3.89% / 5.11% / 0.89%	-	-
01/10	4.66%	3.05% / 1.63%	-	-	10.21%	4.69% / 0.77% / 4.73%	-	-
02/10	4.55%	2.03% / 2.39%	-	-	11.38%	7.99% / 1.75 % / 1.64%	-	-
03/10	4.24%	2.52% / 1.75%	-	-	12.51%	2.18% / 4.42% / 5.87%	-	-

From April 2009 to March of 2010; minor differences relate to approximations made. [1] from CMB Source Apportionment; [2] from integrated CMB+CALPUFF Source Apportionment.

Table 20. Ungrouped contributions for RAMQAR stations 4 and 5.

RAMQAR 4 ENSEADA	COAL[1]	COAL / COKE[2]	GROUP A[1]	ORE / PELLETS / OVENS[2]	GROUP B[1]	BLAST FURNACES/ SINTERING / STEELWORKS[2]	GROUP C[1]	LTQ OVENS / THERMOELECTRICS[2]
04/09 – 09/09	4.17%	2.91% / 1.26%	10.60%	6.74% / 2.42% / 1.44%	5.43%	2.07% / 1.92% / 1.44%	-	-
11/09	8.46%	6.47% / 1.96%	41.01%	26.05% / 10.92% / 4.04%	-	-	-	-
12/09	5.74%	4.34% / 1.41%	32.01%	18.43% / 9.03% / 4.55%	1.06%	0.36% / 0.46% / 0.24%	-	-
01/10	7.78%	4.46% / 3.33%	50.21%	27.51% / 12.06% / 10.64%	8.43%	5.09% / 2.63% / 0.71%	-	-
02/10	5.62%	3.84% / 1.75%	36.84%	22.51% / 8.43% / 5.90%	4.09%	2.23% / 1.53% / 0.33%	-	-
03/10	1.14%	0.81% / 0.37%	35.51%	20.61% / 6.18% / 8.71%	-	-	-	-
RAMQAR 5 VITORIA	**COAL[1]**	**COAL / COKE[2]**	**GROUP A[1]**	**ORE / PELLETS / OVENS[2]**	**GROUP B[1]**	**BLAST FURNACES/ SINTERING / STEELWORKS[2]**	**GROUP C[1]**	**LTQ OVENS / THERMOELECTRICS[2]**
04/09 – 09/09	2.49%	1.42% / 1.09%	-	-	2.78%	0.42% / 0.58% / 1.78%	1.44%	1.14% / 0.3%
11/09	1.23%	0.96% / 0.28%	3.53%	2.11% / 0.69% / 0.73%	1.33%	0.70% / 0.43% / 0.20%	0.70%	0.09% / 0.61%
12/09	-	-	6.99%	3.97% / 1.54% / 1.47%	-	-	-	-
01/10	4.38%	2.61% / 1.75%	16.68%	8.81% / 4.44% / 3.43%	4.63%	2.03% / 2.37% / 0.23%	-	-
02/10	1.95%	1.22% / 0.70%	14.50%	8.35% / 3.20% / 2.95%	4.19	1.52% / 2.14% / 0.53%	-	-
03/10	1.55%	0.98% / 0.54%	5.18%	3.01% / 1.16% / 1.01%	0.26%	0.12% / 0.06% / 0.08%	1.34%	0.21% / 1.13%

From April 2009 to March of 2010; minor differences relate to approximations made. [1] from CMB Source Apportionment; [2] from integrated CMB+CALPUFF Source Apportionment.

Table 21. Ungrouped contributions for RAMQAR stations 6 and 7.

RAMQAR 6 IBES	COAL[1]	COAL / COKE[2]	GROUP A[1]	ORE / PELLETS / OVENS[2]	GROUP B[1]	BLAST FURNACES/ SINTERING / STEELWORKS[2]	GROUP C[1]	LTQ OVENS / THERMOELECTRICS[2]
04/09 – 09/09	1.62%	0.98% / 0.59%	7.65%	4.42% / 1.72% / 1.51%	3.48%	0.67% / 0.91% / 1.90%	-	-
11/09	5.02%	3.66% / 1.40%	33.95%	19.44% / 6.98% / 7.50%	-	-	-	-
12/09	2.58%	1.74% / 0.81%	24.25%	14.52% / 5.54% / 4.20%	-	-	-	-
01/10	1.88%	1.04% / 0.88%	32.72%	17.52% / 7.89% / 7.26%	-	-	-	-
02/10	2.67%	1.39% / 1.25%	28.81%	16.83% / 6.21% / 5.77 %	0.19%	0.08% / 0.09% / 0.02%	-	-
03/10	-	-	17.11%	9.38% / 4.07% / 3.66%	0.57%	0.17% / 0.20% / 0.20%	-	-
RAMQAR 7 V. VELHA	**COAL[1]**	**COAL / COKE[2]**	**GROUP A[1]**	**ORE / PELLETS / OVENS[2]**	**GROUP B[1]**	**BLAST FURNACES/ SINTERING / STEELWORKS[2]**	**GROUP C[1]**	**LTQ OVENS / THERMOELECTRICS[2]**
04/09 – 09/09	1.72%	1.21% / 0.49%	8.41%	4.92% / 1.83% / 1.66%	-	-	-	-
11/09	1.56%	0.98% / 0.57%	19.58%	10.47% / 4.96% / 4.18%	-	-	-	-
12/09	-	-	20.78%	12.70% / 3.98% / 4.12%	-	-	-	-
01/10	1.66%	0.96% / 0.67%	20.58%	12.26% / 4.44% / 3.88%	-	-	-	-
02/10	-	-	29.29%	17.34% / 5.97% / 5.97%	-	-	-	-
03/10	-	-	20.25%	12.00% / 4.19% / 4.06%	0.93%	0.36% / 0.44% / 0.13%	-	-

From April 2009 to March of 2010; minor differences relate to approximations made. [1] from CMB Source Apportionment; [2] from integrated CMB+CALPUFF Source Apportionment.

Table 22. Ungrouped contributions for RAMQAR stations 8 and 9.

RAMQAR 8 CARIACICA	COAL[1]	COAL/COKE[2]	GROUP A[1]	ORE / PELLETS / OVENS[2]	GROUP B[1]	BLAST FURNACES/ SINTERING / STEELWORKS[2]	GROUP C[1]	LTQ OVENS / THERMOELECTRICS[2]
04/09 – 09/09	-	-	-	-	12.01%	1.08% / 1.75% / 9.17%	-	-
11/09	-	-	-	-	10.85%	6.79% / 1.34% / 8.70%	-	-
12/09	-	-	-	-	9.84%	1.05% / 1.97% / 6.79%	-	-
01/10	-	-	-	-	8.54%	2.26% / 3.34% / 3.20%	-	-
02/10	-	-	-	-	9.26%	2.16% / 3.14% / 3.91%	-	-
03/10	-	-	-	-	14.31%	1.52% / 2.79% / 10.16%	-	-

RAMQAR 9 SENAC	COAL[1]	COAL/COKE[2]	GROUP A[1]	ORE / PELLETS / OVENS[2]	GROUP B[1]	BLAST FURNACES/ SINTERING / STEELWORKS[2]	GROUP C[1]	LTQ OVENS / THERMOELECTRICS[2]
04/09 – 09/09	5.47%	4.09% / 1.46%	21.37%	13.89% / 4.51% / 2.97%	19.00%	7.33% / 5.03% / 6.64%	4.00%	0.76% / 3.24%
11/09	8.19%	5.85% / 2.35%	67.81%	42.25% / 14.76% / 10.80%	15.25%	10.86% / 2.65% / 1.74%	2.29%	1.52% / 0.77%
12/09	11.86%	9.38% / 2.50%	61.56	38.89% / 15.59% / 7.08%	15.90%	6.43% / 6.13% / 3.34%	5.27%	1.06% / 4.21%
01/10	4.52%	2.74% / 1.78%	79.33%	43.33% / 19.84% / 16.16%	9.17%	5.83% / 2.56% / 0.78%	0.70%	0.15% / 0.55%
02/10	-	-	78.91%	49.47% / 16.95% / 12.49%	10.40%	6.07% / 3.48% / 0.85%	1.69%	0.23% / 1.46%
03/10	-	-	52.93%	31.20% / 10.71% / 11.02%	14.14%	8.36% / 3.48% / 2.30%	2.49%	0.38% / 2.01%

From April 2009 to March of 2010; minor differences relate to approximations made. [1] from CMB Source Apportionment; [2] from integrated CMB+CALPUFF Source Apportionment